Modeling fetal cardiac valve intervals and fetal-maternal interactions

Faezeh Marzbanrad

Submitted in total fulfilment of the requirements of the degree of

Doctor of Philosophy

Department of Electrical and Electronic Engineering
THE UNIVERSITY OF MELBOURNE

November 2015

Produced on archival quality paper

Abstract

Despite the advances in fetal healthcare, in Australia around 9-10 out of 1000 babies die in perinatal period, which is defined as starting from 22 weeks of pregnancy and extending to the first week after birth. This mortality rate is three to four times higher in some developing countries. Furthermore, false alarms produced by the current fetal surveillance technology impose unnecessary interventions, which involve additional costs and potential maternal and fetal risks. Therefore there is a critical need for more accurate fetal assessment methods for reliable identification of fetal risks. Fetal heart assessment is one of the main concerns in fetal healthcare and provides significant information about the fetal development and well-being. The aim of this research is to develop automated and accurate fetal heart assessment methods using noninvasive and less specialized techniques.

In this research, automated methods were developed for estimation of the fetal cardiac valve intervals which are fundamental and clinically significant part of the fetal heart physiology. For this purpose simultaneous recordings of one dimensional Doppler Ultrasound (1-D DUS) signal and noninvasive fetal Electrocardiography (fECG) were used. New methods were developed for decomposition of the DUS signal into the component manifesting the valves' motion. Opening and closing of the valves were then identified automatically based on the features of the DUS component, their temporal order and duration from the R-peak of fECG. Result of evaluating the cardiac intervals over healthy gestational ages and in heart anomaly cases, showed evidences of their effectiveness in assessing fetal development and well-being.

Fetal heart activity is influenced by not only the fetal conditions and maturation, but also the maternal psychological and physiological conditions. Therefore this research

also focused on the relationship between maternal and fetal heart rates. To this aim, a model-free method based on Transfer Entropy (TE) was used to quantify directed interactions between maternal and fetal heart rates at various time delays and gestational ages. The changes of the coupling throughout gestation provided detailed information on the fetal-maternal relationship, which can provide novel clinical markers of healthy versus pathological fetal development.

Declaration

This is to certify that

1. the thesis comprises only my original work towards the PhD,
2. due acknowledgement has been made in the text to all other material used,
3. the thesis is less than 100,000 words in length, exclusive of tables, maps, bibliographies and appendices.

Faezeh Marzbanrad, November 2015

Publications

Book Chapter:

1. F. Marzbanrad, Y. Kimura, M. Palaniswami, et al., "Fetal Heart Rate Variability". ECG Time Series Variability Analysis: Engineering and Medicine, (eds:H. Jelinek, D. Cornforth, A. Khandoker), Chapter 18, CRC Press, ISBN 9781482243475, 2015.

Journal Papers:

2. F. Marzbanrad, Y. Kimura, K. Funamoto, et al., "Model based Estimation of Aortic and Mitral valves Opening and Closing Timings in Developing Human Fetuses". IEEE Journal of Biomedical and Health Informatics vol.PP, no.99, pp.1, 2014. doi: 10.1109/JBHI.2014.2363452.

3. F. Marzbanrad, Y. Kimura, K. Funamoto, et al., "Automated estimation of fetal cardiac timing events from Doppler ultrasound signal using hybrid models". IEEE Journal of Biomedical and Health Informatics, vol.18, no.4, pp.1169-1177, 2014. doi: 10.1109/JBHI.2013.2286155.

4. F. Marzbanrad, Y. Kimura, M. Palaniswami, et al., "Quantifying the Interactions between Maternal and Fetal Heart Rates by Transfer Entropy". PlosOne journal, 10.12, 2015.

Conference Papers:

5. F. Marzbanrad, M. Endo, Y. Kimura, et al., "Transfer Entropy Analysis of Maternal and Fetal Heart Rate Coupling", IEEE Engineering in Medicine and Biology Conference EMBC 2015.

6. F. Marzbanrad, A. Khandoker, M. Endo, et al., "Classification of Doppler Ultrasound Signal Quality for the Application of Fetal Valve Motion Identification". Computing in Cardiology Conference (CinC), 2015.

7. F. Marzbanrad, A. Khandoker, M. Endo, et al., "A Multi-dimensional Hidden Markov Model Approach to Automated Identification of Fetal Cardiac Valve Motion". IEEE Engineering in Medicine and Biology Conference EMBC 2014, pp.1885-1888.

8. F. Marzbanrad, Y. Kimura, M. Palaniswami, et al., "Application of Automated Fetal Valve Motion Identification to Investigate Fetal Heart Anomalies". IEEE EMBS Healthcare Innovation Conference (HIC), 2014 IEEE , vol., no., pp.243-246, 2014. doi: 10.1109/HIC.2014.7038920

9. F. Marzbanrad, Y. Kimura, M. Endo, et al., "Automated measurement of fetal Isovolumic Contraction Time from doppler ultrasound signal without using fetal electrocardiography", Computing in Cardiology Conference (CinC), 2014 , vol., no., pp.485-488, 2014.

10. F. Marzbanrad, Y. Kimura, K. Funamoto, et al., "Development of fetal cardiac intervals throughout 16 to 41 weeks of gestation". In Computing in Cardiology Conference (CinC), 2013, pp. 1155-1158. IEEE, 2013.

11. F. Marzbanrad, A. H. Khandoker, K. Funamoto, et al., "Automated Identification of fetal cardiac valve timings". Engineering in Medicine and Biology Society (EMBC), 2013 35th Annual International Conference of the IEEE, pp. 3893-3896. IEEE, 2013.

Other related publications:

Journal paper:

12. A. Khandoker, F. Marzbanrad, A. Voss, et al., "Analysis of Maternal-Fetal Heart Rate Coupling Directions with Partial Directed Coherence". Journal of Biomedical Signal Processing and Control, 2015 (Major revision).

Conference papers:

13. F. Marzbanrad, A. H. Khandoker, Y. Kimura, et al., "Estimating Fetal Gestational Age Using Cardiac Valve Intervals". Computing in Cardiology Conference (CinC), 2016 (Under review).

14. A. H. Khandoker, F. Marzbanrad, Y. Kimura, et al., "Assessing the development of fetal myocardial function by a novel Doppler myocardial performance index". IEEE Engineering in Medicine and Biology Society Conference (EMBC), 2016 (Under review).

15. Q. Wang, A. H. Khandoker, F. Marzbanrad, et al., "Investigating the beat by beat phase synchronization between maternal and fetal heart rates". Engineering in Medicine and Biology Society (EMBC), 2013 35th Annual International Conference of the IEEE, pp. 3821- 3824. IEEE, 2013.

Acknowledgements

I would like to express my gratitude to my supervisors Professor Marimuthu Palaniswami and Dr. Ahsan Khandoker for their guidance, support and knowledge. I would like to thank the team of clinical support service at the School of Medicine, Tohoku University, in Japan, for providing the data for this research, especially Professor Yoshitaka Kimura for giving invaluable support and insight on the clinical aspect of the research.

I am very grateful for my friends and colleagues at the Department of Electrical and Electronic Engineering, and the Intelligent Sensors, Sensor Networks and Information Processing (ISSNIP) center. I would like to express my appreciation to Professor Len Stevens and Melbourne School of Engineering for offering me the Len Stevens scholarship, which provided me with an outstanding opportunity to visit the University of Oxford, Emory University and Georgia Institute of Technology, during my candidature and thank Professor Gari Clifford for supervising me during my visit.

I am thankful for my loving parents and brother for their encouragement and perspective. Special thanks go to my father who introduced me to the world of electrical and electronic engineering and for his knowledge and support. I warmly thank my mother who inspired me to apply my engineering knowledge in the medical field. Finally, I am deeply grateful to my husband for his endless love, continuous support and his companionship throughout our PhD journeys.

Contents

List of Figures

List of Tables

Chapter 1

Introduction

FETAL healthcare is a field of increasing interest and significance around the globe. In Australia around 9-10 out of 1000 babies die in perinatal period which is from 22 weeks of pregnancy to the first week after birth [9]. This mortality rate is three to four times higher in some developing countries [170]. Perinatal mortality is mostly caused by congenital malformations and perinatal hypoxia [27]. The most common of major congenital diseases is Congenital Heart Diseases (CHD), which is the cause of over half of neonatal mortality and morbidity due to structural defects [51]. The incidence of CHD is 1 out of 125 babies each year and even with the current improved treatment options, every fifth child with CHD dies during the first year of life. The mortality rate correlates closely with the severity of the heart defect and its early clinical manifestations. Early detection of CHD and perinatal hypoxia may reduce perinatal morbidity and mortality [128], while providing tremendous medical, psychological and economical benefits [61]. Since 85% of fetuses with CHD are not detected and classified in the high risk category, screening of low risk cases is also necessary [87].

Another indication for fetal assessment is to investigate the fetal development, which can be affected by conditions which restrict the normal growth of the fetus. Intrauterine growth restriction (IUGR) indicates a higher risk for perinatal morbidity and mortality [33]. IUGR fetuses have 50% higher neonatal mortality rates. Furthermore IUGR results in 10%-30% higher incidence of minor and major congenital anomalies, leading to 30% to 60% of the IUGR perinatal deaths [33,145]. The incidence of IUGR is approximately 4% to 8% of children born in developed countries and 6% to 30% in developing countries [33]. Detection and management of IUGR in clinical practice are through the fetal assessment

methods, such as ultrasound and biophysical profile (BPP), amniotic fluid volume (AFV) and Doppler assessment of the fetal circulation, which will be discussed in detail in the next chapter.

Despite the advances in fetal surveillance which reduced perinatal morbidity and mortality rate in the high risk population, the majority of stillbirths and anomalies still occur in low risk pregnancies [27]. Furthermore, false alarms produced by the current fetal surveillance technology impose unnecessary interventions, which involve additional costs and potential maternal and fetal risks. Therefore there is a need for more effective and sensitive methods of identifying fetal risks, as well as simple and less specialized techniques applicable to the larger population of low risk pregnancies.

1.1 Research aims

To estimate the fetal cardiac valve intervals automatically based on the electrical and mechanical activities of the fetal heart

Fetal Cardiac valve intervals are fundamental and clinically significant part of the fetal heart physiology and can be used as sensitive markers for fetal development and well-being. In this research automated methods were investigated for estimation of the cardiac intervals, through noninvasive and easy-to-operate devices. Simultaneous use of one-dimensional Doppler Ultrasound (1-D DUS) signal and noninvasive fetal Electrocardiography (fECG) provides information on the electrical and mechanical activity as well as electromechanical coupling of the fetal heart. As will be discussed in the literature review, previous studies used signal processing techniques to extract the information content of the 1-D DUS signal, from which the cardiac intervals were manually determined. However, the DUS signal is nonstationary, highly susceptible to noise and has a transient nature which complicates the extraction of the information on the mechanical activity of the heart. Furthermore manual identification of the cardiac valve timings is time consuming, requires special expertise and is subject to inter and intra observer and visual errors. As such, improved approaches to extract the information content of the DUS signal and automated estimation of fetal cardiac intervals were investigated in

this research. The effect of gestational progression and fetal development as well as fetal heart anomalies on the intervals were investigated to provide novel markers of healthy versus pathological development.

To investigate the relationship between maternal and fetal heart rates with advancing gestation

Evidence of the relationships between maternal and fetal heart rates have been found in previous studies. However the knowledge about the mechanism, directionality and development of this relationship throughout gestation is still limited. The second part of the thesis is aimed at investigating any linear or nonlinear interactions between maternal and fetal heart rates in both directions. Another purpose of this part is to study the changes in the coupling with gestational progression, which may provide clinical marker to assess fetal development.

1.2 Overview of thesis

The first part of the thesis is on the background of the research, including chapter two which reviews the fetal health assessment methods. It begins with conventional fetal screening methods in clinical practice, then highlights the methods for fetal heart assessment. These methods include the techniques currently in use in clinical practice and research. More detailed reviews of literature are included at the beginning of the following parts.

The second part of the thesis includes chapter 3 to 8 aimed at estimating and analyzing fetal cardiac intervals. It begins with chapter 3 is focused on the automated estimation of fetal cardiac intervals from simultaneous recordings of DUS and fECG signals. This chapter provides a background on the previous studies and describes the new automated methods developed for this purpose. Chapter 4 and 5 address the shortcomings of the methods in chapter 3 and present two new methods for improved estimation of fetal cardiac intervals. Chapter 4 introduces a more efficient method than the technique proposed in chapter 3, and chapter 5 is focused on a more accurate technique. The methods described in chapters 3 to 5 estimate fetal cardiac intervals from DUS and fECG. Al-

though fECG has a crucial role as a reference in these methods, simultaneous recording with DUS, extraction and processing of fECG complicate these methods. Therefore in chapter 6, the estimation of the cardiac intervals from DUS signal without fECG, is investigated. Considering that the DUS signal is highly susceptible to noise and variable on a beat-to-beat basis, it is crucial to assess the signal quality to ensure its validity for a reliable estimation of the cardiac timings. Therefore an automated quality assessment is investigated in chapter 7 to classify the quality of the DUS signal. In chapter 8, fetal cardiac intervals are estimated for normal fetuses as well as the cases with heart anomalies to investigate the effect of anomalies on the intervals which can be used as clinical markers.

In chapter 9, beat-by-beat estimated fetal heart rate from fECG is used to investigate its relationship with the maternal heart rate. The transfer of information between maternal and fetal heart rate is also analyzed for different stages of pregnancy to provide a marker for fetal development throughout gestation.

Finally, chapter 10 summarizes the major contributions of this thesis and provides suggestions for future studies to fill the gaps and further develop the research in this area.

Part I

Background

Introduction to Part I

A large body of research advocates improved fetal assessment techniques for early and reliable detection of antepartum fetal risks, aimed at reducing perinatal morbidity and mortality. This Part provides a background to the fetal health screening techniques with a focus on cardiac assessment methods.

Chapter 2
Fetal health assessment methods

This chapter first provides a general review of the current fetal health assessment methods in clinical practice and research and then reviews the methods specific to fetal cardiac assessment. More detailed reviews of literature are included at the beginning of the thesis parts. This chapter is a slightly modified version of the published book chapter:

- *F. Marzbanrad, Y. Kimura, M. Palaniswami, et al., "Fetal Heart Rate Variability". ECG Time Series Variability Analysis: Engineering and Medicine, (eds:H. Jelinek, D. Cornforth, A. Khandoker), Chapter 18, CRC Press, ISBN 9781482243475, 2015.*

2.1 Conventional fetal screening methods

EARLY identification of fetal risks is a field of increasing interest and significance around the globe. A large body of research advocates various fetal assessment techniques to evaluate antepartum fetal risks. Such risks indicate the need for intervention which is aimed at reducing the risk of intrauterine death [40, 109, 156]. The risks include but not limited to utero-placental insufficiency, hypoxia or fetal abnormalities. Antenatal fetal assessment may particularly have an impact for some maternal or pregnancy related conditions associated with increased perinatal morbidity and mortality, which are summarized in table 2.1 [178]. Fetal assessment is not only necessary for high risk pregnancies, but also recommended for all pregnancies in general, since it has been reported that low risk pregnancies have a larger contribution in perinatal mortality than high risk pregnancies [176].

Conventional techniques of fetal assessment include: fetal movement counting, Amniotic Fluid Volume (AFV) test, sonographic assessment and Biophysical Profile (BPP), Contrac-

tion Stress Test (CST), Non Stress Test (NST), Vibroacoustic Stimulation (VAS), Doppler velocimetry and integrated methods [19, 37, 40, 109, 156]. These techniques are briefly introduced in this chapter.

2.1.1 Fetal movement counting

Fetal movement counting is one of the oldest and simplest techniques, aimed at identifying reduced fetal movement which indicates the need for further assessment. This method can be performed in different ways including Cardiff and Sadovsky, which vary in the procedure and required time of the test [56]. Although the test can be done by mother, the perception of movement is usually not accurate nor reliable, as it may be confused by uterine contractions or aortic pulsation. A diverse range of movement counts is suggested for maternal perception which further complicates the assessment and diminishes the reliability of the test. Furthermore, routine and daily movement counting by mother followed by appropriate action in the case of reduce motion, is reported to offer no advantage over informal inquiry about movements and selective use of formal

Table 2.1: Maternal, fetal and pregnancy related conditions which are indications for fetal surveillance; modified from the table in [16, 103, 156, 178, 197].

Maternal Conditions	Fetal and pregnancy related conditions
Antiphospholipid syndrome	Pregnancy-induced hypertension/Pre-eclampsia
Hypertensive disorders	Insulin requiring gestational diabetes
Hyperthyroidism	Decreased fetal movements
Hemoglobinopathies	Multiple gestation (with significant growth discrepancy)
Cyanotic heart disease	Intrauterine growth restriction (IUGR)
Systemic lupus erythematosus	Small for gestational age (SGA) fetus
Chronic renal disease	Post-term pregnancies ($>$ 294 days)
Pre-pregnancy diabetes	Isoimmunization (moderate to severe)
Advanced maternal age	Previous fetal demise (unexpected/recurrent)
Morbid obesity	Preterm prelabor rupture of membranes (PPROM)
	with oligohydramnios
	Polyhydramnios
	Chronic abruption

counting in high-risk cases [56].

2.1.2 Amniotic fluid volume

Established in early 1980s, Amniotic Fluid Volume (AFV) has been used as a chronic marker of the intrauterine environment [196]. The gold standard for this measurement is based on the dye-dilution measurement which cannot be applied repeatedly during pregnancy. Instead, ultrasound based methods such as maximum vertical pocket (MVP) and amniotic fluid index (AFI) have been advocated, which are both correlated with actual AFV, specially in the normal range [34, 163]. According to a study by Magann et al., both methods are useful for predicting variable decelerations, low Apgar scores and caesarean delivery for fetal distress [106]. Although both MVP and AFI techniques are similar in prediction of adverse perinatal outcomes, neither of them is used as an effective sole test for fetal assessment [40].

2.1.3 Doppler velocimetry

The process of Doppler assessment of umbilical artery involves the use of continuous or pulsed wave Doppler to determine arterial flow in a segment of umbilical cord, which is identified using B-mode sonography. The pattern of the waveform is then evaluated mostly through the ratio of Systolic/Diastolic (S/D) and the resistance index, based on quantifying the end diastolic velocity relative to the peak systolic velocity. The presence of diastolic flow has a higher impact than S/D value, e.g. the absence or reversed end diastolic flow is associated with increased incident of perinatal morbidity and mortality [77], as well as 80% and 46% risk of hypoxia and acidosis, respectively [137].
Using Doppler velocimetry is recommended in pregnancies complicated by hypertension and specially in the case of growth restriction [4]. However, according to the large number of controlled, randomized, nonrandomized and observational Doppler studies, examination of the fetoplacental circulation is of little value in unselected low-risk pregnancies [109]. Therefore it is not used as a screening test in general pregnancies.

2.1.4 Nonstress test by Cardiotography

Fetal Heart Rate (FHR) provides a reliable evaluation of the Autonomic Nervous System (ANS) function, which regulates the heart beat dynamics. FHR monitoring is commonly used to assess fetal well-being, and can also provide information about the development of fetal ANS. As discussed earlier, fetal movement counting is one of the basic techniques of fetal assessment. Based on a study in 1978, around 99.8% of fetal movements which last for more than 3 seconds are associated with FHR accelerations [186]. Therefore monitoring of FHR as a Non-Stress Test (NST) has become popular for fetal assessment. Movement of the fetuses with no acidosis and no neurological depression shows intermittent FHR acceleration [186]. FHR deceleration is another parameter which is associated with an abnormal status of the pregnancy, especially when followed by a womb contraction occurring within a given time period [26, 87]. NST aims to reduce the rate of fetal compromise caused by fetal hypoxia or placental insufficiencies.

FHR monitoring is generally performed by Cardiotography (CTG) for which the noninvasive DUS transducer is used during a 20 minute test. Additionally, a strain gauge or a tokodynamometer is also used to monitor the uterine activity. NST is defined as reactive if at least two accelerations of more than 15 bpm from the baseline (which is 110-160 bpm) lasting more than 15 seconds, occur within the 20 minute test. However the absence of accelerations may be due to the fetal sleep and in that case the test is extended to 40 minutes [19]. In practice, if the fetus does not show reactivity after 40 minutes, further assessment is performed by contraction stress test or biophysical profile test. Vibroacoustic stimulation can also be used to interrupt fetal sleep and provoke FHR acceleration which results in a decrease in the test duration and the number of false positive results due to fetal sleep [184]. Another factor involved with false positive results is the gestational age, since 50% of the normal fetuses in 24-28 weeks and 15% of the ones in 28-32 weeks of pregnancy fail to show reactivity in FHR [44, 96].

Overall, nonreactive FHR may be associated with prolonged fetal sleep, immaturity of the fetus, ingestion of sedatives by the mother and cardiac or neurologic anomalies of the fetus. The false negative rate of this test is quite low 0.3%, but the false positive rate is around 50% [46].

DUS signal has been the main tool for CTG. However this signal is susceptible to noise and is nonstationary mainly due to the movement of the fetus and distortion of the ultrasound signals while passing through the amniotic fluid and abdominal layers. These characteristics of the DUS signal complicates finding fiducial points to detect fetal beats and FHR estimation. Therefore advanced signal processing techniques are required to retrieve the fetal cardiac information from this signal. The DUS signal can provide more details about the fetal heart other than only the fetal heart rate. The Doppler shift of the ultrasound beam reflected from moving valves of the fetal heart and collected by the transducer uncovers the opening and closure of the fetal cardiac valves [134, 135, 174]. Using this DUS signal, the timings of cardiac valve motions are estimated and used to evaluate different systolic and diastolic cardiac intervals [79, 85, 174]. This is one of the main focuses of this work and will be discussed in detail in chapters 3 to 7.

2.1.5 Contraction stress test

The Contraction Stress Test (CST) was introduced in 1970s based on an intrapartum observation of the association between recurrent late FHR decelerations and fetal hypoxemia [158]. Since then, it has been used to detect the fetal hypoxemia prior to the acidemia development. The process begins with a nonstress test. If during NST a minimum frequency of 3 uterine contractions in 10 minutes does not occur, CST is performed for which either intravenous admission of dilute oxytocin or maternal nipple stimulation is used to achieve adequate contractions. The result of this test can be categorized as: ”negative”, if no late or significant variable decelerations observed; ”positive”, if late decelerations with at least 50% of contractions detected; ”suspicious”, when intermittent late or variable decelerations are found; ”hyper-stimulation”, in the case of decelerations with contractions of more than 90 seconds’ duration or 2-minute frequency and ”unsatisfactory” if fewer than three contractions per 10 minutes or an un-interpretable tracing is observed [40].

A study by Lagrew shows that nonreactive positive CST is well associated with fetal growth restriction, increased incidence of late decelerations in labor and low 5-minute Apgar scores [91]. Compared to NST, this technique is less dependent on the fetal sleep

and age. The positive predictive value of CTS is as high as 50% and the predicting value of negative cases is significantly high, such that the rate of only 1 still birth per 1000 normal fetuses within 1 week of a negative test is reported [53, 69].
However CST has some disadvantages such as the multiple time requirement of the test to provoke contractions and 10% to 15% rate of equivocal tests. Moreover it can not be used in certain maternal or fetal conditions in which testing might be necessary, for example, in the case of maternal uterine rapture or bleeding; or for the fetuses with the age of less than 37 weeks with the risk of preterm labor [19, 37].

2.1.6 Biophysical profile

Beginning in 1980s, fetal biophysical profile (BPP) method was developed based on real time ultrasound technique to investigate not only AFV but also the fetal breathing movements as well as body and reflex movement. The sonographic parameters are proposed to be considered together with FHR monitoring to assess both short term and long term fetal status and placental function and reserve [156]. Manning proposed a combination of five parameters to be assessed for BPP which are NST, fetal breathing movements, fetal body movements, fetal tone and AFV [114] each scored at 0-2 to provide an overall score of 0-10 for BPP. The idea was to improve specificity of the test by including breathing and tone, since breathing movements decrease during hypoxemia; and to improve sensitivity by considering AFV evaluation [19]. Manning observed correlations between BPP score and the risk of intrauterine asphyxia or death. Based on studying 90000 patients, the false negative rate of BPP was found 0.06% for a weekly interval of normal tests [38, 111, 112]. However the false positive rate was 50% [110].
Some of the disadvantages of this method are the requirement of both FHR and sonography which results in increased cost and time and it may not be used as a fetal surveillance technique for unselected populations [19, 109]. A number of modified versions of BPP have been proposed, such as the elimination of the NST test if sonography shows normal conditions, resulted in no negative predictive value loss based on an experiment on 2500 cases [113]. The combination of NST and AFV may also be investigated as a modified BPP, which provides similar scores to full BPP for fetuses with abnormal NST

Table 2.2: Summary of the major conventional fetal assessment methods and their evidence and indication, adopted from [40].

Test	Level of Evidence	Recommendation level for high risk patients
Contraction stress test	II-2	B
Nonstress test	II-2	C
Vibroacoustic stimulation	II-1	
Amniotic fluid volume	II-2	C
Biophysical profile	II-2	B

Level of evidence: I, at least one adequate randomized controlled trial; II-1, well-designed nonrandomized controlled trial; II-2, well-designed cohort or case-control trial; Strength of recommendation: A, good evidence to support recommendation; B, fair evidence to support recommendation; C, insufficient evidence to support or reject recommendation.

results [130, 136].

2.1.7 Summary of the fetal screening methods

The major conventional methods are summarized in Table 2.2. The level of evidence and strength of recommendations are also indicated for each method based on the criteria recommended by the US Preventive Services Task Force [40].
However these tests are not completely supported by the most rigorous essays required for assessment of screening, diagnostic or therapeutic interventions [40].

2.2 Fetal cardiac assessment

Fetal circulation is one of the main concerns in fetal assessment which has a crucial importance; especially the evaluation of the heart action may give more useful information about the fetus during pregnancy [109]. As discussed earlier, FHR monitoring is commonly used for this purpose.
As discussed in the first chapter, another indication for evaluating fetal heart is congenital heart disease [7], which is the most common among major congenital diseases. Even now that there are improved treatment options available, every fifth child with CHD dies

during the first year of life. The mortality rate correlates closely with the severity of the heart defect and its early clinical manifestations. Therefore early detection of these conditions may reduce perinatal morbidity and mortality [128]. Furthermore, it provides tremendous medical, psychological and economical benefits [61]. The examination for identification of CHD is not only necessary for high risk populations, but screening of low risk cases is also important; because 85% of fetuses with CHD are not detected and classified in the high risk category [87].

Although FHR monitoring has been used as NST or CST to find accelerations, decelerations and baseline variability of fetal heart rate, it is not enough for a thorough assessment of the fetal state. Beat by beat evaluation of fetal heart rate is required for more detailed analysis, such as short-term heart rate variability. There are several methods that can be used for monitoring FHR noninvasively, such as CTG, Ultrasound M-mode analysis, fECG, magnetocardiography (MCG) and Phonocardiography (PCG) [149]. The fECG and MCG methods can provide information about the electrical activity of the fetal heart. The structure of the heart and blood flow through the valves can be visualized and examined by fetal echo-cardiography. This method is a useful mean for diagnosing structural heart defects, but it is a highly specialized and expensive technique, which is not generally used for screening low risk population. Systolic and diastolic cardiac intervals can also be evaluated based on the opening and closure timings of the valves as well as the onset of the QRS complex of fECG. Although valve motions can be visualized by echocardiography, there is a simpler and less expensive method for identification of opening and closing of the valves, using 1-D DUS. These methods are described in detail in the next chapters.

In following section, a short description of the fetal heart physiology is provided, then the cardiac assessment techniques are reviewed.

2.2.1 Fetal heart physiology

Similar to the heart after birth, fetal heart is a muscular organ which provides a continuous blood circulation. However it undergoes significant changes during its development and even with the first breaths or in few hours after birth, which makes it structurally

and functionally different from the newborn's heart. While its critical development between the 3rd and 7th weeks of gestation, it changes from a simple tube to a structure with four chambers. Although it is capable of pumping to circulate the blood in its early form in the 3rd week, the heartbeat can be heard after 20 weeks and the fECG and MCG can be recorded through the maternal abdomen after 16 to 20 weeks of pregnancy [82, 149, 166, 192].

A developed fetal heart consists of 4 chambers, similar to the heart after birth: right atrium (RA), right ventricle (RV), left atrium (LA) and left ventricle (LV). The atria are thin-walled structures mainly responsible for holding the blood, while the ventricles are larger and thick-walled chambers for pumping the blood. As a pump, the heart has valves to ensure the blood flow in the right direction. Atrioventicular valves which swing from the atria into the ventricles, include a three-leafed tricuspid valve on the right, and a two-leafed mitral valve on the left side of the heart. There are also two semilunar valves from the ventricles, namely the Aortic and Pulmonary valves opening to the Aorta and the pulmonary artery, respectively.

The heart has a nerve system which stimulates it to beat repeatedly in the following sequence. Each heartbeat begins in the right atrium stimulated by an action potential signal from the sinoatrial (SA) node. The signal causes the atrial muscle cells to depolarize and contract during the atrial systole phase, corresponding to the P wave of the fECG. Then the signal leaves the atria to enter the ventricles via atriaventicular or AV node, in the inter-atrial septum. It spreads through the bundle branches and the large diameter purkinje fibers along the ventricle walls. As signal spreads through the ventricles, the contractile fibers depolarize and contract very rapidly during ventricular systole. The period of conduction that follows atrial systole and precedes the contraction of the ventricles is depicted on the ECG by the PR segment. The ECGs QRS complex represents the rapid ventricular depolarization. It is followed by the ventricular diastole, when the signal leaves the ventricles and the ventricular wall recovers and repolarizes. Ventricular repolarization corresponds to the T-wave of the ECG and the total time for both depolarization and repolarization of the ventricles is represented by the QT interval. Figure 2.1 illustrates the connection of ECG tracing with the electrical and mechanical events in a

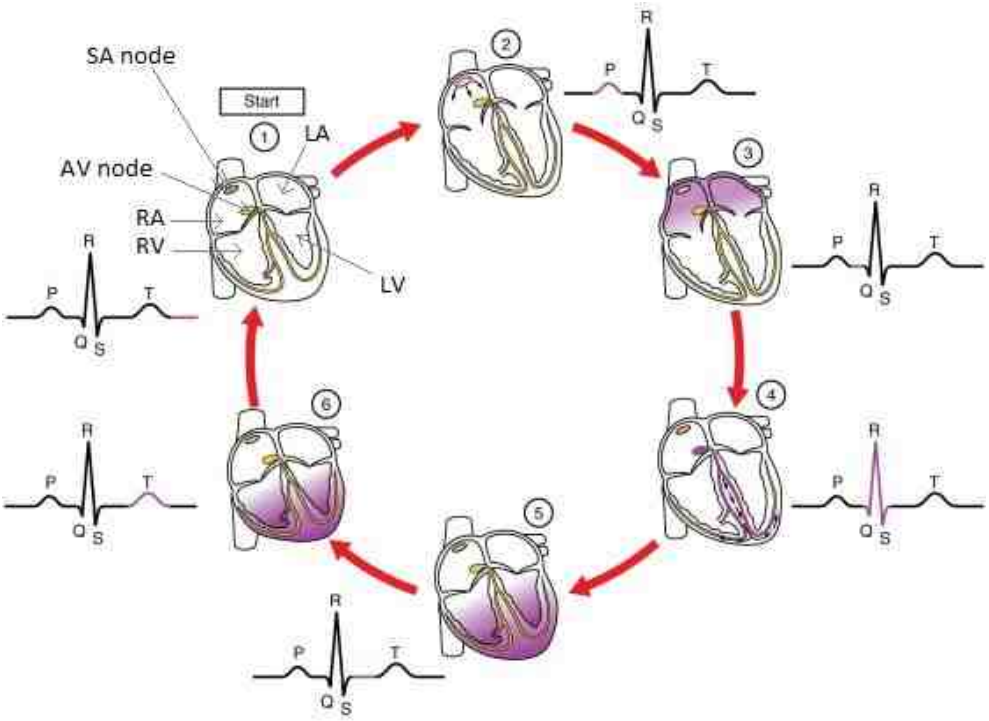

Figure 2.1: The ECG tracing corresponding to the electrical and mechanical events in a cardiac cycle is illustrated. The figure is modified from the e-book "Anatomy and Physiology II", originally published by OpenStax College, and released under the CC-By license: https://creativecommons.org/licenses/by/3.0/ [143].

cardiac cycle [143].

The fetal heart has the same basic structure and function as the newborn heart, except some important differences. Since all of the oxygen that the fetus requires is provided by the placenta, fetal lungs do not need to operate and the majority of fetal blood detours away from the lungs, via two openings: Foramen ovale opens between the right and left atria and Ductus Arteriosus links aorta and pulmonary artery. When the blood enters into the right atrium, some of it flows into the right ventricle, similar to the adult heart; while some blood flows to the left atrium through the Foramen ovale. The latter passes directly to the left ventricle to be pumped out to the body without passing the lungs. Some of that blood in the right ventricle which would normally go to the lungs through the pulmonary artery, bypasses the lungs and enters the aorta via Ductus arteriosus. Ductus arteriosus and the flap of the foramen will remain open until 30 minutes after the newborns first breathing. Their closure is due to an increase in pressure on the

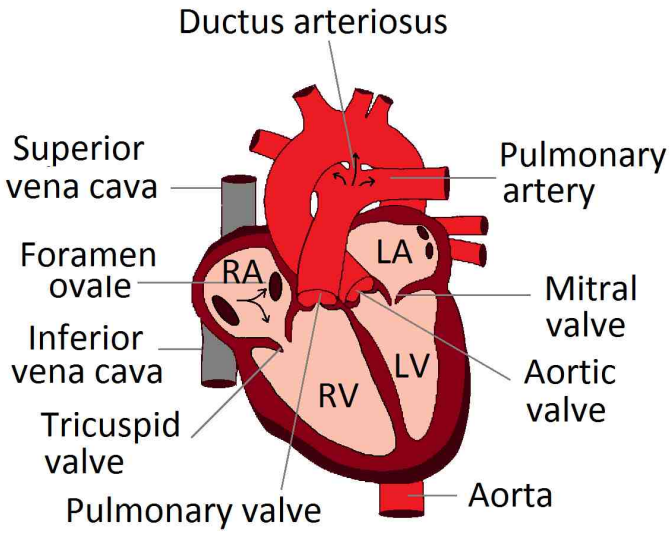

Figure 2.2: The anatomic structure of the fetal heart is illustrated.

left side and a decrease on the right side of the heart. Therefore the blood can flow to the lungs to provide oxygen to the body [50]. Figure 2.2 illustrates the anatomic structure of the fetal heart.

2.2.2 Fetal echocardiography

Fetal echocardiography is the most informative and noninvasive technique for fetal cardiac assessment, based on ultrasound. The four chamber view of the heart is one of the easiest and most useful views to obtain in fetal echocardiography, by which the position and the size of the heart in the chest and its inner parts, the structure and the function of the heart are examined. For example the size and contractility of the ventricles and the appearance of the atrioventricular valves are among the features evaluated from the four-chamber view [5].

As an extended basic examination, views of the outflow tracts can be also evaluated which includes the right and left ventricular outflow tracts of the heart. The latter is also called "five chamber view" and demonstrates the four chambers and the aorta emerging from the left ventricle. The pulmonary artery which opens to the right ventricle is illus-

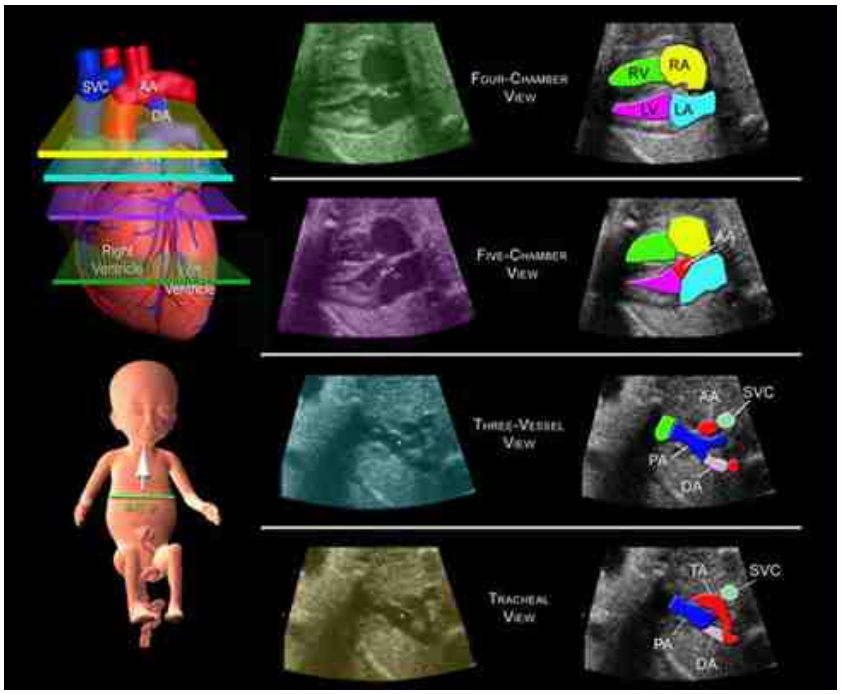

Figure 2.3: Summary of the views, showing the four-chamber view and the outflow tracts of the heart, by first imaging the four-chamber view and then moving towards the fetal neck; to view the five-chamber, 3-vessel, and tracheal views. Adopted with permission from [42]

trated in the right outflow tract view[3]. According to a study of the low risk population for CHD screening with prospective study design, the sensitivity of 60.3% was obtained using the four chamber view examination and the sensitivity of the extended examination was found to be 65.5% [142].

The speed and accuracy of cardiac analysis has been enhanced by the introduction of Doppler color mapping about two decades ago [41]. The presence and direction of the blood flow and the presence of small vessels as well as the areas of turbulence can be found and confirmed by means of color doppler. Figure 2.3 illustrates a summary of four-chamber view, the five-chamber, three-vessel, and tracheal views of the fetal heart [42].

Pulsed wave Doppler is recommended for a complete evaluation of the fetal heart, specially in the case of fetal cardiac malformation or compromise. This technique demonstrates the blood flow velocity through the cardiac valves. Figure 2.4 shows four ex-

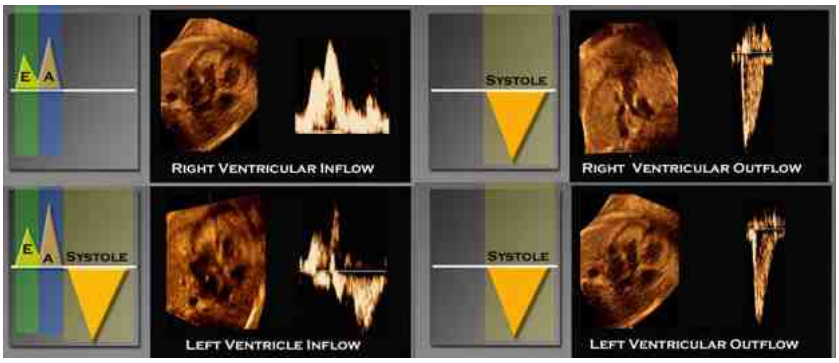

Figure 2.4: Pulsed Doppler waveforms captured from the inflows within ventricles and the aortic and pulmonary outflow tracts. The waveform in early diastole is shown with the green bar. The E wave occurs when the mitral valve opens and the blood flows into the ventricles. The blue bar shows atrial systole and specified as A wave, when the atria contract and the remaining blood is forced into the ventricle. The contraction of the ventricles is shaded with yellow, as the systolic waveform. Adopted with permission from [42].

amples of the pulsed Doppler waveforms recorded from inflows to the left and right ventricles, as well as the pulmonary and aortic outflow tracts [42]. Overall, the following aspects of Doppler evaluation are examined: the direction, pattern and velocity of the flow and measuring volume flow and function. M-mode echocardiography is less used in fetal cardiac evaluation but has the main following applications: measurement of cardiac structures, estimation of left ventricular function and evaluation of atrial and ventricular contraction sequence [5]. Moreover, three dimensional (3D) and four dimensional (4D) fetal echocardiography are other more recently developed means of the fetal heart assessment. They enable a real-time 3D/4D of the examination of the fetal heart, which can provide a reliable reassurance of normality or to accurately diagnose major structural heart defects for the fetuses at risk for cardiac anomalies [15, 28, 70]. Overall, fetal echocardiography is an expensive method and only particular maternal and fetal conditions indicate the need for it. Furthermore, in most cases, primary care physicians or obstetricians cannot appropriately analyze the heart views and only qualified specialists can perform this highly specialized examination [24].

2.2.3 Fetal electrocardiography

Invasive fetal electrocardiography

Though a series of studies in 1960s, Hon et al. proposed capturing the details of fECG directly recorded through an electrode attached to the fetal scalp and improving its signal to noise ratio [65–67]. The process was invasive and required the rupture of membrane, by inserting the electrodes through the cervix and attaching to the presenting part of the fetus, e.g. via a scalp clip. The problem of noise reduction was partly solved using an 8-50 Hz filter, which however potentially obscured the P and T waves. Hon et al. also developed an online averaging technique performed on a Mnemotron CAT digital computer. The signal-to-noise ratio was improved by a factor of 10 to 20, enabling consistently recording of fECG with P and T waves and minor baseline changes during labor [67, 182].

In an early study in 1962, Larks et al., suggested the importance of the morphological changes of the ST segment, such as an association between depression or elevation of ST segment with apparent intrauterine and neonatal difficulties [94, 95]. Later, ST waveform analysis of fECG for intrapartum surveillance (STAN) became a method for fetal surveillance. STAN combines the standard FHR tracing by CTG with an automated analysis of fECG through ST-waveform analysis (STAN, Neoventa Medical, Moelndal, Sweden) [6, 139]. It was shown that the rates of umbilical artery metabolic acidosis and operative delivery for fetal distress were significantly lower when a combination of FHR monitoring and ST-waveform analysis was used, than the FHR monitoring alone [6]. A significant reduction in term neonates suffering from moderate to severe neonatal encephalopathy was observed using this method [140]. Improvements in fetal outcome by increasing usage of STAN was also reported by Noren et al. [139]. The general indications for STAN include completion of 36 weeks of gestation and situations where internal monitoring was the preferred fetal surveillance method. High-risk pregnancies, suspicious or abnormal CTG antenatally or in early labor, labor induction, oxytocin augmented labor, and presence of meconium stained amniotic fluid are other examples [139]. This invasive technique is more suitable during labor and not feasible for the antepartum period, and

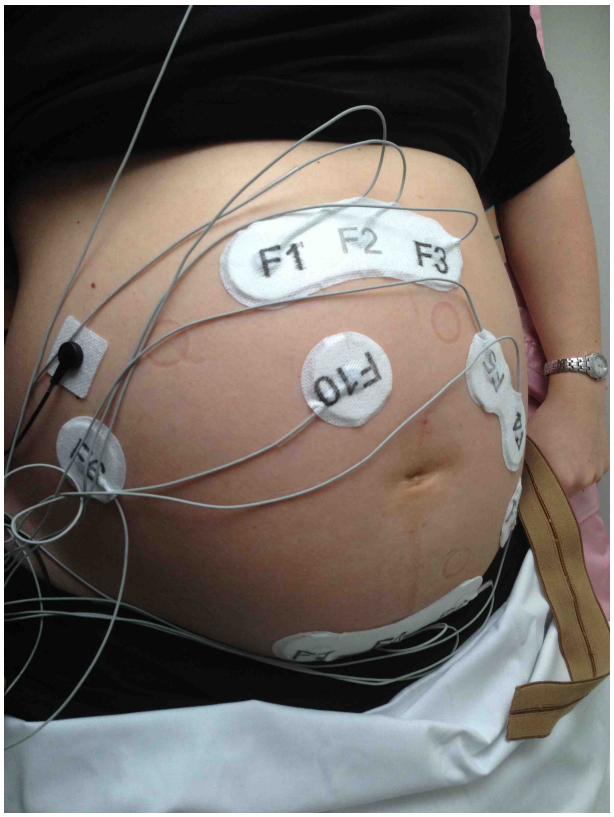

Figure 2.5: An example of the configuration of electrodes for noninvasive fECG.

is only for monitoring singletons. Furthermore, only one differential electrode is possible, therefore it does not provide a three dimensional electrical field emanating from the fetal heart [30].

Noninvasive fetal electrocardiography

Noninvasive fECG through the maternal abdomen has been a challenging area of research in engineering and clinical technology over the last decade [82,99,166]. For noninvasive fECG, data are collected using a set of electrodes placed on the maternal abdomen, while as discussed above, invasive fECG requires uterine rupture for intrauterine electrodes with direct contact to fetal skin [92,146]. Figure 2.5 shows a sample configuration of the electrodes in practice. Noninvasive fECG can be used during pregnancy as early as 16th week of gestation. The obtained signal by this method contains a weak fECG with a low signal to noise ratio, because of the small size of the fetal heart and several low

conductive layers through which the signal passes to reach the maternal abdomen surface. Furthermore, fECG is not the only recorded signal, but is mixed with the maternal ECG (MECG) overlapping in time and frequency domain. It is also contaminated by maternal respiratory, motion artifacts and uterine contractions. Therefore signal processing is highly necessary to recover the fECG from the abdominal mixture. The movement of fetus itself also has an influence depending on the orientation of the fetus. Moreover, limitation of clinical knowledge about the fetal cardiac function, compared to adult's have limited the advancement in this field [30, 166]. Nevertheless, noninvasive fECG, even in its current stage of development, provides a comparable or higher accuracy of FHR than an ultrasound method, while allowing additional interpretation of the electrical activity of the fetal heart [30, 74].

Although the main purpose of analyzing fECG is to estimate R peaks and find heart rate on a beat to beat basis, a more accurate estimation of fECG waveform with more details of P-wave and T-waves as well as accurate QRS complex will provide additional morphological information based on PR, ST, QT intervals. Different factors have influence on the fECG waveform, including hypoxia, ion channel activity of myocardial cells, autonomic nervous activity and congenital heart defects. For example, the ST segment waveform of fECG is changed in case of hypoxia [57, 82]. The QT interval can be used to detect long QT (LQT) syndrome, which is a high risk for developing life-threatening arrhythmias and sudden cardiac death in children and adults [173]. PR and QT intervals also change with gestational age as investigated by Kimura et al., [82] and shown in figure 2.6 [82,169]. Therefore these intervals can be used to assess the development of the fetus during pregnancy. However beat by beat identification of T waves from noninvasive fECG is more difficult and challenging than the R wave, because of noise and interferences which contaminate the fECG [30, 166]. In addition to the beat-to-beat FHR and morphological information, fECG can also provide contraction monitoring [63] or fetal movement and position [30, 165].

Availability of public gold standard databases is also crucial for improving the extraction of fECG. Early public data bases include: (i) the Daisy database constituted of 8 channels (4 abdominal and 3 thoracic) and the abdominal ECG (AECG) lasting for 10 sec sampled

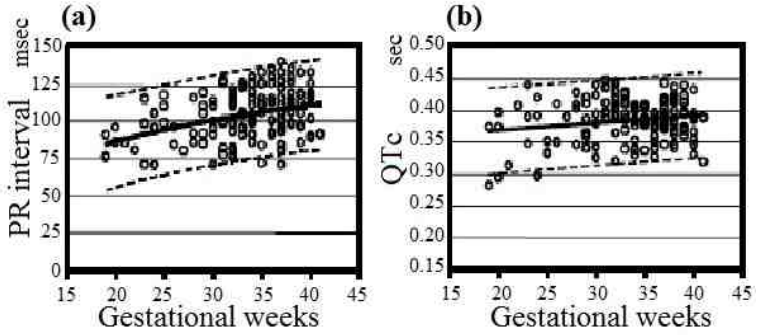

Figure 2.6: The standard values of PR intervals (a) and QTc (b) throughout gestation weeks [82, 169]

at 250 Hz. (ii) The Non-Invasive Fetal Electrocardiogram Database (NIFECGDB), available on PhysioNet [55] sampled at fs = 1 kHz. 55 multichannel abdominal ECG recordings taken from a single subject (21 to 40 weeks of gestation), fs = 1 kHz, without reference annotations. (iii) Abdominal and Direct Fetal Electrocardiogram Database (ADFECGDB), available on PhysioNet [55] sampled at fs = 250 Hz with 5 min of recordings (4 abdominal channels) from 5 women in labor (38 to 41 weeks of gestation), fs = 1 kHz, scalp ECG available for reference. All these databases are low dimensional (number of recordings, number of abdominal channels available) and few data have any reference annotations, which are fetal QRS complex location from a single annotator [30, 166]. The PhysioNet/Computing in Cardiology Challenge in 2013 provided a public set of noninvasive fECG data to facilitate the evaluation of signal processing techniques for fECG extraction. The database contained 447 records from the following resources: ADFECGDB [126], Simulated fECGs [13], NIFECGDB [55], noninvasive fECG and Scalp fECG database [30]. It was aimed at improving the estimation of not only the QRS complex, but also the QT interval. Reference QRS annotations and QT intervals were reviewed as a gold standard, using simultaneous direct fECG wherever available [30].

Extraction of fECG typically involves preprocessing of the abdominal ECG, estimation and then removal of the MECG, estimation of fECG, identification of RR intervals and postprocessing. The preprocessing is the first step, which includes removal of noise and artifacts, power-line noise and baseline wandering, using filtering and averaging approaches. Various approaches has been attempted for separation of fECG by cancellation

of MECG. As reviewed in [30, 166], major achievement in recovering the fECG has been through the techniques described as follows. Adaptive filtering is one of the techniques used to cancel MECG or other artifacts or to extract fECG by training an adaptive or matched filter [146,161,202]. Partition-based weighted sum filters [175], least square error fittings [115], Kalman filtering methods [8,60,167] and template subtraction [8,25,115,187] are other alternatives. The complication of some of these methods is that they require a reference which may be MECG or a waveform similar to the interfering signal, in order to exclude it from the mixture. Linear decomposition techniques are based on single or multichannel decomposition of the collected data which are assumed to be linear and stationary mixtures of the signals and noises. The applied methods may use time, frequency or scaling properties of the signals, such as Wavelet Analysis methods [78, 101], spatial filtering, such as singular value decomposition (SVD) methods [22, 36, 76], using the independency of the mixing components in Blind Source Separation (BSS) techniques [10, 39, 208] or a combination of these approaches [72, 195, 206]. For example a number of papers used Principal Component Analysis (PCA) [76, 102], Independent Component Analysis (ICA) [207], or Periodic Component Analysis [164]. Nonlinear decomposition techniques assume that fECG is not necessarily linearly mixed with interferences and noise, therefore some methods use nonlinear transform or nonlinear projection to recover the fECG [159, 172]. The fusion of different techniques, such as a subset of the aforementioned methods was also proposed for an improved estimation of fECG [12, 14].
Considering the large noise contamination and low signal to noise ratio, sole use of BSS may not be promising and it may not be stable for this application, as it tends to extract noise rather than the tiny fECG signal [82]. A more stable method is Blind Source Separation with Reference (BSSR) which improved BSS methods by adding a learning process with reference signals. The references might be periodic signals mimicking the fECG or a reference using one dimensional (1-D) DUS [169]. This method was used for fECG extraction in our research, benefitting from the availability of the simultaneous 1-D DUS signal as a reference. The schematic illustration of this method is shown in figure 2.7, and it is discussed in detail in chapter 3.

Validity of the BSSR method was also tested by comparing with invasively recorded

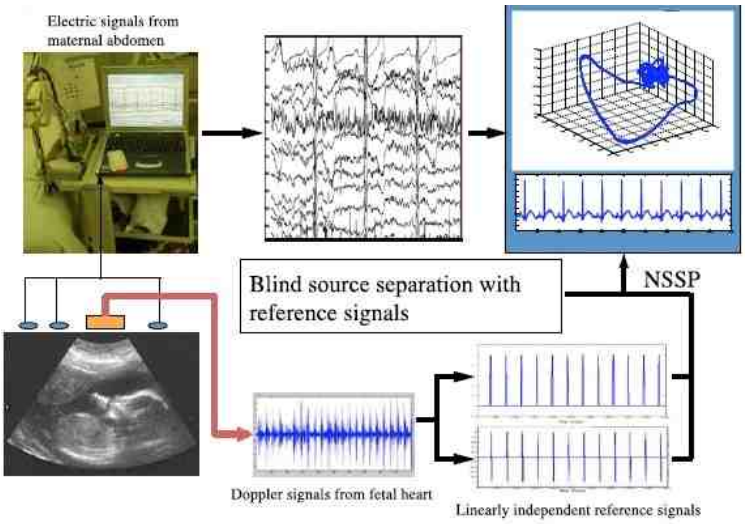

Figure 2.7: The schematic diagram of the BSSR fetal ECG extraction system [82, 169]

fECG in a previous study [82]. Beat to beat fetal heart rate variability was found to be precisely consistent and coincident for invasively and noninvasively recorded fECG, as shown in figure 2.8 (correlation coefficient: 0.998 and less than 0.51 bpm bias according to Bland-Altman test) [82]. Heart rate variability measures calculated from fECG and Doppler CTG were also compared based on 10 subjects between 24-38 gestation weeks by Kimura et al., [82]. An example of results for a 24-week subject is illustrated in figure 2.9 [82]. The correlation coefficient and Bland Altman plots were used to evaluate the comparisons. It was found that compared to Doppler Ultrasound method, FHR from fECG provides more details on short term variability (STV) of heart rate [82]. STV is shown to be associated with fetal autonomic activity [81] and can be used as an effective tool for fetal assessment.

Using the BSSR method, reliable fECG traces can be extracted and were shown to be useful for detecting the fetal heart arrhythmia including Premature Atrial Contractions (PAC), Premature Ventricular Contractions (PVC) and Sick Sinus Syndrome (SSS) [82]. If these kind of Arrhythmia is diagnosed during pregnancy, it can be a marker of congenital heart defects. There are also transient arrhythmia, usually with functional causes by physiological phenomena such as hyperactivation of ion channels in the fetal myocardial

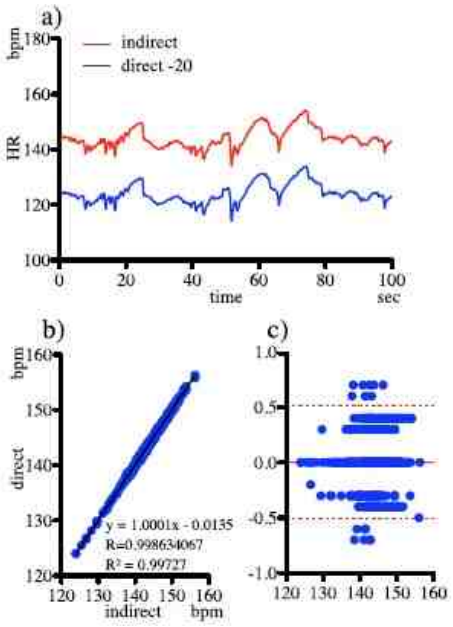

Figure 2.8: Accuracy of noninvasive fECG, a) The red graph shows an instantaneous heart rate tracing pattern of a deceleration calculated from noninvasive fECG. The blue graph shows an instantaneous heart rate tracing of the deceleration calculated from the scalp electrode fECG. Both heart rates are almost coincident. b) A linear correlation between the two heart rates (correlation coefficient: 0.9986). c) The Bland-Altman plots showing a small bias of 0.51 bpm. The minimum value for the limits of agreement was -0.51 bpm and the maximum was +0.51 bpm whereas 95% intervals of the points lie within $\pm$1bpm [82].

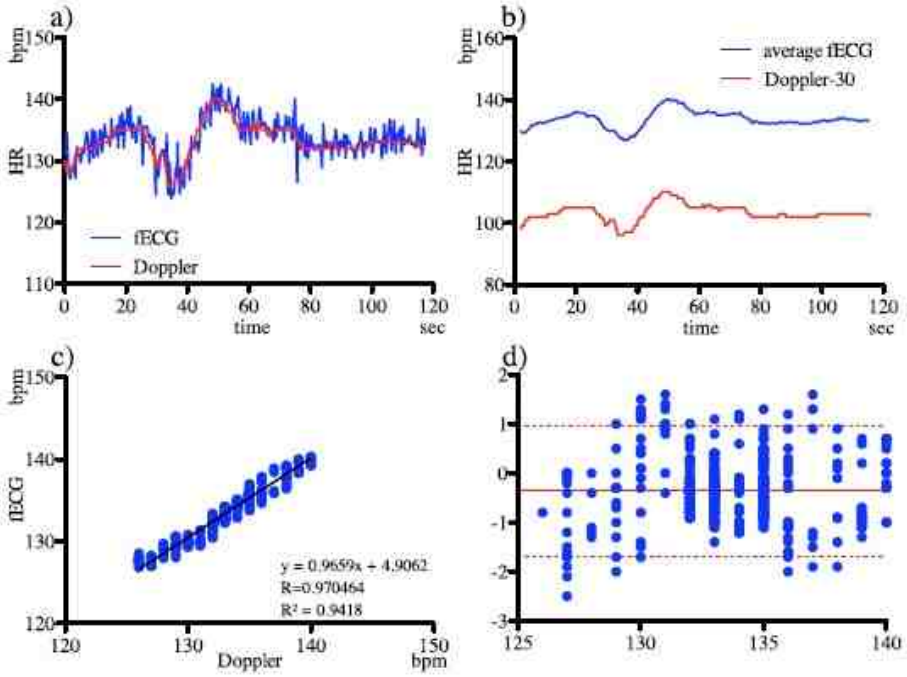

Figure 2.9: Comparison of Doppler CTG with noninvasive fECG extracted by BSSR. a) One example of comparison between fetal heart rate from fECG (blue line) and fetal heart rate from traditional Doppler CTG (red line) in a singleton fetus at 24 weeks of gestation. b) The blue line shows the moving average of fECG over each of the 15 time points (3.75sec) (average fECG). The red line represents the Doppler -30bpm line. c) A linear relationship between the two signals (the correlation coefficient: 0.970). d) Bland-Altman plot showing a significantly small bias of 1.3bpm. The minimum value for the limits of agreement was -1.6bpm and the maximum was +1.0bpm, whereas 95% intervals of the points lie within $\pm$5bpm [82].

cell. Furthermore ectopic beats, which might be recognized as an important pathologic association, can be detected using fECG.

2.2.4 Fetal magnetocardiography

Fetal Magnetocardiography (MCG) is the recording of a very weak magnetic field (10^{-12} tesla) generated by the flowing currents in the fetal heart. Superconductive Quantum Interface Device (SQUID) is a very sensitive sensor which is used to record fetal MCG. Liquid helium has to be used to cool SQUID and overall the instruments of the fetal MCG are expensive, large size and complex [149, 150]. Examples of the signals recorded by fECG and MCG were compared in [149] and the averaged waveforms are illustrated in figure 2.10. The fECG is the best of twenty channels while MCG is compromised by the noise due to simultaneous recording of fECG [149]. This fECG trace is of the best quality recordings which is not guarantied for any recording at any time. However, MCG provides good quality waveforms as well as a map on the maternal abdomen by means of a trigger, therefore fECG can be averaged over that. Thus the fetal MCG can be used as a complement of fECG. The detailed waveforms obtained by fetal MCG can be used for diagnosing the conduction disorders of the fetal heart and arrhythmias. During fetal MCG the patient is advised to have minimal movements during recording and the duration of the test is usually short, but fECG can be measured at any time or even at home during pregnancy [149].

2.2.5 Phonocardiography

Fetal Phonocardiography (fPCG) is performed by placing a special microphone on the maternal abdomen to detect fetal heart sounds. Different from adult's, fetal heart sound has low intensity and narrow frequency band. It is weakened while traveling to the maternal abdomen surface. The ambient noise is also one of the disturbances for this technique and one of the causes for low SNR. However more prominent disturbances are

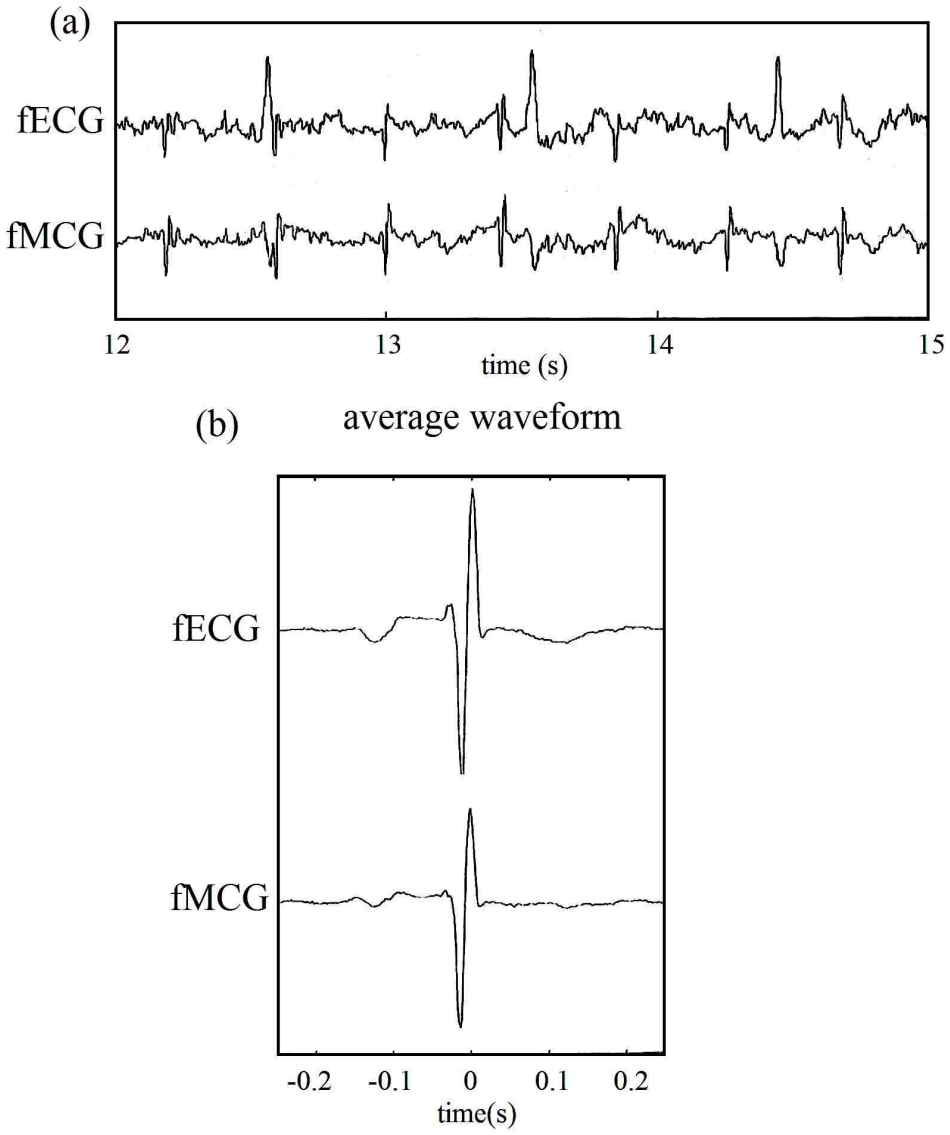

Figure 2.10: The traces of fECG and MCG (a) which are simultaneously recorded, as well as the average waveform for one cardiac cycle of fECG and fMCG (b). Modified from the figure in Peters et al., 2001 [149]

caused by the fetal movement and breathing as well as maternal heart sound, internal movements and breathing. Fetal PCG is generally used after 30th week of pregnancy, although some useful sounds may be recorded in 28th week as well [87]. In 1986, fPCG was investigated by Colley et al., and compared with a simultaneous ultrasound record of fetal activity. They found the pattern of fPCG correlated with 86% of the total fetal breathing detected with ultrasound and a further distinctive pattern was found to be associated with 90% of fetal movements [31].

The fPCG signal mainly consists of two sounds; S1 which is produced by the closure of the atrioventricular (Mitral and tricuspid) valves and S2 that originates from the closure of semilunar (Aortic and pulmonary) valves. The systolic time interval is defined as the interval from S1 to S2 and the diastolic interval is the duration from S2 to the next S1. The S1 sound is of a lower frequency band (peaking around 20 Hz) than S2 signal (peaking around 32 Hz) and the maternal heart sound is mostly lower than 25Hz. The features obtained by this method include the fetal heart rate (long term measurement) from which heart rate variability parameters can be obtained, valve sound, systolic and diastolic time intervals, heart murmur due to the turbulent blood flow, which can be used to diagnose CHD and assess the fetal breathing [87].

2.2.6 Summary of the cardiac assessment methods

Table 2.3 shows an overview of the advantages and disadvantages of different heart monitoring techniques [149].

Table 2.3: overview of different methods for FHR monitoring, modified from the table in Peters et al., 2001 [149].

Methods	Apparatus	Gestational age	Accuracy	Remarks
Doppler ultrasound	inexpensive; easy to handle	$\geq$20 weeks*	95+% reliable , FHR short-term variability may not be observable, valve movements (through further processing)	can also be used during labor and recorded from 16th week.
Fetal Echocardiography	expensive, specialized, skilled personnel required	$\geq$18 weeks	90-95% reliable FHR, anatomy, physiology of heart depends on quality images; accuracy intervals limited	cardiac scanning is possible from 11th week by transvaginal probe
Noninvasive fECG	inexpensive; easy to handle	$\geq$20 weeks* possibly with a dip around 32 weeks	60% reliable in last month, for FHR beat to beat accuracy, limited fECG morphology	can be used during labor, good for long term ambulatory use
FMCG	expensive, skilled personnel required	$\geq$20 weeks	fully reliable, waveforms observable in an averaged signal; accuracy intervals about 5 ms	measured in 13th week.
FPCG	inexpensive; easy to handle	$\geq$30 weeks	FHR, systolic and diastolic intervals and heart murmurs can be detected	good for long term use

* In our study noninvasive fECG was recorded and successfully separated for the fetuses in as early as 16 weeks, together with simultaneous 1-D DUS.

Part II

Estimation of Fetal Cardiac Valve Intervals

Introduction to Part II

SIMULTANEOUS recording of the electrical and mechanical activities of the fetal heart provides the measurement of fetal cardiac intervals which are sensitive markers for fetal development and well-being. This section provides a review of the previous methods and the proposed automated methods for estimation of fetal cardiac valve intervals.

Chapter 3

Estimation of fetal cardiac valve intervals by 1-D Doppler ultrasound and fetal electrocardiography

Fetal cardiac intervals can be estimated using simultaneous recording of Doppler Ultrasound and fECG signals. This chapter provides a background on the conventional and the new automated methods developed for this purpose.
This chapter is a slightly modified version of the published articles [119, 122, 123]:

- *F. Marzbanrad, Y. Kimura, K. Funamoto, et al. Automated estimation of fetal cardiac timing events from Doppler ultrasound signal using hybrid models, IEEE Journal of Biomedical and Health Informatics, vol.18, no.4, pp.1169-1177, 2014. doi: 10.1109/JBHI.2013.2286155.*
- *F. Marzbanrad, A. H. Khandoker, K. Funamoto, et al. Automated Identification of fetal cardiac valve timings, In Engineering in Medicine and Biology Society (EMBC), 2013 35th Annual International Conference of the IEEE, pp. 3893-3896. IEEE, 2013.*
- *F. Marzbanrad, Y. Kimura, K. Funamoto, et al. Development of fetal cardiac intervals throughout 16 to 41 weeks of gestation, In Computing in Cardiology Conference (CinC), 2013, pp. 1155-1158. IEEE, 2013.*

3.1 Introduction and literature review

3.1.1 Extended application of 1-D Doppler ultrasound

FETAL heart rate monitoring is commonly performed by CTG for which noninvasive 1-D DUS signal is used. This signal can provide more details about the fetal heart, other than only the heart rate. The Doppler shift of the ultrasound beam which is

reflected from the moving valves of the fetal heart and collected by the transducer, uncovers the opening and closure of the fetal cardiac valves [134, 135, 174]. Although valve motion timings can be also detected by fetal echocardiography, as discussed in chapter 2, this method is expensive and highly specialized, requires skilled specialists to operate and is only performed for particular fetal and maternal conditions. Using 1-D DUS signal, the timings of cardiac valve movements are estimated with less expertise and cost, which efficiently provide different systolic and diastolic cardiac intervals [79, 85, 174]. However, a reference such as fECG is also required for this purpose. The main reason is that there is no single well defined fiducial point in the waveform to identify each heart cycle [149]. Furthermore, fECG is required to estimate the electromechanical coupling indices, which are fundamental and clinically significant parts of the heart physiology [100, 199].

3.1.2 Fetal cardiac intervals

The opening and closure timings of the cardiac valves are the main bases for estimating the mechanical and electromechanical indices of the fetal heart [134]. These intervals are illustrated in figure 3.1. Considering the synchronous operation of both sides of the fetal heart, the semilunar and atrioventricular valve motions are expressed as the aorta and mitral valve movements respectively throughout the thesis. Among the cardiac intervals, Systolic Time Intervals (STI) have received considerable attention as indicators of myocardial function. The STI interval is the time from the onset of the QRS complex of the fECG to the closing time of Aorta (Ac) and offers assessment of ventricular function. It consists of the Pre-Ejection Period (PEP) and the Ventricular Ejection Time (VET). PEP starts with the onset of ventricular depolarization (Q-wave of fECG) and ends at the onset of ejection which is the aorta opening (Ao) time. VET is the systole phase which corresponds to the ventricular ejection of blood into the arterial system, characterized by the time between opening and closing of Aorta. PEP is further divided into Electromechanical Delay Time (EDT) and Isovolumic Contraction Time(ICT). EDT is the period from the onset of ventricular depolarization (Q-wave of fECG) to the moment that mitral valve closes (Mc). It is followed by ICT which is the time between closing of mitral and

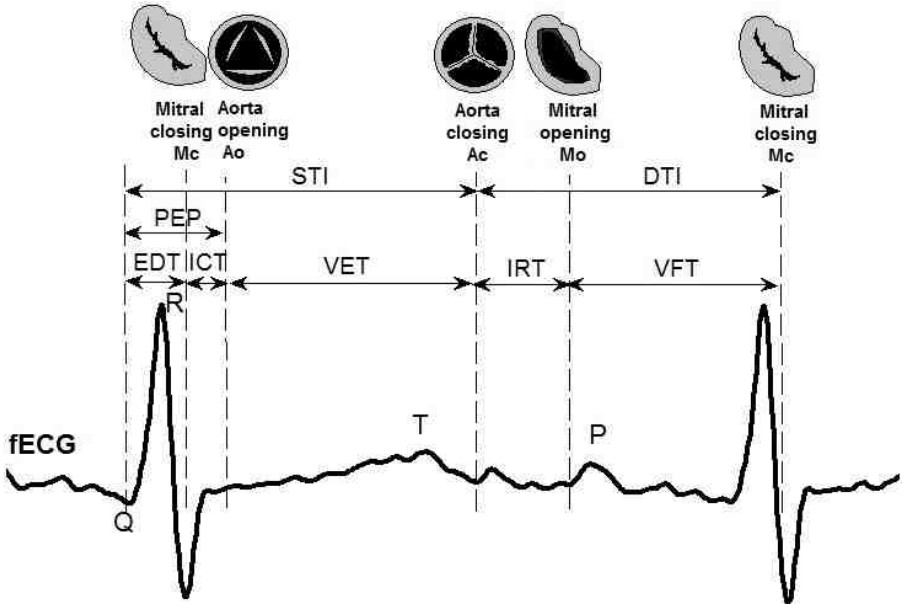

Figure 3.1: An illustrative example of fetal cardiac intervals: Systolic Time Interval (STI), Electromechanical Delay Time (EDT), Isovolumic Contraction Time(ICT), Pre-Ejection Period (PEP), Ventricular Ejection Time (VET), Diastolic Time Interval (DTI), Isovolumic Relaxation Time (IRT), Ventricular Filling Time (VFT).

opening of Aorta. The diastolic time follows the STI interval and is also important for assessing the myocardial blood flow and ventricular filling. During the diastolic period, Isovolumic Relaxation Time (IRT) occurs from Ac to mitral opening (Mo) time and is followed by Ventricular Filling Time (VFT) from opening to closing time of mitral [20].

From a clinical standpoint, PEP, ICT and VET are the most useful cardiac intervals for fetal assessment [134]. For example, PEP is reported as a sensitive indicator of the function state of the fetal myocardium and the loading conditions of the heart, which can indicate the fetal cardiac performance [47,127]. Furthermore, the development of hypoxemia and acidosis is early manifested by prolongation of PEP [134,144]. Another study suggested to use ICT as a reliable index to be substituted for fetal cardiac contractility [204]. Other cardiac intervals are also valuable in clinical practice [134,205]. Additional uses of these intervals for identification of abnormalities and assessment of the fetal development throughout gestation are discussed in the following chapters.

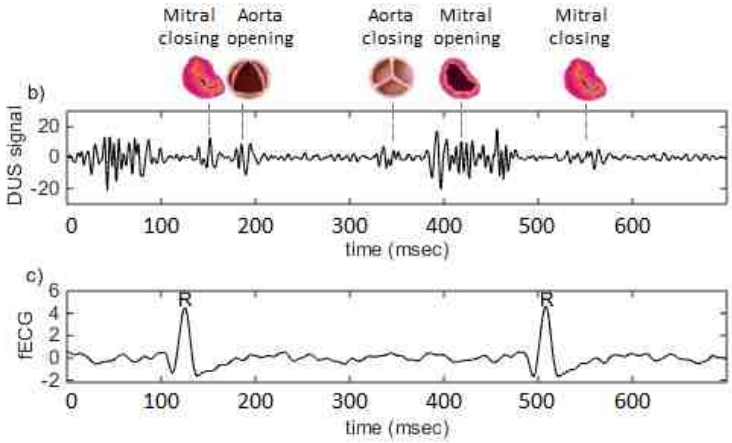

Figure 3.2: An illustrative example of mitral and aorta opening and closing identification from the raw 1-D DUS signal (b), and fECG as a reference (c).

.

3.1.3 A review of the previous methods

Previous studies found that the high-frequency component (e.g. $>$ 100 Hz, for ultrasound frequency of 1.15 MHz) of the DUS signal is linked to the valve movements, as the valves move faster than the heart walls. The lower frequency content is associated with the cardiac wall motion and the movement of other organs, which are relatively slower than the valve motion [134, 135, 174]. Therefore in order to identify the valve motion using the DUS signal, the component corresponding to valve motion should be extracted from the components related to the movement of the cardiac wall or other organs.

An example of the DUS signal with the corresponding valve motion events is shown in figure 3.2. The DUS signal shown in figure 3.2 (b) is one of the best quality signals. As the figure shows, the valve motion events can not be easily identified from the raw DUS signal, therefore the DUS signal needs to be processed. The signal is also contaminated by noise and interferences from the movement of maternal and fetal organs; the content of the DUS signal is highly variable and it depends on the respective fetus and transducer orientation [174].

Early studies in the 1980s proposed noninvasive methods which mainly aimed to analyze the systolic time interval, using noninvasive abdominal ECG and the DUS signal [86, 135, 144, 168]. All of these methods were based on band pass filtering approaches to

extract the high frequency component of the DUS, from which the valve movements were identified manually by experts. There were three main issues with these methods needed to be resolved. Firstly, due to the noisiness and variability of the DUS data on a beat-to-beat basis, as well as the wide changes in the signal contents and spectral characteristics over time, band pass filters could not effectively provide the component originated by the valve motion. Secondly, as also discussed in chapter 2, extraction of the fECG from the abdominal mixture requires is still a challenge [82, 99, 166]. Finally, manual identification of beat-to-beat opening and closing of valves is time consuming, requires special expertise and is subject to inter and intra observer and visual errors. Improvement in the aforementioned aspects is essential to make this technique more reliable and applicable with less expertise.

Several studies suggested applying improved signal processing techniques and more powerful processors to extract the information content of the DUS signal [79,90,119,174]. Shakespear et al., used Short Time Fourier Transform (STFT) analysis of the DUS signal and showed that the component with a higher frequency band is generally linked to valve movement, while the low frequency component is associated with the cardiac wall motion [174]. However the frequency range of the valve motion related component was not constant over time. They showed that using averaged spectrogram data the Doppler frequency shifts associated with cardiac motion events can be visualized (fECG was used as reference), as illustrated in figure 3.3. The variation in the content of the signal across the examples are also evident in these figures. It is not always possible to capture and visualize all valve and wall motion events using this technique. As shown in Figure 3.3 (b), the valve motions may not be detectable from the spectrogram [174]. Considering the nonstationarity and transient nature of the DUS signal as well as the wide changes in the signal content and spectral characteristics over time, it was proposed by Khandoker et al., to apply the multi-resolution wavelet analysis to the DUS signal [79]. Using the wavelet analysis, valve movements were visualized as peaks in the detailed signal (at level 2 wavelet decomposition). Figure 3.4 shows two examples of the DUS signals decomposed by this method and the detected valve motions. It is proposed in this work to use Empirical Mode Decomposition (EMD) as an alternative which is a data-driven

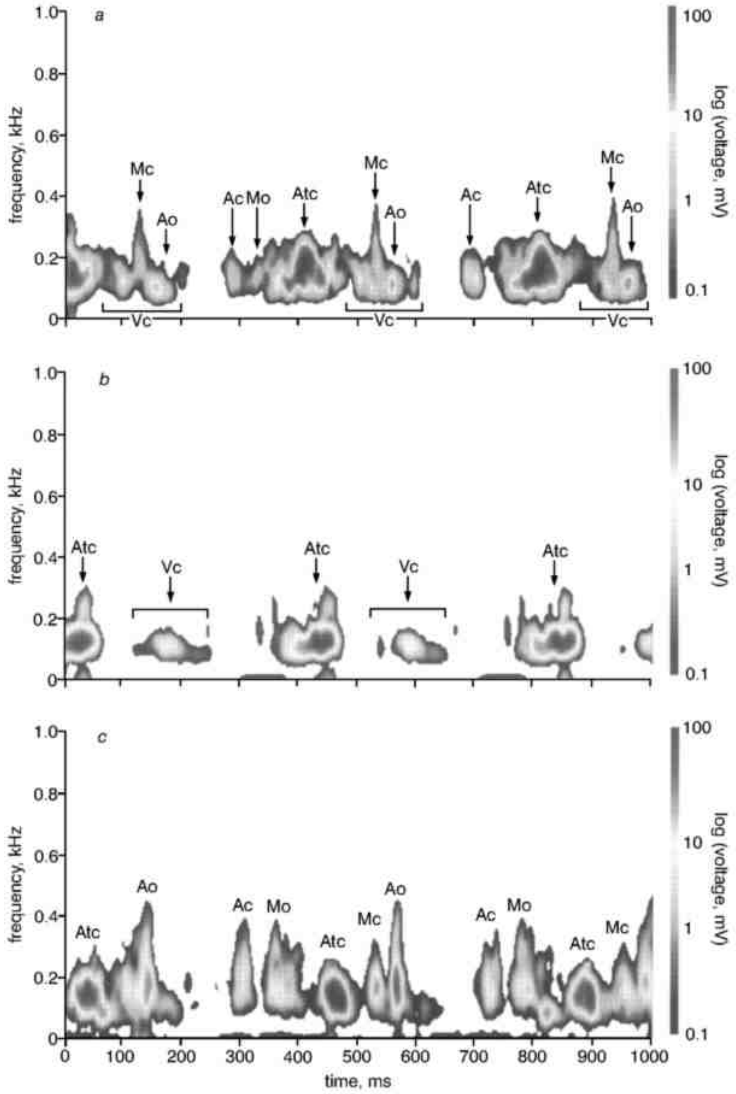

Figure 3.3: Three examples of DUS spectrograms annotated to show how the cardiac activity including atrial wall contraction (Atc), ventricular wall contraction (Vc), aorta opening and closing (Ao and Ac), mitral opening and closing (Mo and Mc) are manifested [174].

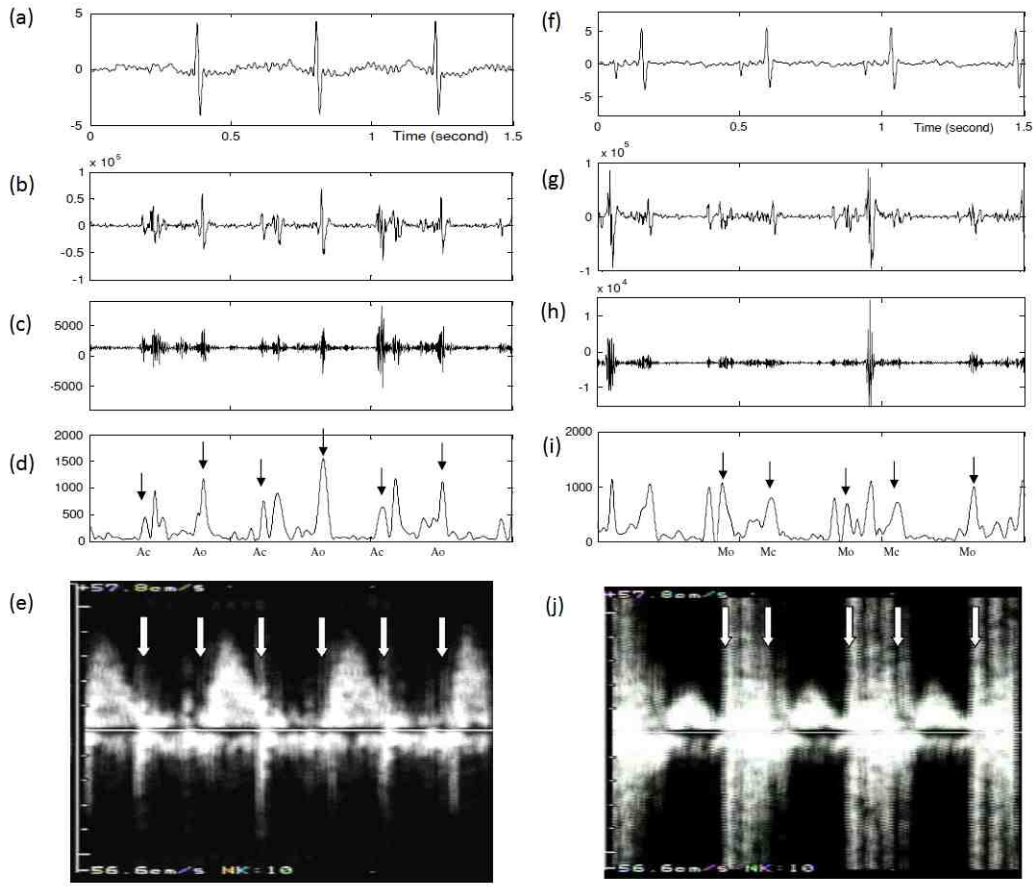

Figure 3.4: Figures (a) and (f) show two examples of fECG extracted from abdominal ECG signals using BSSR [169]. Figures (b) and (g) Show the raw DUS signals recorded simultaneous with fECG. The detailed signals after wavelet decomposition of (b) and (g) at level 2 are shown in figures (c) and (h), respectively. The cubic splines envelope of maxima of the detailed signal is then taken as illustrated in figures (d) and (i). In order to verify the detected valve motions, Pulsed wave Doppler signals of fetal aortic and mitral valve movements are shown in figures (e) and (j) and annotated to illustrate the connection of the signals with the valve motions [79].

algorithm used for decomposing nonlinear and nonstationary time series. As discussed in the next section, this algorithm can effectively separate the component linked to valve movements [119,123].

Since fECG is used as a reference, it is necessary to have a reliable and precise detection of the R waves from the fECG. A blind source separation with reference method was proposed by Sato et al., to separate the fECG used in this current research [169].

Another challenge is the need for automated identification of valve movement. Different from the previous manually techniques for detection of the valve motion, a number of methods are proposed for automated detection of the valve events, as described in the current and following chapters.

3.2 Methods

3.2.1 Data

Simultaneous recordings of the abdominal ECG and Doppler ultrasound signals from 45 pregnant women at the gestational age of 16 to 41 weeks with normal single pregnancies were collected at Tohoku University Hospital in Japan. A total of 45 recordings (each of 1 minute length) were sampled at 1 kHz with 16-bit resolution. The reason we used 1-minute recordings was that the standard fetal ECG measurement protocol was set up to that duration. Also ethics committee allowed only one minute ECG to be recorded to minimize the inconvenience for the participating mothers. All 45 subjects were divided into three age groups for analysis: 16-29 weeks, 30-35 weeks and 36-41 weeks, including 15, 12 and 18 fetuses, respectively. The study protocol was approved by Tohoku University Institutional Review Board and written informed consent was obtained from all subjects. The continuous DUS data were obtained using Ultrasonic Transducer 5700 (fetal monitor 116, Corometrics Medical Systems Inc.) with 1.15 MHz signals. To compare the actual appearance of the aortic valve's opening and closing pattern with valve timing events appeared in DUS signals, pulsed-wave Doppler signals were obtained from convex 3.5 Hz of HITACHI ultrasound scanner (Ultrasonic diagnostic instrument Model

EUB-525; HITACHI health medical corporation). The detailed procedure for experimental set up and transabdominal ECG data collection was described in a previous study by Sato et al., [169].

3.2.2 fECG extraction

Data from 12 channels were recorded bipolarly from the electrodes placed on the maternal abdomen, sampled every 1 ms (1 kHz sampling) with 16-bit resolution and bandpass filtered by 1 - 100 Hz finite impulse response filter. Twelve electrodes were used for abdominal ECG recording, ten of which were arranged on the maternal abdomen, one reference electrode on the back and one electrode was set at the right thoracic position. To separate fECG from the composite abdominal signal, a combination of maternal ECG cancelation and blind source separation with the reference signal (BSSR) was used [169]. In brief, electrical activities of the heart can be modeled as a vector in the direction of excitation called the heart vector [183]. The recorded signal in each electrode was modeled as a projection of the heart vector on the axis spanned by the electrode and the reference. The maternal ECG component was excluded by subtracting the linear combination of mutually orthogonal projections of the heart vector. After that, fECG was extracted from the complex mixture based on its correlation with DUS signal as a reference, using BSSR which is a kind of neural network method [169].
The R-peaks of fECG were then automatically detected by applying a lower threshold (e.g. 5 times the mean of fECG over 10 second intervals) and peak-detection based on zero crossing of the decreasing first derivative of the signal.

3.2.3 Decomposition of the DUS signal by Empirical Mode Decomposition

One of the main methods used in this work is EMD which was first introduced by Huang et al. [68]. It is a single channel method for decomposing a complicated signal into a set of different oscillatory modes. These components are called Intrinsic-Mode functions (IMF) and are zero mean, orthogonal and spectrally independent. The IMFs do not necessarily have constant frequency or amplitude range.

EMD is an empirical procedure which is defined only by an algorithm and basically does not focus on any analytical formulation for theoretical analysis. It has been used extensively in image, speech and audio processing applications as well as biomedical signal processing [21,45,129,141,181] where its effectiveness is shown.

In brief, the EMD adaptively decomposes a signal into the IMFs through a specific algorithm, namely "sifting procedure". Therefore for each mode, the highest frequency component is locally extracted out of the input signal.

The sifting process is based on two constraints:

1. The number of zero crossing and extrema in the whole data must be the same or at most differ by one.

2. At each point, the mean value of the upper and lower envelopes which are constructed based on the local maxima and minima is zero.

The sifting algorithm begins with identifying local maxima and minima of the signal to be decomposed. Then the local maxima and minima are interpolated to find the upper and lower envelopes respectively. The mean of these two envelopes is subtracted from the signal. The process is repeated for the residue until it meets a stoppage criteria which limits the size of the standard deviation computed for two consecutive residues. The first IMF is then obtained from the residue of the final subtraction. The whole procedure is performed on the residue of this IMF to find the second IMF. This process continues to obtain all IMFs and the final residue has zero or one extrema. More details can be found in [68].

In this study it is proposed to apply EMD to the DUS signal to decompose it to the IMFs which naturally have different frequency bands. An example of applying EMD to the DUS data is shown in figure 3.5. The peaks of the envelope of the first IMF provide the features for identification of the cardiac valve events.

3.2.4 Automated valve motion detection

After applying EMD to the DUS data as shown in figure 3.5, according to the findings in the previous studies, the component with the higher frequency band (higher than 100 Hz) i.e. the first IMF, is linked to the valve motions [174]. On the other hand the low

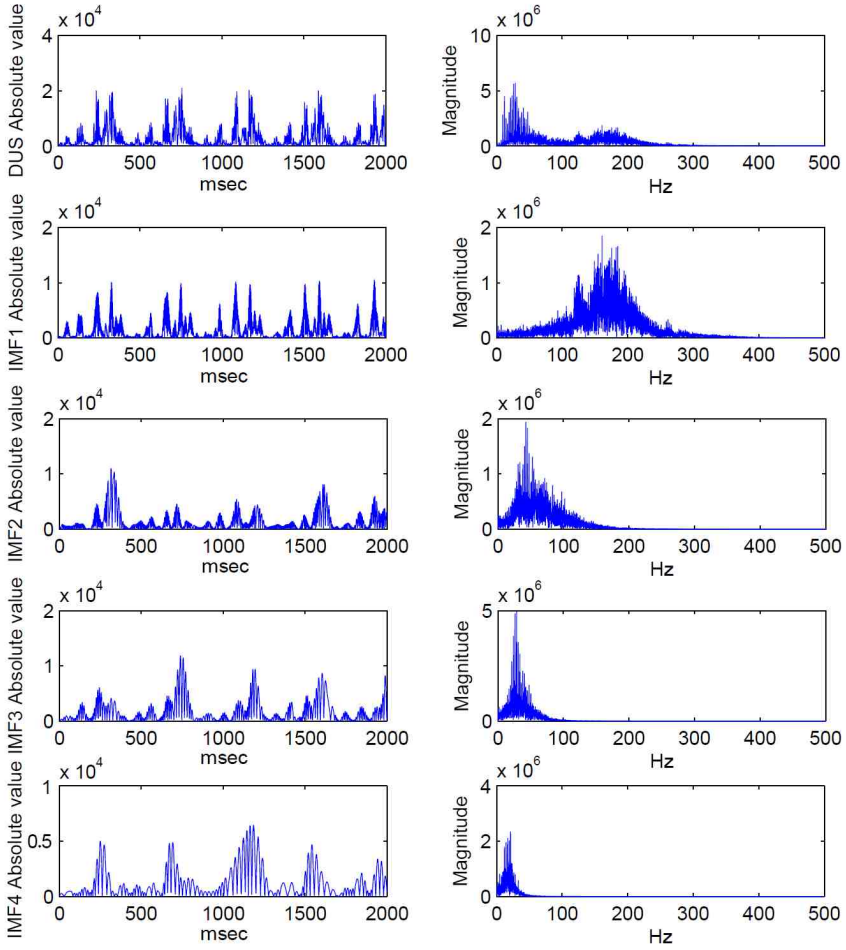

Figure 3.5: The decomposition of the DUS signal to different IMFs using EMD

frequency components generally correspond to the wall motion. More precisely, the absolute value of the first IMF has a sequence of peaks which is associated with opening and closure of the atrioventricular and semilunar valves. For a better assessment, the envelope of that IMF was obtained using spline interpolation over local maxima and then (low-pass) filtered. The intervals of the cardiac cycles were also found using R-R intervals of the fECG. Then the filtered IMF was normalized over each cardiac cycle and its peaks were detected.

In previous studies, the cardiac events were manually assigned to the peaks and the intervals were calculated. In this study we aim to identify them automatically. To this aim, each peak should be classified as an indicator of one of the cardiac valve timing events or

none of them. The first approach is based on Hidden Markov Model (HMM). It can find the events based on the probabilistic model of their occurrence sequence and timings. However it was found that the amplitude as well as the timing of the peaks can also be used to classify them. Therefore in the next approach, Support Vector Machine (SVM) was used as a powerful classifier to identify the events. Because the temporal dependency of the occurrence of events is not considered in SVM, some extra peaks might be classified as the same event in some cardiac cycles, or an incorrect order of events might be noticed. Thus the Hybrid HMM-SVM approach is proposed to be used in order to overcome the defects of SVM and HMM. The time segment of each cardiac cycle was set by using fECG as a reference.

3.2.5 Hidden Markov Models (HMM)

HMM was developed in the 1960s [11] and has been widely used in various applications. Different from the Markov Model, observed symbols in HMM are emitted from some hidden states. The formal definition of HMM is [18]:

$$\lambda = (A, B, \pi) \tag{3.1}$$

A is a transition matrix, B is the emission matrix and π is the initial probability. Given a sequence of observations, the HMM process is aimed to find the sequence of the hidden states that the model went through, based on the transition probability that each state follows another one and the emission probability of the observations from each state. More details can be found in [18]. If there is an available set of examples from a process, the model can be estimated by either supervised or unsupervised training. In this study the supervised approach was used because both input and output of the process were available as a training set, for which we had prior information. In our experiments Hidden Markov Models from statistics toolbox of MATLAB was used.

In the first approach, HMM was applied to the filtered version of the first IMF for recognizing valve movements. The sample procedure for detecting a cardiac event is shown

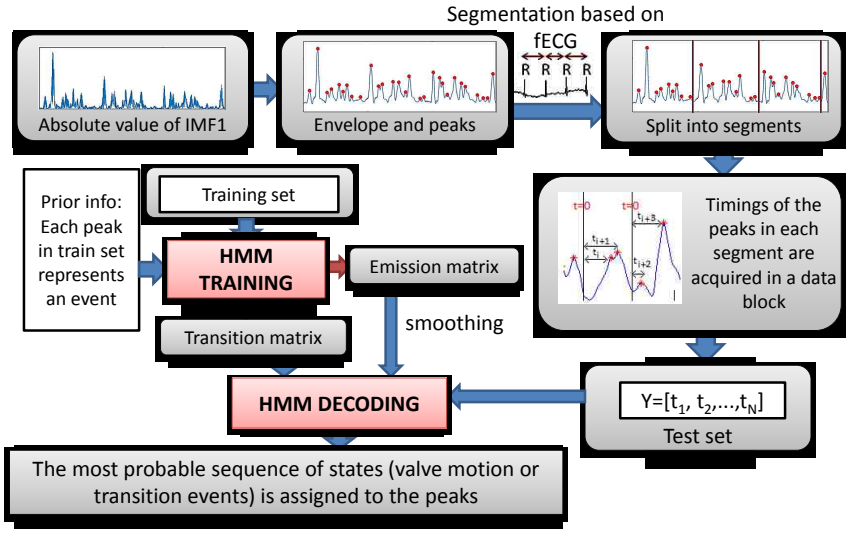

Figure 3.6: HMM approach block diagram

in figure 3.6. First, the peaks of the first IMF were identified based on the declining zero crossing first derivative and negative second derivative criteria. In order to find the timing of the peaks of the IMF envelope in each cardiac cycle, the whole sequence had to be split into different segments using the R-R intervals of the fECG. The time difference from the beginning of the segment to the occurrence of each peak in that segment was then calculated, assigned to each peak and denoted by t_i. This data set made our observation set. The hidden states $S = (s_1, s_2, ..., s_N)$ were set as the opening (o) and closure (c) of the Mitral and Aortic valves: Mo, Mc, Ao, Ac and four transitional states: T1, T2, T3, T4, which may occur between each pair of valve motion states.

A training set for which we had prior information about the timings of cardiac events was then used for the HMM training process. First, HMM was trained based on the prior information about the training set (if each peak represented one of the valve motion or transitional events) to provide an estimation of the transition and emission matrices. Each element ij of the transition matrix was estimated as the number of times the event s_j followed s_i in the training set, divided by the total number of s_i in that set. Each element $b_j(k)$ of the emission matrix was estimated by the number of times an observation

(peak timing) was linked to the state s_j in the training set, divided by the total number of s_j. Since the training set may not be rich enough to estimate the emission probability for every time bin, the estimated emission matrix may contain many zeros and isolated spikes. Therefore the estimated emission matrix was filtered by a low pass filter and then normalized. This filtered matrix and the transition matrix were then used to decode the new data. By decoding, a matrix containing the probability of the occurrence of each event was obtained for each peak. Then the event with the highest estimated posterior probability of occurrence among all states was assigned to each peak.

3.2.6 Support Vector Machines (SVM)

In this approach, SVM was used to classify the peaks of the IMF envelope as a sign of each event (or no event). SVM developed by Vapnik [193] is a powerful technique for classification. Two class SVM is designed to find a separating hyperplane with the maximum margin with the classes. In the case of nonlinear classification, the data is first transformed by a Kernel function into the higher dimensional space in which it becomes linearly separable. SVM is based on the "structural risk minimization" criteria in order to attain low probability of generalization error [64]. More details on SVM can be found in [2].

To construct SVM, a kernel function $K(\mathbf{x}_i, \mathbf{x})$ must be first selected. The choice of the kernel may affect the performance of SVM. The Radial Basis Function (RBF) is one of the kernels which is used in many applications. It is defined as follows:

$$K(\mathbf{x}_i, \mathbf{x}_j) = exp(-\frac{||\mathbf{x}_i - \mathbf{x}_j||^2}{2\sigma^2}) \tag{3.2}$$

where σ is the width of the RBF function. In this study, the RBF kernel was used and σ was experimentally chosen to be 1.

SVMs are usually formulated for binary (two-class)problems. However they may be extended to multiclass problems. In this study the one-against-all approach was used for multiclass SVM [2]. The classes were the same as the states in HMM approach.

SVM was used as the second approach for classifying the peaks corresponding to one of

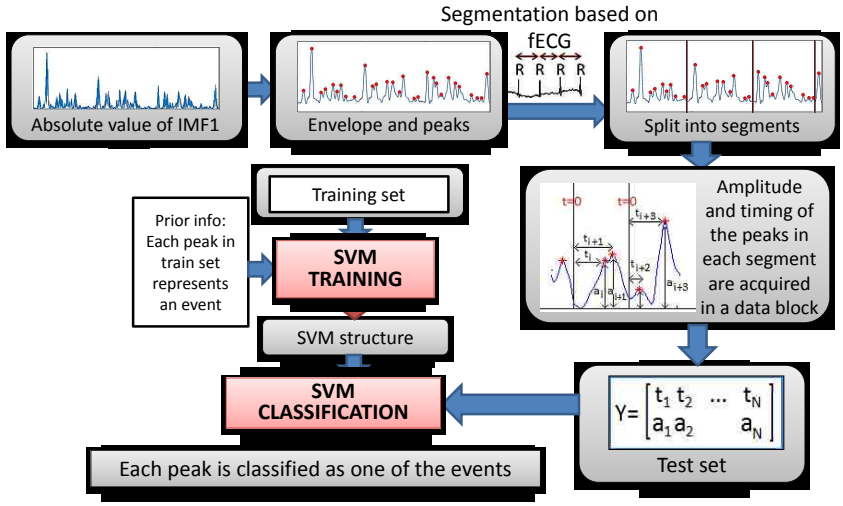

Figure 3.7: SVM approach block diagram

the valve motion or other transitional events. For example, the procedure for recognizing an event from the first IMF is shown in figure 3.7. In order to obtain the features, first EMD was applied to the DUS data, the envelope of the IMF was taken and all peaks were determined based on the derivative of the signal. Then, the signal was broken into segments using R-R intervals of fECG as the reference. The time interval from the beginning of each segment to the occurring time of each peak in that segment and the amplitude of the peak were acquired as the features in a matrix **Y**. SVM uses a training set with the prior knowledge which assumes the events associated with the peaks. The SVM structure was developed based on the training set. The new data were classified by SVM to find the event represented by each peak, based on the amplitude and timing of the peaks. The Support Vector Machine functions from Bioinformatics toolbox of MATLAB were used for this study.

3.2.7 Hybrid SVM-HMM

The Hybrid SVM/HMM method has been developed for the speech recognition [54,59]. In this research we propose to use it for recognizing the cardiac events. It is a combination of HMM and SVM. In order to combine SVM and HMM, a probabilistic output of SVM must be obtained, because HMM is based on probability models. Platt's SVM method [152] can provide such an output. In this method the distance of each sample from the separating hyperplane is transformed to the posterior probability of classifying the sample. The posterior probability output of the SVM, $P(class|input)$, is obtained by calculating: $P(y = +1|f(x))$, where:

$$f(x) = \sum_{i=1}^{l} \alpha_i y_i K(x, x_i) + b \tag{3.3}$$

and parametric Sigmoid is fitted to the output of the SVM classifier:

$$P(y = +1|f(x)) = \frac{1}{1 + exp(Af(\mathbf{x}) + B)} \tag{3.4}$$

The parameters A and B are determined by minimizing the negative log likelihood of the training data which has the form of a cross-entropy error function. In the hybrid SVM/HMM process the transition matrix and the initial probability is first determined based on the HMM training process. The SVM is also trained using the training set. The SVM classification process is then performed on the new data and the emission probability distribution is obtained by using the output of the Platt's SVM through the Bayes' rule. Therefore the HMM model is constructed. Based on this model, the most probable hidden states are recognized through the decoding process.

For example the procedure of identifying the events from first IMF is shown in figure 3.8. First the data were broken into segments. Here again, the fECG was used as a reference for segmentation. Then the time and the amplitude of the peaks were taken into the matrix $\mathbf{Y}$. A training set for which we had prior information was used for SVM and HMM training. The new data were then classified by the hybrid SVM/HMM method to obtain the probability of the occurrence of the events for each peak. Then one of the valve

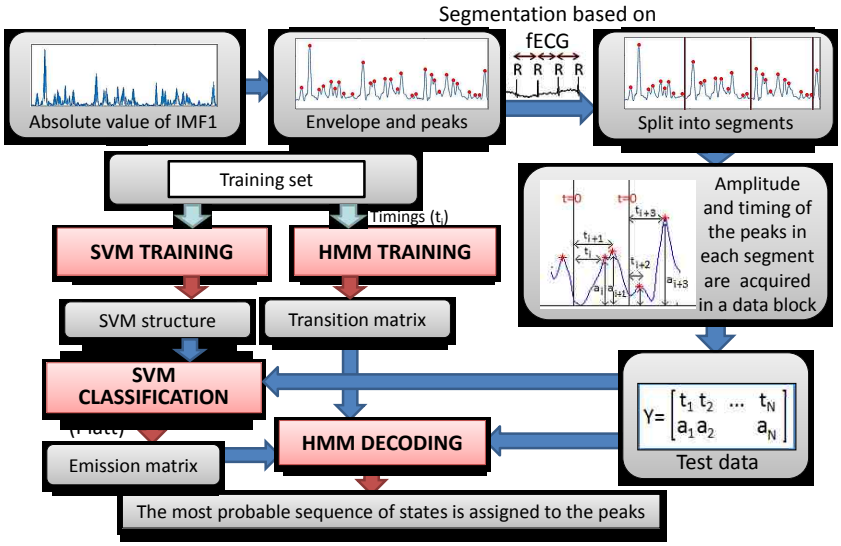

Figure 3.8: Hybrid SVM-HMM approach block diagram

motion or transitional events for which the estimated occurrence probability was higher than other events was assigned to each peak.

3.3 Results

In order to evaluate the results, the timings of opening and closure of the valves were verified by the Pulsed-wave Doppler images. It visualizes the direction and the characteristics of the blood flow through the valves. In this technique, the aortic blood flow Doppler waveform is recorded from the long axis of the five-chamber view of the heart. The M-mode cursor is placed perpendicular to the inter-ventricular septum at the level of the mitral valve to examine end-systole and end-diastole (closure of atrioventricular valves).

In this study the total number of 45 different data sets of DUS and corresponding fECG were used for testing the algorithm and obtaining the timings. In order to train the hybrid SVM/HMM classifier, the timings of the events for 30 cardiac cycles from three different normal fetuses were determined manually based on expertise. The algorithm was then

Table 3.1: Mean ± standard error of the average time intervals (msec) over 45 normal fetuses and the accuracy of identified events.

intervals	Mean± Standard Error	rate (new method)	rate (previous study [79])
R-R	413.6 ± 26.0	100.0%	100.0%
R-Mc	14.3 ± 2.3	91.1%	84.0%
R-Ao	51.1 ± 3.4	95.3%	87.0%
R-Ac	204.6 ± 5.5	98.8%	97.6%
R-Mo	276.4 ± 5.4	94.5%	89.7%
Ao-Ac	153.5 ± 6.3	94.6%	87%

Table 3.2: Results of Kruskal-Wallis test (p-values) and pairwise comparison with Mann-Whitney-Wilcoxon method for changes of the estimated intervals versus different age groups. The mean ± Standard Error (SE) (msec) of the timings for different age groups are shown. Significant differences between pairs of age groups: 16-29 vs 30-35, 16-29 vs 36-41 and 30-35 vs 36-41 are marked by (a), (b) and (c), respectively.

Interval	p-value	Mean±SE age group 16-29	Mean±SE age group 30-35	Mean±SE age group 36-41
EDT	0.0967	25.3±4.8	24.2±5.5	26.4±4.0
ICT	0.0558	36.4±2.6	35.6±2.7	37.7±3.4
IRT	0.0218	73.0±4.6 $^{(A)}$	69.7±4.5 $^{(A,C)}$	72.2±4.9 $^{(C)}$
PEP	0.0026	61.7±4.8 $^{(A)}$	59.9±5.2 $^{(A,C)}$	64.0±4.0 $^{(C)}$
STI	1×10^{-8}	213.9±5.2 $^{(B)}$	214.0±7.1 $^{(C)}$	218.2±7.1 $^{(B,C)}$
VET	0.0333	152.2±3.7 $^{(A,B)}$	154.2±6.9 $^{(A)}$	154.2±7.7 $^{(B)}$

applied to new data sets from different fetuses to find the timings during 40 cardiac cycles for each data set. Figure 3.9 shows an example of the high frequency IMF and the identified events, the fECG and the Pulsed Doppler image of the mitral valve movement for three cardiac cycles from one of the test sets. Figure 3.10 shows the result of using another data set with the fECG and the Pulsed Doppler image of the aortic valve movement. Figure 3.11 shows estimated timings of the valve movements from one of the test data sets. Only few event timings were missed using this method. Table 3.1 shows the percentage of the estimated events using all data sets from 45 fetuses for a total of 1777 cardiac cycles and the mean and standard error of the average estimated time intervals over all fetuses.

The identification of the events by using the SVM, HMM and the hybrid SVM/HMM method were compared in Figure 3.12. By comparing the results with the Pulsed Doppler

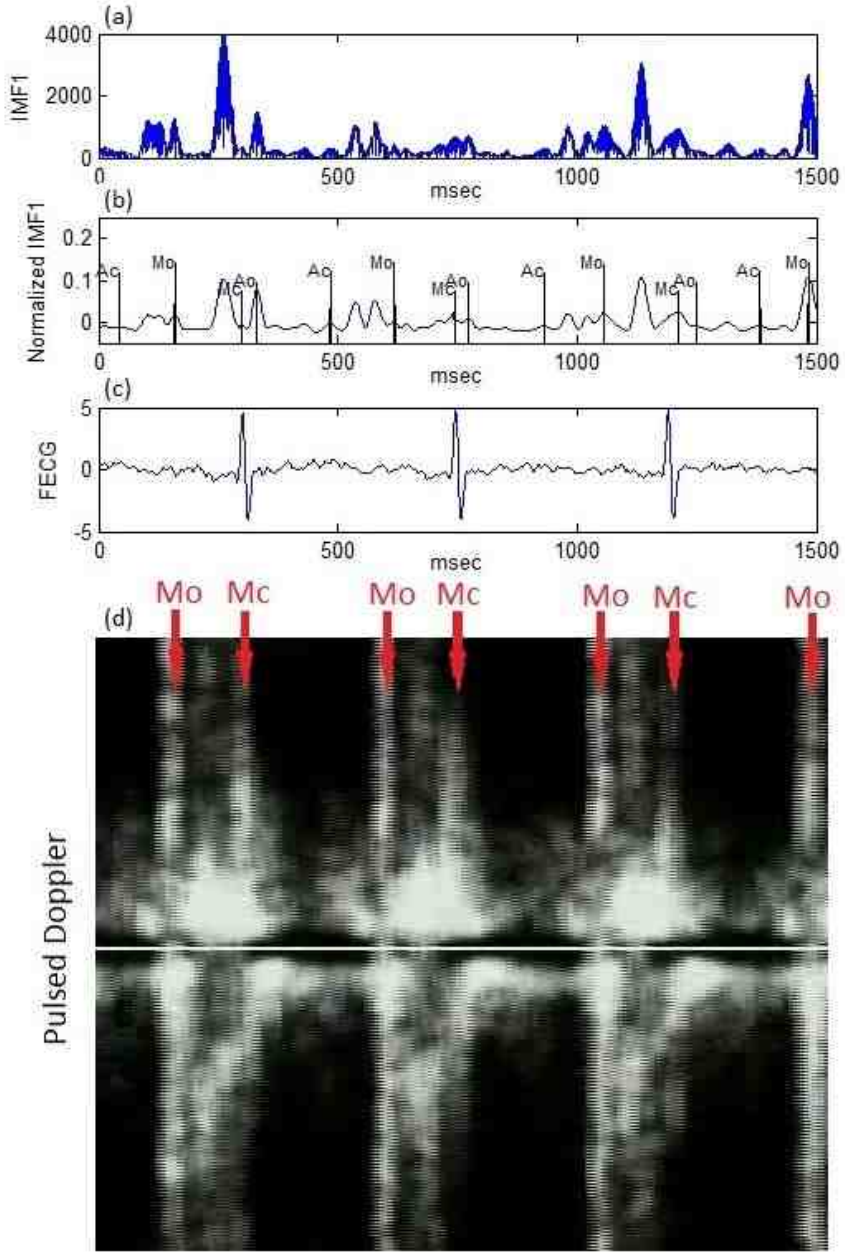

Figure 3.9: (a) First IMF of the Doppler ultrasound signal decomposed by EMD. (b) Envelope of the normalized IMF and the identified timings. (c) The simultaneous fetal electrocardiogram signal extracted from abdominal ECG signals using BSSR. (d) Pulsed wave Doppler signal of fetal mitral valve movements annotated to show how the specific signals are linked with opening and closing events. Mo and Mc represent the opening and closing of mitral valve. The fetus was at 35 weeks of gestation.

image, it is shown that the hybrid method performs better than the previous study by Khandoker et al. [79].

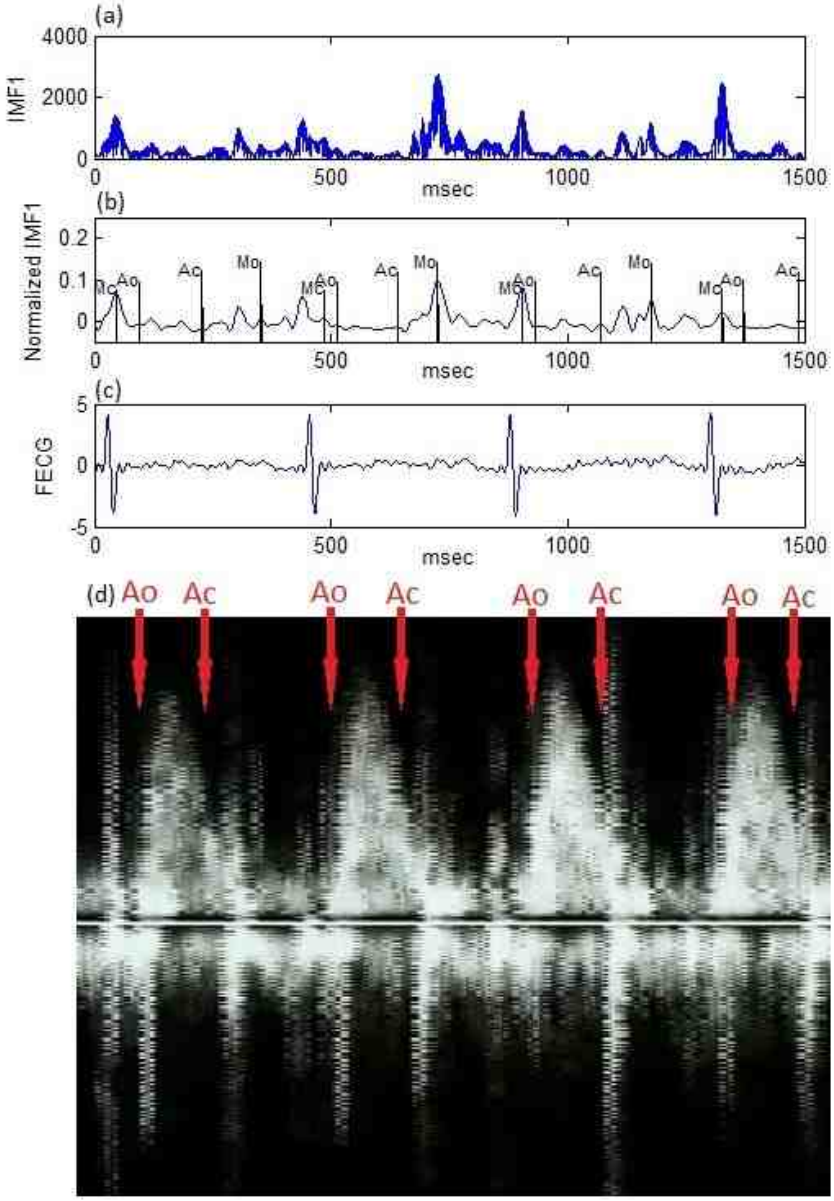

Figure 3.10: (a) First IMF of the Doppler ultrasound signal decomposed by EMD. (b) Envelope of the normalized IMF and the identified timings. (c) The simultaneous fetal electrocardiogram signal extracted from abdominal ECG signals using BSSR. (d) Pulsed-wave Doppler signal of fetal Aortic valve movements annotated to show how the specific signals are linked with opening and closing events. Ao and Ac represent the opening and closing of aortic valve. The fetus was at 29 weeks of gestation.

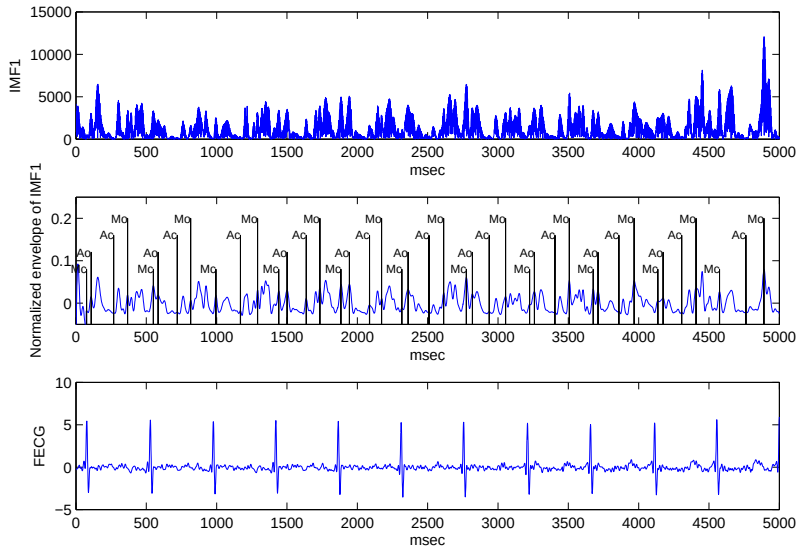

Figure 3.11: An example of identified events: mitral opening and closing (Mo and Mc) and aortic valve opening and closing (Ao and Ac).

Table 3.3: Results of Multiple comparison by Mann-Whitney-Wilcoxon method (P-values).

intervals	16-29 vs 30-35	16-29 vs 36-41	30-35 vs 36-41
IRT	0.0032	0.1973	0.0222
PEP	0.0095	0.0966	0.0004
STI	0.4588	0.0000	0.0000
VET	0.0192	0.0091	0.4808

3.3.1 Changes of the cardiac intervals with gestational progression

The estimated intervals were also analyzed by Kruskal-Wallis test to investigate their changes during pregnancy. Data from all 45 fetuses were divided into three different age groups: 16-29, 30-35 and 36-41 weeks, including 15, 12 and 18 fetuses, respectively. Table 3.2 and 3.3 show the results of Kruskal-Wallis test (p-values), mean and standard error of the timings for each age group as well as their pair-wise comparison with Mann-Whitney-Wilcoxon method.

Figure 3.13 shows the result of comparison of the changes in PEP with the findings of an earlier study by Mensah et al., [127].

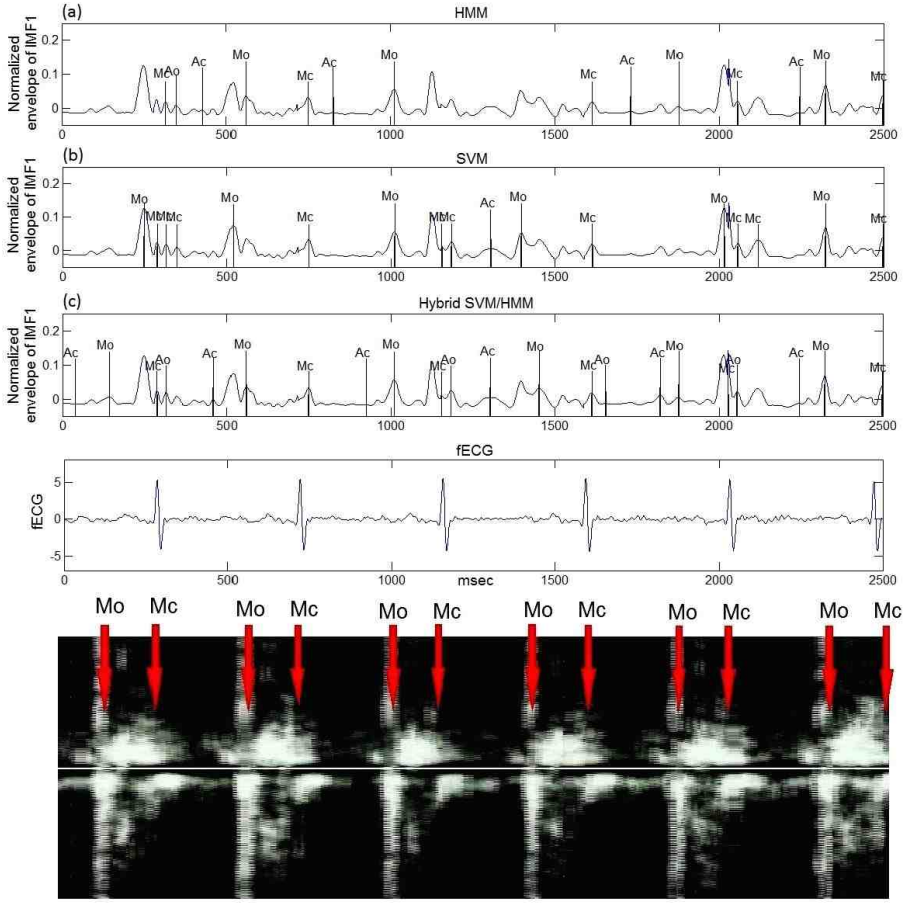

Figure 3.12: Comparison of the identification of the valve movements by using HMM (a), SVM (b) and Hybrid SVM/HMM (c)

3.4 Discussion

In previous studies, intervals of cardiac events have been estimated from DUS signal by using digital filtering, STFT or wavelet [79, 80, 90, 134, 174]. The DUS signal is nonlinear and nonstationary and wide changes in the signal content and spectral characteristics are noticed on a beat-to-beat basis. The transient nature of the DUS signal and its variability are also shown in previous papers [174]. Therefore it is not convincing to use fixed parameters such as cut off frequency for filtering methods for the whole signal and different subjects. Thus EMD which is a data driven method is more suitable for this application. EMD has been extensively used for decomposing nonlinear and nonstationary signals, including the DUS signal but for estimating the fetal heart rate [88, 162] and it has not

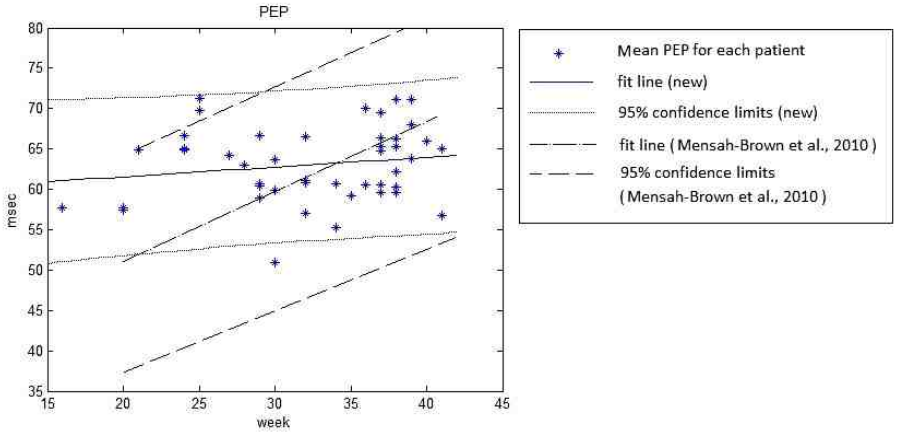

Figure 3.13: Changes of the mean and 95% confidence interval of PEP compared to the results of the previous study by Mensah et al., [127].

been used for this specific application before. The results show that by applying EMD the component which is linked to valve movements is practically separated and its peaks which correspond to the events can be discriminated.

All previous studies were based on manual identification of the cardiac event timings. However it is difficult to recognize the peaks manually, especially for nonexperts. Moreover the appearance of particular types of events in DUS signal strongly depends on the location of the ultrasound transducer and the fetus. Some peaks which are linked to the cardiac events may not be visible in some situations or some extra peaks may appear which may be confusing for manual recognition. It also takes time to carefully investigate the DUS signal component in order to recognize the events. There are some visual errors as well as inter- and intra- observer errors when events are recognized based on human observation. Therefore in this research an automated method was proposed to recognize the events. For this purpose the hybrid SVM/HMM method was proposed to be used, which has been previously employed only in speech processing applications. Furthermore, to our best knowledge, the combination of EMD and the hybrid SVM/HMM has never been used before. The hybrid method classifies the peaks of the decomposed component of the DUS signal to be linked to each cardiac event, based on the pattern of the peaks, the timings and the sequence of the events. The better training of the classifier with the DUS signals with different patterns, the more powerful automated recognition

of the cardiac events. As shown in table 3.1, by using this method, a higher percentage of the valve movement events was identified, compared to the previous manual method. The results were also compared with the Pulsed Doppler images which verified the successful identification of the events.

The estimation of the timing of cardiac events would be very difficult without using fECG as a reference for segmentation. In this study the position of the R-waves was used for segmentation of the signal into different cardiac cycles. Results of this method provide the continuous and beat-to-beat identification of cardiac intervals, which can be used for clinical purposes.

The relationship between the cardiac intervals and the gestational age was also investigated in this study. According to the Kruskal-Wallis test and pairwise comparison with Mann-Whitney-Wilcoxon, STI was found to be the most changeable with the age. On the other hand ICT was more stable during pregnancy as also reported by Koga [86]. According to a recent study by Mensah-Brown et al., PEP increases with the gestational age (r= 0.57 , $p < 0.0001$)[127]. In this study based on the pairwise comparison, it is found that PEP slightly decreases ($p < 0.0095$) from the age group of 16-29 to 30-35, and then significantly increases to the age of 36-41 ($p = 0.0004$, table 3.3). As shown in figure 3.13 the estimated timings are mostly in the same range of 95% confidence interval of the previous study [127], especially after 30 weeks. The disagreement between the results before 30 weeks may be caused by the lower accuracy of our technique compared to the ultrasound imaging for the early gestation fetuses. The results of pairwise comparison indicate that except for EDT and ICT, all intervals of the age group 36-41 are significantly different from previous ages. For example STI does not change significantly from the age of 16-29 to 30-35 ($p = 0.4588$), but after that sharply increases toward the final weeks of pregnancy ($p < 0.0001$). The trend of changes in PEP is also different in the final stage. Therefore the final weeks of pregnancy are the most critical.

IRT intervals were found to be longer in this study than the timings reported in [108]. The reason may be that the age of the fetuses analyzed in [108] was from 6 to 10 weeks of gestation, but the average age of the fetuses we analysed was 31 weeks. The cardiac function changes with the development of the fetal heart. A part of the difference may be

related to this developmental change.

A limitation of this study is that the quantitative comparison with the pulsed wave Doppler image based valve motion timings was not provided. More accurate methods such as trans-vaginal pulsed Doppler imaging can be used in the first trimester fetuses [108]. However our system is compatible with this wide-continuous monitoring of fetal heart during second to third trimesters. More accurate quantitative comparison of the results of the proposed method with pulsed Doppler images requires image processing and recognition process which are beyond the scope of this study.

3.5 Conclusion

DUS signal is nonlinear, nonstationary, noisy and variable on a beat to beat basis. Therefore using a combination of EMD as a data driven method for decomposing nonlinear and nonstationary signal and hybrid SVM/HMM for automated identification of the events improved the estimation of cardiac intervals. Results showed that 94.5% of mitral opening, 91.1% of mitral closing, 95.3% of aortic valve opening and 98.8% of aortic valve closing were identified by this method, which were higher than the manual approaches. The identified timings were verified by pulsed doppler images.

Furthermore the trend of changes of the cardiac intervals for growing gestational age groups was analysed. Results showed significant changes in STI, IRT, VET and PEP from early to late gestation. In particular the intervals which corresponded to the last weeks before delivery were significantly different from their values during the earlier weeks.

Chapter 4

A multi-dimensional hidden Markov model approach to automated identification of fetal cardiac valve motion

The focus of this chapter is on an improved automated identification of the fetal cardiac valve opening and closing from Doppler Ultrasound signal and fECG as a reference. A novel combination of EMD and multi-dimensional Hidden Markov Models (MD-HMM) was employed which provided beat-to-beat estimation of cardiac valve event timings with improved precision and recall compared to the one dimensional HMM and hybrid SVM-HMM approaches.
This chapter is a slightly modified version of the published article [116]:

- *F. Marzbanrad, A. Khandoker, M. Endo, et al. A Multi-dimensional Hidden Markov Model Approach to Automated Identification of Fetal Cardiac Valve Motion, IEEE Engineering in Medicine and Biology Conference EMBC 2014, pp.1885-1888.*

4.1 Introduction

A Challenge in identification of the fetal cardiac valve motions is to automate this task. In earlier studies [79, 85, 135, 144, 168, 174], the opening and closing of the valves were identified manually from the peaks of the DUS component by skilled specialists. Manual identification process requires special skills and is time consuming and subject to inter and intra observer errors. Therefore an automated technique was proposed in chapter 3, using HMM to find the cardiac valve opening and closing as hidden states, from the peak timings of the DUS signal component as observation [119]. HMM

only takes one observation symbol at each time, which was the peak timing as proposed in chapter 3 [119], while other features such as the amplitude of the peaks can also be used for identification. To incorporate additional features, the hybrid Support Vector Machines (SVM)-HMM was proposed to recognize the events as discussed in chapter 3 [123]. However combining SVM with HMM made it more complicated, by additional processes such as: nonlinear transformation with Kernel, solving an optimization (dual) problem, repetition of procedure for multiclass SVM and estimating the probabilistic output.

The focus of this chapter is to improve the precision and recall of the automated identification of fetal cardiac valve movement by incorporating additional features using MD-HMM which is less complex than hybrid SVM-HMM.

4.2 Method

4.2.1 Data

Similar to the process described in chapter 3, the Doppler ultrasound and abdominal ECG signals were recorded simultaneously at the Tohoku University Hospital, Sendai, Japan. Furthermore, 16 additional recordings were received from Japan at the time this study was conducted, made a total of 61 recordings available. Pregnant women and fetuses were all healthy with single pregnancy and the gestational age of 16 to 41 (33 ± 6) weeks. All recorded signals were 1 minute in length and sampled at 1 kHz with 16-bit resolution. The study protocol was approved by Tohoku University Institutional Review Board and written informed consent was obtained from all participants. Ultrasonic Transducer 5700 (fetal monitor 116, Corometrics Medical Systems Inc.) with 1.15 MHz signal was used to collect the continuous DUS.

Data were divided into training and testing sets. Training set was obtained from 345 cardiac cycles of DUS components and fECG from 21 fetuses. The cardiac valve motion events of the training set were identified manually based on expertise. Data from the remaining subjects were used for test set. M-mode and pulsed wave Doppler fetal echocardiography were performed simultaneous with DUS and fECG for two test sub-

jects to verify the mitral and aortic valve timings. Convex 3.5 Hz of HITACHI ultrasound scanner (Ultrasonic diagnostic instrument Model EUB-525; HITACHI health medical corporation) was used for this purpose. The fECG recording and processing were the same as the procedures described in chapter 3.

4.2.2 DUS signal decomposition and segmentation

DUS signal was decomposed by EMD as described in the previous chapter. By applying EMD to the DUS signal, the first IMF corresponding to valve motions was obtained [119, 123]. The envelope of its absolute value was taken by interpolating its maxima and smoothing by low pass filter. The peaks of the envelope provided the features for identification of the opening and closing of the valves. The envelope was segmented into cardiac cycles using R-R intervals of the simultaneous fECG and then normalized.

4.2.3 Identification of valve timing events by multi-dimensional HMM

The valve timings can be automatically identified from the peaks of the envelope of the first IMF using HMM, as described in chapter 3 [119]. The timings of the observed peaks of the first IMF envelope were used as observations to find the hidden states: Mitral closing (Mc), transition 1 (TR1), Aorta opening (Ao), transition 2 (TR2), Aorta closing (Ac), transition 3 (TR3), Mitral opening (Mo), transition 4 (TR4).
The identification process was performed in training and decoding phases. In the training phase, the probability of emissions and transition between states were estimated. Each element ij of the transition matrix was found by dividing the number of times the event s_j followed s_i in the training set by the total number of s_i in that set. Each element $b_i(t)$ of the emission matrix was calculated from the number of times an observation was linked with the state s_i in the training set, divided by the total number of s_i. Viterbi algorithm was used for decoding the observation set and finding the most probable sequence of states linked to the peaks of the IMF envelope.
In this chapter, it is proposed to use multi-dimensional HMM which was developed for telerobotic applications [62, 203], in order to add new features to the observation, such as

the amplitude of the peaks to improve identification.

To add a new dimension, an additional set of emission probabilities was estimated in the training phase which was the probability of observing a peak amplitude given a hidden state at that peak time. The peak amplitudes were quantized and scaled to be mapped into a range of integers from 1 to 200. The emission probability can be expressed as follows:

$$b_{i,d}(o_d(t)) = P(o_d(t)|s = i) \tag{1}$$

where i is the state number, o indicates the observation sequence in discrete time t, which has two dimensions, the timing ($d = 1$) and amplitude ($d = 2$) of the peaks. Since the training set was not rich enough to estimate the emission probability for every time bin and amplitude value, the estimated emission matrices contained some zeros and isolated spikes. Therefore the estimated emission matrix was filtered by a low pass filter and then normalized. Figure 4.1 shows emission probability trained based on 345 cardiac cycles from 21 fetuses.

The amplitude and timing of the peaks given each state were independent as verified by Hilbert-Schmidt Independence Criterion (HSIC) test with a Gamma approximation and the median distance as kernel size (type I error upper bound was < 0.17 for Mc, < 0.03 for Ao and < 0.01 for other states)[58]. Therefore the probability density function of the observation, specific to each state (e.g. state i) was modified as follows and used in Viterbi algorithm.

$$B_i(O(t)) = \prod_{d=1}^{n} b_{i,d}(o_d(t)) \tag{2}$$

where n indicates the dimension of the observation which is 2 in this application. More details about the multi-dimensional Viterbi algorithm can be found in [62].

4.2.4 Cross-validation

The MD-HMM approach was compared to one dimensional HMM and hybrid SVM-HMM, using 10-fold cross validation. The training set was randomly partitioned into 10 subsets with almost equal size; one subset for validation and 9 subsets for training. The whole process was repeated 10 times with different subsets for validation.

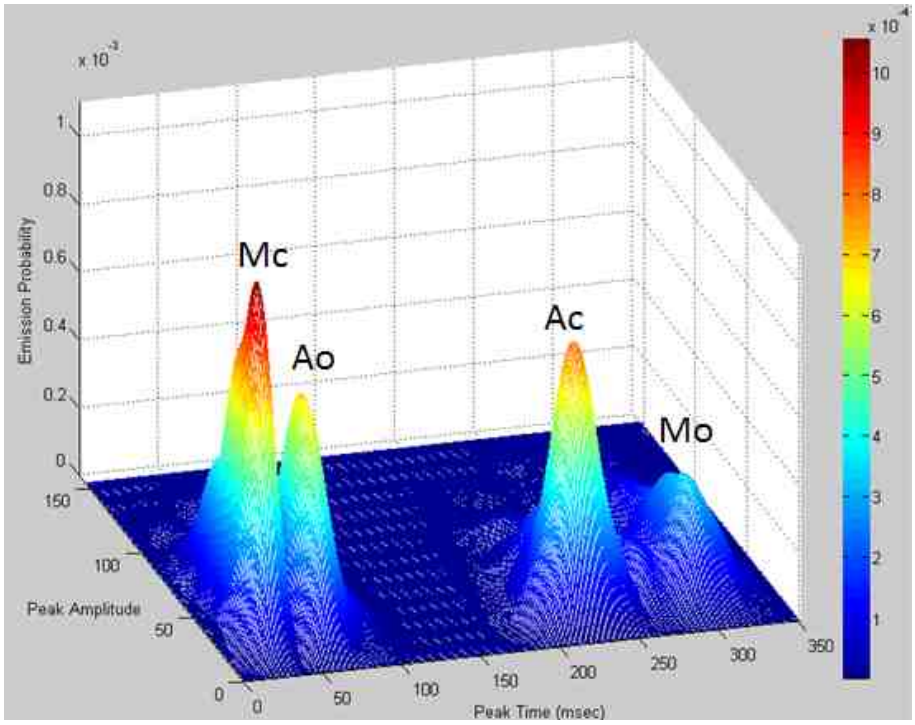

Figure 4.1: Emission probability distribution trained based on 345 cardiac cycles from 21 fetuses, for different observed peak amplitude and timing from the preceding R-peak.

The precision and recall of the identification of each valve timing event was calculated as follows and averaged over the 10 folds:

$$Precision_i = \frac{T_i}{T_i + \sum_j F_{ij}} \tag{4.1}$$

$$Recall_i = \frac{T_i}{T_i + \sum_j F_{ji}} \tag{4.2}$$

where i refers to one of the valve motion events (Mo, Mc, Ao or Ac), T_i is the number of true estimation of event i and F_{ij} indicates the number of times event j was mistakenly identified as event i.

4.3 Results

The precision and recall of identifying valve motion events was obtained from 10-fold cross-validation of the training set including 345 cardiac cycles of DUS signal and fECG

Table 4.1: Precision (%) of identification of valve motion events by cross validation of different methods applied to the training set including 345 cardiac cycle recordings from 21 fetuses.

Methods	Mc	Ao	Ac	Mo	Average
MD-HMM	91.5	89.1	81.5	69.4	82.9
SVM-HMM	90.8	90.6	77.9	60.0	79.8
HMM	90.8	88.1	71.2	59.4	77.4

Table 4.2: Recall (%) of identification of valve motion events by cross validation of different methods applied to the training set including 345 cardiac cycle recordings from 21 fetuses.

Methods	Mc	Ao	Ac	Mo	Average
MD-HMM	92.9	91.2	81.5	69.6	83.8
SVM-HMM	93.8	92.7	77.9	60.2	81.2
HMM	91.3	89.4	71.2	59.6	77.9

from 21 fetuses. The new MD-HMM method, one dimensional HMM approach [119] and hybrid SVM-HMM [123] were compared in tables 4.1 and 4.2 which show the improved precision and recall using the new method.

The MD-HMM method was applied to two test data (not involved in training) for one of which, the simultaneous M-mode image of the aortic valve motion and for the other one the pulsed wave Doppler image from mitral was collected. Figure 4.2 and 4.3 show the m-mode and pulsed wave Doppler images which verify the identification of the aorta and mitral valve motions respectively. As shown in figure 4.3, the last Mc event did not appear nor was it identified from the DUS signal. However Mc was identified for 95.1% of all cardiac cycles combined from 61 subjects. The rate of identified events across 61 subjects (8510 cardiac cycles) from training and testing sets, the mean and standard error (SE) of the average interval of fECG R-wave to each valve motion are summarized in table 4.3.

4.4 Discussion

In this study a new automated method was proposed to identify the beat-to-beat fetal cardiac valve timings with improved precision and recall. The shortcoming of the (one

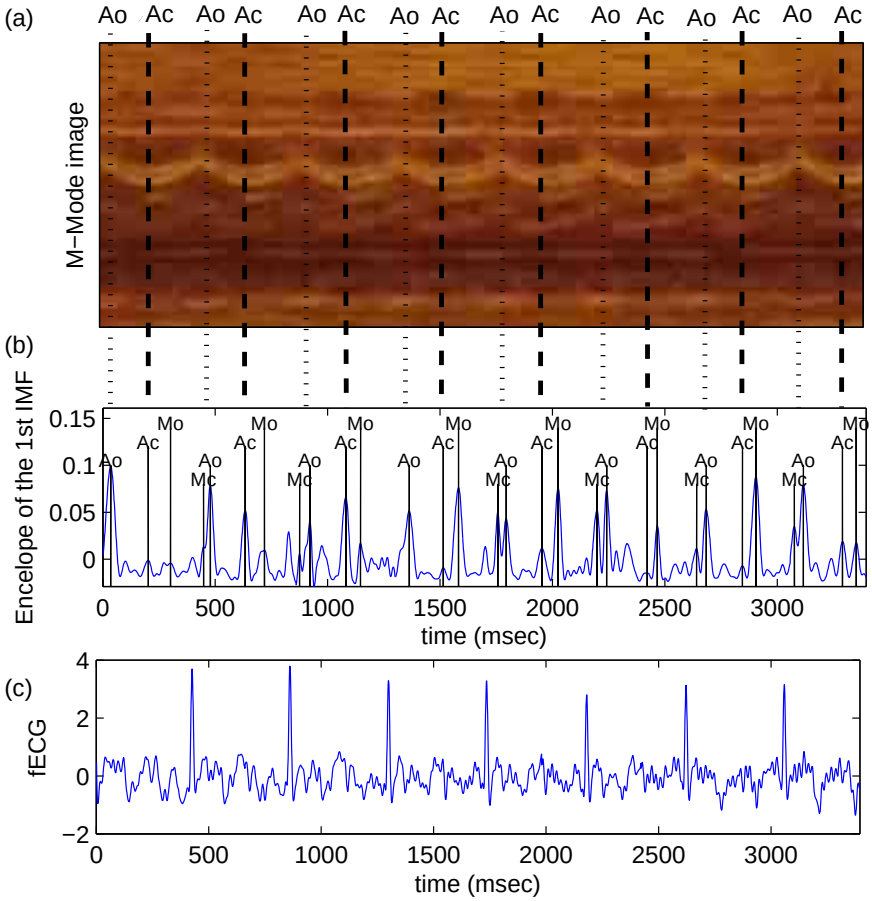

Figure 4.2: (a) The M-mode image of the aortic valve operation. The aorta opening (Ao) and closing (Ac) events are depicted by dashed lines. (b) The envelope of the first IMF and the events identified by the MD-HMM method. (c) Simultaneously recorded fECG.

dimensional) HMM is that it only takes one observation symbol at each time [119]. By extending it to the multi-dimensional HMM, multiple features can be used for identification. By adding the peak amplitude feature, the average precision and recall were improved from 77.4% to 82.9% and from 77.9% to 83.8%, respectively. Other parameters such as the width of the peaks can also be used in future studies.

Another method to incorporate multiple features for this application is the hybrid SVM-HMM which was described in the previous chapter [123]. The precision and recall of the MD-HMM was slightly higher than the hybrid SVM-HMM method. Furthermore, the MD-HMM method is simpler than the hybrid method. The procedures added to

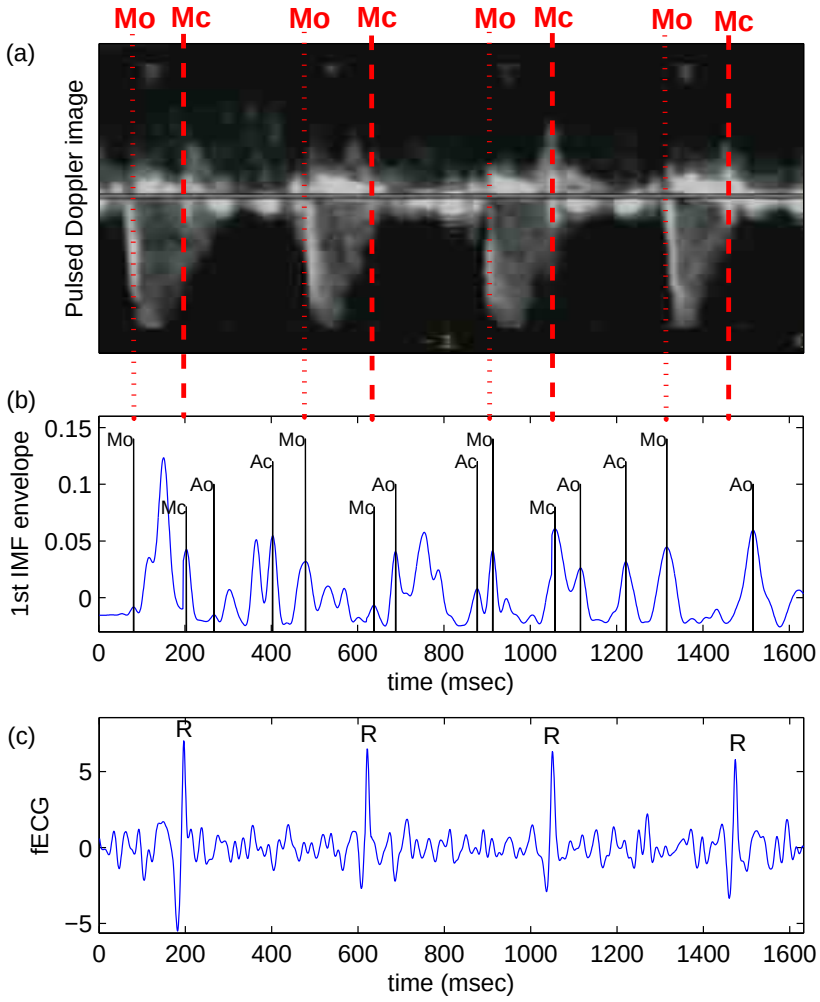

Figure 4.3: (a) Pulsed wave Doppler image of fetal mitral valve movements. Dashed lines show mitral opening (Mo) and closing (Mc), (b) The envelope of the first IMF and the valve motion events identified by the proposed method, (c) Simultaneously recorded fECG.

HMM for SVM-HMM include: nonlinear transformation with Kernel, solving an optimization problem (dual problem [193]), repetition of procedure in the one-against-all scheme for multiclass SVM and fitting sigmoid (Platt's method) to obtain a probabilistic output. While for MD-HMM training, an extra estimation of the emission matrix is added for each extra dimension which is simply calculated from the number of times an observation is to linked each state, divided by the total number for that state. For decoding, the emission probabilities are multiplied under the condition of their independence, to obtain the probability density function of the observation for each state required in

Table 4.3: Mean ± SE of cardiac intervals and the rate of identified events for 61 fetuses are summarized. The identification rate was calculated from the number of identified cardiac valve events out of 8510 beats from 61 fetuses.

Intervals	Mean ± SE	rate* (%)
R-R	420.9 ± 34.1	100
R-Mc	26.5 ± 2.9	95.1
R-Ao	64.1 ± 3.7	98.8
R-Ac	220.7 ± 4.7	99.9
R-Mo	297.1 ± 7.4	99.9

Viterbi algorithm. Overall, the process of MD-HMM is less complex than the SVM-HMM specially for low dimension, but detailed comparison of their complexity requires further study.

Mitral closing event had the lowest identification rate (table 4.3) and also did not appear in the last beat shown in figure 4.3. Mitral closes when the pressure of the left ventricle exceeds the left atrial pressure, which is followed by opening of aorta. A reason for lower identification rate of Mc is that time difference between Mc and Ao is very short and in some cases their corresponding peaks of IMF cannot be distinguished. As reported in the results of this and the next chapter, mitral opening was identified with the least precision and recall. This is mostly because mitral opens in two phases (E phase followed by A phase) which is not the case for other valve movement events. This complicated the identification of the peak corresponding to the onset of the E phase.

4.5 Conclusion

In this chapter a new method was proposed for automated identification of fetal cardiac valve motions using a combination of EMD and multi-dimensional HMM. Employing MD-HMM enabled the use of amplitude of the peaks of the first IMF as well as their timings, which improved the precision and recall of the identification of cardiac valve motion. The average precision obtained by the MD-HMM was 82.9%, which was higher than one dimensional HMM (77.4%) and hybrid SVM-HMM (79.8%). More than 95.1% of valve motion timing events were identified using this method and they were also verified by M-mode and pulsed Doppler images for two fetuses.

Chapter 5

Model-based estimation of Fetal Cardiac Timing Events

In this chapter, an efficient model is proposed using K-means clustering and hybrid SVM-HMM modeling techniques. As described in chapter 3, the valve motion can be automatically identified by hybrid SVM-HMM based on the amplitude and timing of the peaks of the DUS high frequency component. Different patterns of the DUS components were found in this study which were variable on a beat to beat basis and throughout gestation. The amplitude of the peaks linked to the valve motion was different across the patterns and this affected the valve motion identification by the previous hybrid SVM-HMM method. Therefore, clustering of the DUS components based on K-means was proposed and the hybrid SVM-HMM was trained for each cluster separately. The valve motion events were consequently identified more precisely by beat-to-beat attribution of the DUS component peaks. It was an improvement compared to the hybrid method without clustering and this model would be useful for reliable screening of fetal wellbeing.

This chapter is a slightly modified version of the published article [117]:

- *F. Marzbanrad, Y. Kimura, K. Funamoto, et al. Model based Estimation of Aortic and Mitral valves Opening and Closing Timings in Developing Human Fetuses. IEEE Journal of Biomedical and Health Informatics vol.PP, no.99, pp.1, 2014. doi: 10.1109/JBHI.2014.2363452.*

5.1 Introduction

AS discussed in chapter 3, a method based on HMM was proposed for identification of valve motions [119]. Opening and closing of different valves, assumed as hidden states, were identified from the observed sequences of the peaks of the DUS signal component using HMM [119]. It was later found that the amplitude of the peaks can improve valve movement identification, in addition to the timing of the peaks. There-

fore, hybrid SVM-HMM and MD-HMM approaches were proposed in chapter 3 and 4, in which both the transition model of the valve motion and pattern of the peaks were used to identify the valve motion events from the observed peaks of the DUS signal component [123].

Although SVM-HMM provides a better estimation of fetal cardiac timings compared to HMM, nonstationary characteristics of the DUS signal complicate the classification of the peaks. The variable pattern of the DUS component is observed for both inter and intra subjects, which primarily depends on the orientation of the fetal heart to the transducer [174]. For example, the peak corresponding to aortic valve opening is sometimes smaller and sometimes larger than the peak representing the mitral closure. If a common training set is used for all existing patterns of the DUS components, the identification precision of valve motion by hybrid SVM-HMM is decreased.

In this chapter, K-means clustering is first used to find the patterns of the DUS components and match each beat-to-beat DUS components to one of the models. Then, the valve motion events are identified from the peaks of the DUS component using hybrid SVM-HMM trained specifically for its corresponding cluster. In this study, six patterns were identified for DUS components and the occurrence rate of each pattern was also analyzed for the fetuses in different age groups to investigate its relationship with the gestational age.

5.2 Materials and Methods

5.2.1 Data

Similar to the process described in the previous chapters, the DUS signal from 1.5 MHz Ultrasonic Transducer 5700 and the abdominal ECG signals were collected by a multi-channel data acquisition system. Signals were recorded simultaneously from 61 pregnant women at the gestational age of 16 to 41 (33 ± 6) weeks with healthy single pregnancy at Tohoku University Hospital, Japan. DUS signal patterns were compared in two age groups of early gestation (16-32 weeks) and late gestation (36-41 weeks), including 24 and 28 fetuses respectively.

M-mode and pulsed-wave Doppler were acquired simultaneous with DUS and fECG recordings, using convex 3.5 Hz of HITACHI ultrasound scanner, to verify the mitral and aortic valve opening and closing time obtained from the DUS signal. Ultrasonic diagnostic instrument Model EUB-525; from Hitachi health medical corporation and ACCUVIX A30; from Samsung Medison were used in this experiment. More details about the experimental set up can be found in our previous study [169].

5.2.2 fECG extraction

The fECG extraction process was the same as in the previous chapters. Data from 12 channels were recorded bipolarly from the electrodes placed on the maternal abdomen, and fECG was extracted from the composite abdominal signal, using a combination of maternal ECG cancelation and blind source separation with the reference signal (BSSR) [169]. The R-peaks of fECG were then automatically detected by applying a lower threshold (e.g. 5 times the mean of fECG over 10 second intervals) and peak detection using the derivative of the signal.

5.2.3 DUS signal decomposition

The collected DUS signal (figure 5.1-(a)) contained components linked to the movement of the fetal cardiac valves, walls or other organs. As discussed in the previous chapters and shown in [174], the high frequency component of the DUS signal is linked to the valve movement, while the low frequency component is associated with the cardiac wall motion. To obtain the valve motion related component, the DUS signal was decomposed by the multiresolution Wavelet analysis as described in the previous studies [79, 122]. In this part of thesis EMD is not used for decomposition, because wavelet analysis provides the components with more consistent amplitude range which can be better clustered, hence more suitable for the purpose of this study. The wavelet analysis uses a set of basis functions to decompose the signal into the detailed and the approximate signals, which are the higher and lower frequency components, respectively. The decomposition is repeated on the approximation signal to obtain detail and approximation signals at

the next level. In this study, the second order complex Gaussian was used as mother wavelet. The detailed signal of the DUS signal at level 2 is the high frequency component ($100 - 200$ Hz) which corresponds to the valve motion events (figure 5.1-(b)) [79, 174]. The envelope of the absolute value of this signal was taken by interpolating its maxima and smoothing by low pass filter (figure 5.1-(c)). In the rest of the chapter, this envelope is called "DUS component" for simplicity.

5.2.4 Segmentation and normalization

The DUS component was segmented into cardiac cycle sections and then normalized. Segmentation was performed using R-peaks of the simultaneously recorded fECG. Each segment of the DUS component was taken from R-R intervals of the corresponding fECG. It was then normalized by subtracting the mean and dividing by the standard deviation of the DUS component estimated over the segment. An example is shown in figure 5.1-(c).

5.2.5 Training

The training phase consisted of three sections: Clustering in which different models of the segments of the DUS components were automatically obtained using K-means clustering, HMM training in which the transition model was estimated from the training data and SVM training in which the SVM structure was developed. Training data set was obtained from 345 cardiac cycles of DUS components and fECG from 21 fetuses. The cardiac valve motion events for this train set, were identified manually based on expertise.

Clustering

K-means clustering method was used to estimate different templates for the segments of the DUS components. The k-means clustering [105] is a classical, most widely known and well-studied unsupervised learning approach, which iteratively clusters data into groups with members close to each other and far from members of other clusters. It is a fast algorithm with uncomplicated computation for each iteration and converges in few

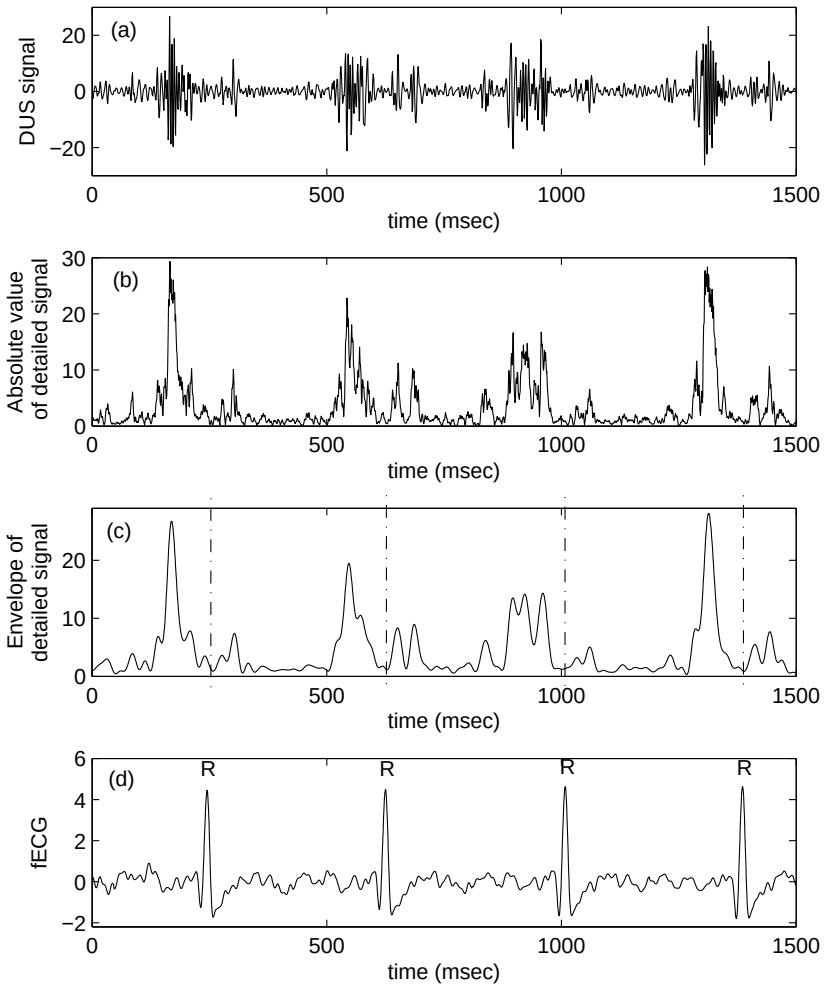

Figure 5.1: The decomposition of the DUS signal using the second order complex Gaussian as mother wavelet; (a) the DUS signal, (b) the detailed signal at level 2, (c) the envelope of the detailed signal (the DUS component) and its segments divided by dash-dot lines, (d) Simultaneously recorded fECG.

iterations [185].

For clustering and template matching, the first 350 samples (350 msec) of the DUS component in each segment were used (x in eq. (5.1)). However for HMM-SVM training and recognition, all samples (full length) of the segments were considered. The K-means clustering algorithm was performed based on Euclidean distance. It was used to find the clusters $C_1, ..., C_k$, such that:

$$\arg\min_{C_1,...,C_k} \sum_{h=1}^{k} \sum_{x_o \in C_h} \parallel x_o - \mu_h \parallel^2, (o = 1, 2, ..., M) \tag{5.1}$$

where x_o is the observed DUS component of segment (o), M is the number of observation segments (e.g. 345 segments) and μ_h is the mean of the observation segments in cluster C_h. Different number of clusters k from 3 to 16 was tested and the mean silhouette value was the highest for 6 clusters. The final number was therefore decided to be six ($k = 6$) which resulted a reasonable combination of the mitral and aortic valve motion peaks with different comparative sizes across the clusters. The centroid of the clusters and the DUS component segments of each cluster are shown in figure 5.2. K-means clustering function from statistics toolbox of MATLAB was used for clustering.

The percentage of observing each pattern was calculated for each fetus. Then the percentage of each pattern was compared for early and late gestation groups applying Mann-MannWhitneyWilcoxon test.

SVM-HMM training

The hybrid SVM-HMM method was proposed for recognizing the fetal valve motion in chapter 3 [123]. In brief SVM and HMM were combined to automatically identify the valve motion events based on the transition of the states and pattern of the observation. This method includes training and testing processes which are described below and in the next section, respectively.

Similar to the chapter 3, in this application eight hidden states were defined, including the valve motion and the transition events between them, namely: Mitral closing (Mc), transition 1 (TR1), Aorta opening (Ao), transition 2 (TR2), Aorta closing (Ac), transition 3

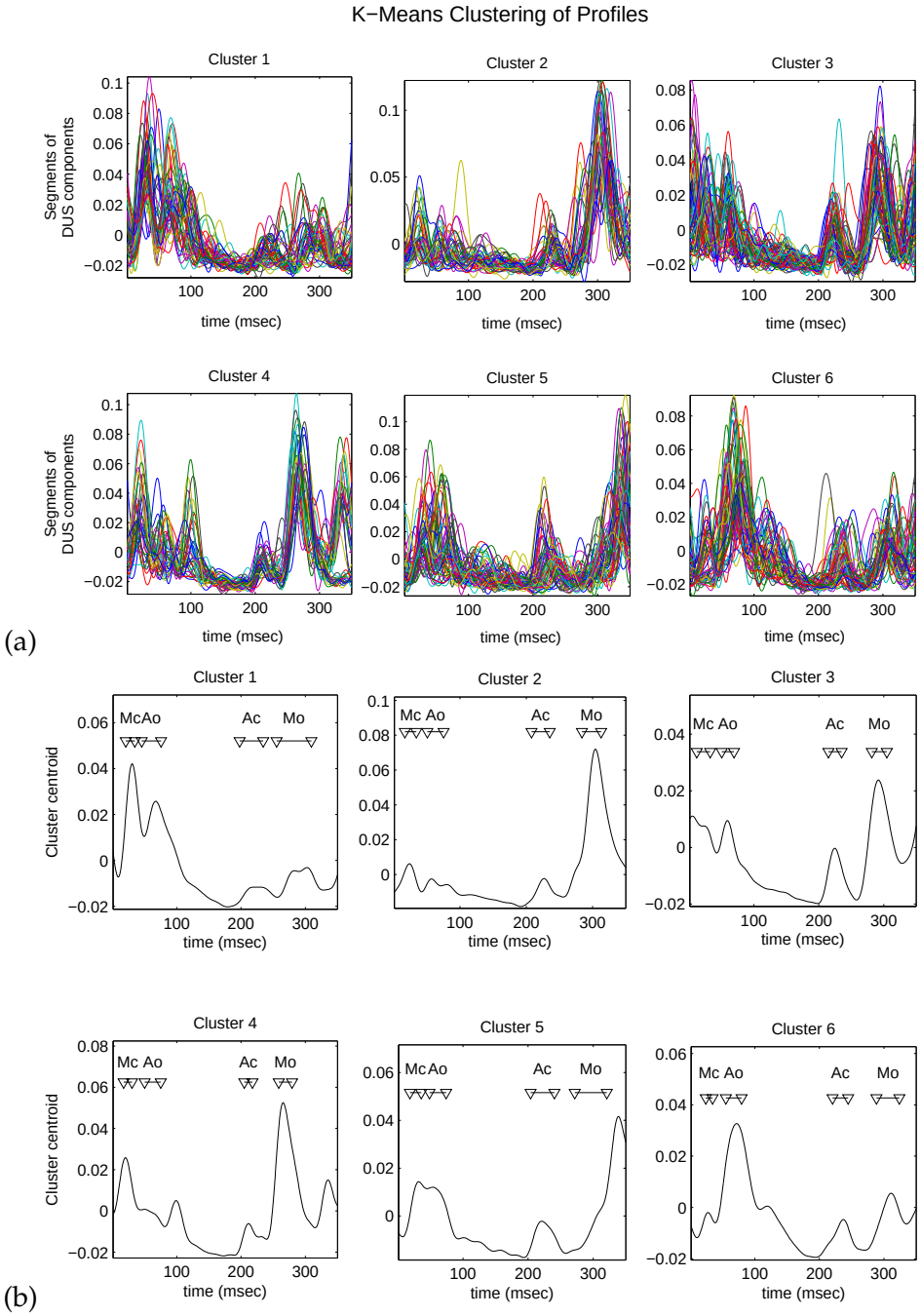

Figure 5.2: The DUS component segments which were clustered into six profiles are shown in the top figure (a), the centroid of each cluster are shown in the bottom figure (b). The mean $\pm$ SD duration of the valve motion timings of the training set for each cluster is marked with downward-pointing triangles in figure (b).

(TR3), Mitral opening (Mo), transition 4 (TR4). The HMM observation is the DUS component and the features are the timing and amplitude of the peaks of each segment of DUS component. In the hybrid SVM-HMM training, the transition matrix is estimated from HMM training process and the emission matrix is obtained from SVM training. The SVM-HMM training process was performed for the training data of each cluster ($C_h, h = 1..., 6$) separately.

Emission matrices were estimated using SVM and the observation was classified into eight classes which were the same as the hidden states as described above, i.e. Mc, TR1, Ao, TR2, Ac, TR3, Mo, TR4. For the training process, all peaks of each segment of DUS components were identified using the derivative of the signal. Then the amplitude of each peak and the interval between the peak and its proceeding R-wave were acquired as the classification features. In the SVM training process, the SVM classifier was trained and the support vectors were identified. This process was performed on the training data of each cluster separately to obtain the SVM classifier specific to each of the six clusters.

5.2.6 Automated recognition of valve motion

The main algorithm for identification of cardiac valve events includes template matching and hybrid SVM-HMM. The latter uses the trained models from the training process to find the valve timings for the new (test) data.

Template matching

The DUS components of the test data were segmented into cardiac cycles using their corresponding fECG R-R intervals. Then each segment was attributed to one of the clusters which gave the minimum Euclidean distance between the first 350 samples of each segment (y) and centroid of the cluster:

$$H(y) = \underset{h}{\operatorname{argmin}} \parallel y - \mu_h \parallel^2, (h = 1, 2, ..., 6) \tag{5.2}$$

where y is a segment of DUS component from test data and H is the cluster index. In order to identify the valve motion events in each segment, the trained model for its matched

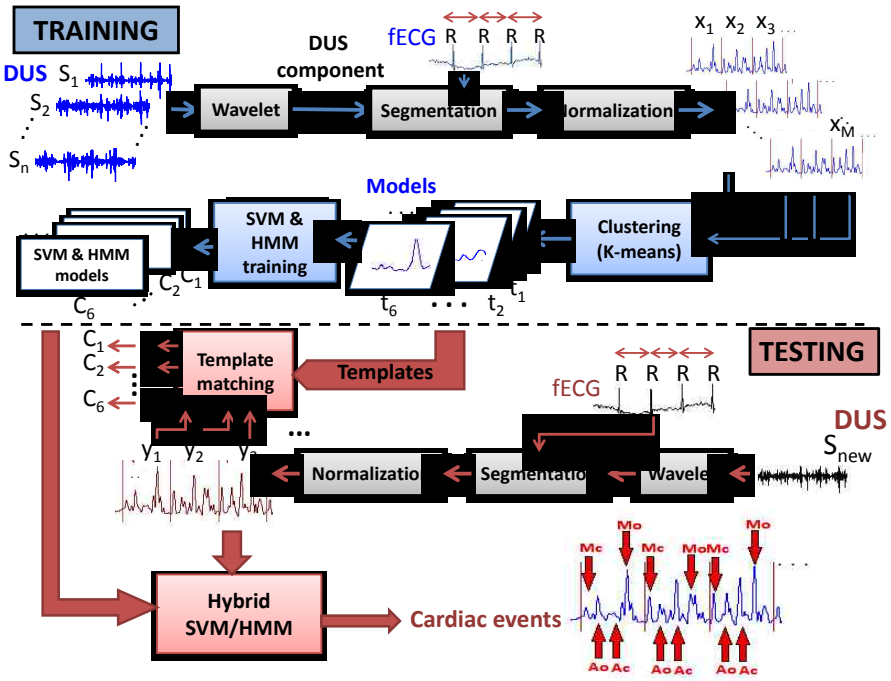

Figure 5.3: Block diagram of the training and testing processes.

cluster was used in hybrid SVM-HMM process.

Hybrid SVM-HMM

For each segment of the DUS components in the test data (y), the time and amplitude of the peaks were used to classify them by SVM classifier trained for the corresponding cluster of that segment ($C_{H(y)}$). As described in chapter 3, since HMM is based on probability models, a probabilistic output of SVM was obtained using Platt's method which provides the posterior probability of classifying the sample, i.e. $P(class|input)$ [152]. The emission probability distribution was estimated using the output of the Platt's SVM through the Bayes' rule [123].

The transition probability (from HMM training) and the emission probability matrices specific to each cluster were used to find the most likely sequence of events for each new segment of the DUS component, using Viterbi algorithm [155]. The block diagram of the training and testing process is shown in figure 5.3.

5.3 Results

5.3.1 Clustering

In the training phase the segments of the DUS components were clustered by K-means method. Six clusters with different patterns of the DUS component segments are shown in figure 5.2. The mean $\pm$ standard deviation (SD) ranges of the valve motion timings are shown in figure 5.2(b) for each cluster. The cluster centroids have peaks in the time range of the valve motion events, but with different comparative amplitude across 6 clusters.

5.3.2 Comparison of patterns for gestational age

The percentage of beats with each DUS pattern was calculated for 24 and 28 fetuses in early (16-32 weeks) and late gestation (36-41 weeks), respectively. The percentage of each pattern was compared between two groups using MannWhitneyWilcoxon test, considering p-value < 0.05 as significant. Table 5.1 shows the p-values for comparing each pattern and figure 5.4 shows the median and 25%-75% quartile ranges of the percentage of occurring for each pattern in early and late gestation groups. The Result shows that

Table 5.1: P-value results for comparison of the percentage of different patterns for the fetuses in early gestation (16-32 weeks) and late gestation (36-41 weeks), applying MannWhitneyWilcoxon.

Patterns	p-value
1	0.0083
2	0.1541
3	0.0422
4	0.0061
5	0.0448
6	0.0258

the patterns 1 and 6 occurred with significantly higher rate after 36 weeks, compared to the cases before 32 weeks. On the other hand patterns 3, 4 and 5 were observed with significantly higher rates for the early gestation group. The percentage difference between two age groups was not significant for pattern 2.

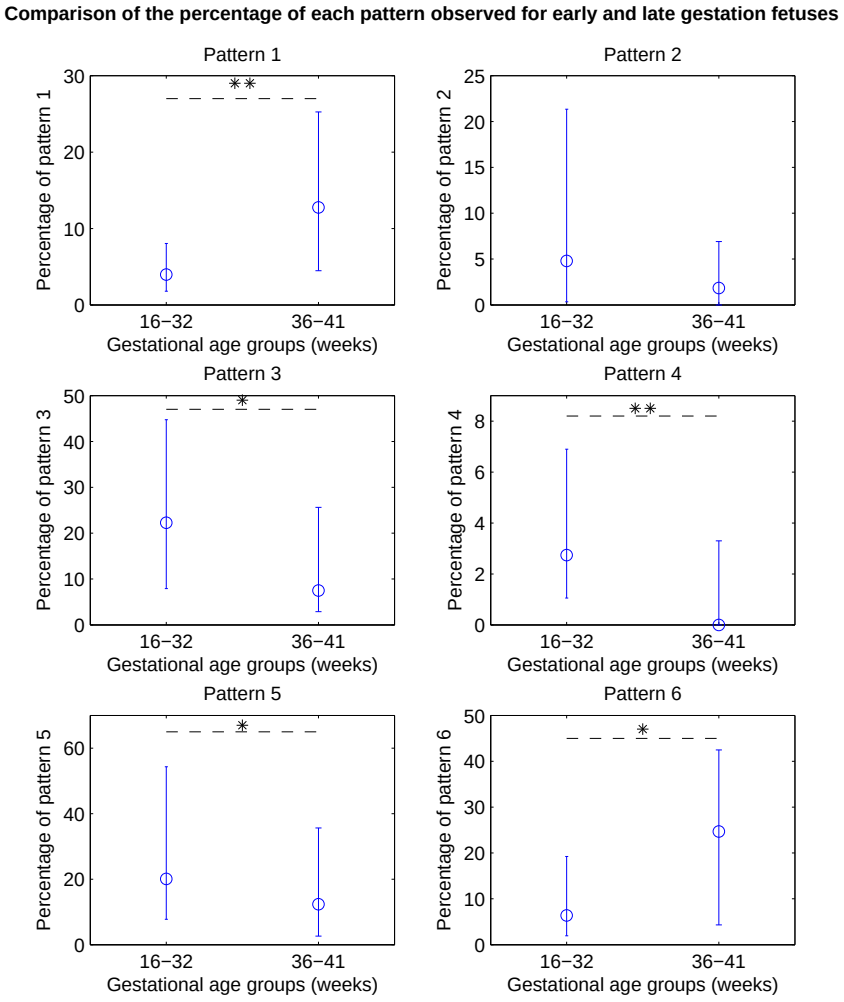

Figure 5.4: The median and 25%-75% quartile ranges of the occurrence percentage of each pattern in early (16-32 weeks) and late (36-41 weeks) gestation groups. Groups were compared by Mann-Whitney U test and significant differences were marked as follows: $P < 0.05$ (*) and $P < 0.01$ (**).

5.3.3 Validation with Echocardiography images

M-mode and pulsed-wave Doppler were acquired simultaneous to DUS and fECG recordings for two fetuses to validate the aorta and mitral motion timings respectively. The data from these two cases were not involved in the training process and only used for testing. M-mode image is used to evaluate the structure and operation of the valves. Figure 5.5 shows opening and closing of the aorta using M-mode recording for 5.7 seconds, which are marked and compared with the results of the proposed method. This figure shows that the aorta opening and closing events identified by the proposed method were aligned with the events shown in the M-mode image. The identified opening and closing events of mitral are not shown to avoid confusion.

The blood flow Doppler waveform through the mitral valve is shown by Pulsed wave Doppler in figure 5.6 (a). The valve motion events were identified in two ways; using K-means clustering and hybrid SVM-HMM for each cluster (figure 5.6(b)) and using the hybrid SVM-HMM without clustering (figure 5.6(c)) [122,123]. For both methods wavelet was used to obtain the DUS component, applying the same training set, but the set was partitioned into the clusters for the new method.

Figure 5.6 shows that the identified mitral movement events by the new method were aligned with the pulsed wave doppler images (figure 5.6(b)), while some of them were misidentified by the previous method (figure 5.6(c)). This comparison can be investigated in more details by considering the mitral opening event occurred at 1543 msec, misclassified by the previous method. The new technique found the segment of 1268-1700 msec closest to the cluster 2. The range of mitral opening event for this cluster is illustrated in figure 5.7(a). It is shown that the amplitude of this peak and its interval from the preceding R-peak of fECG at 1543 msec, is well situated in range of Mo events in figure 5.7(a). On the other hand, the trained range of the Mo peak amplitude in figure 5.7(b) was wider and included even small amplitudes, because clustering was not performed in the previous method and training was based on the DUS components with various patterns. This is one reason why the peak at 1596 msec was wrongly recognized as Mo. It is worth noting that SVM is only a part of classification, and transition of the events takes part in recognition of the events in the HMM part of the hybrid method.

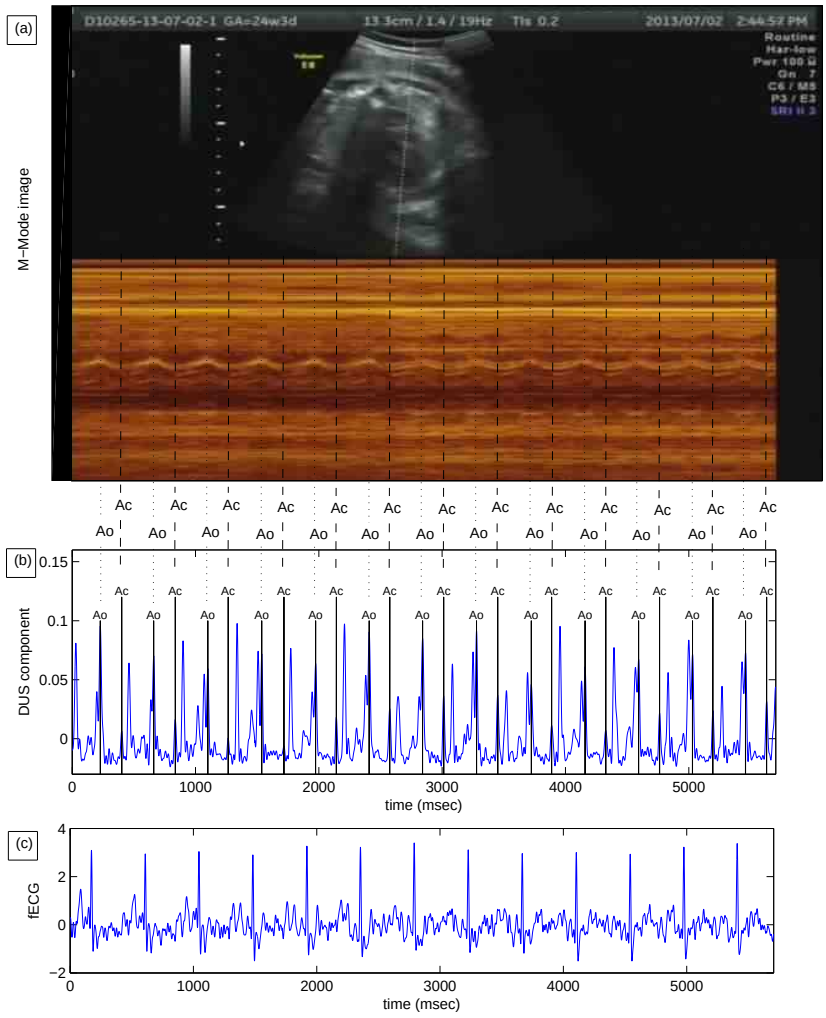

Figure 5.5: (a) The M-mode image of the opening and closing time of the aortic valve for a fetus at 24 weeks of gestation. The dashed lines depict the aorta opening (Ao) and closing (Ac) events. (b) The DUS components and the events identified by the automated method. (c) Simultaneously recorded fECG.

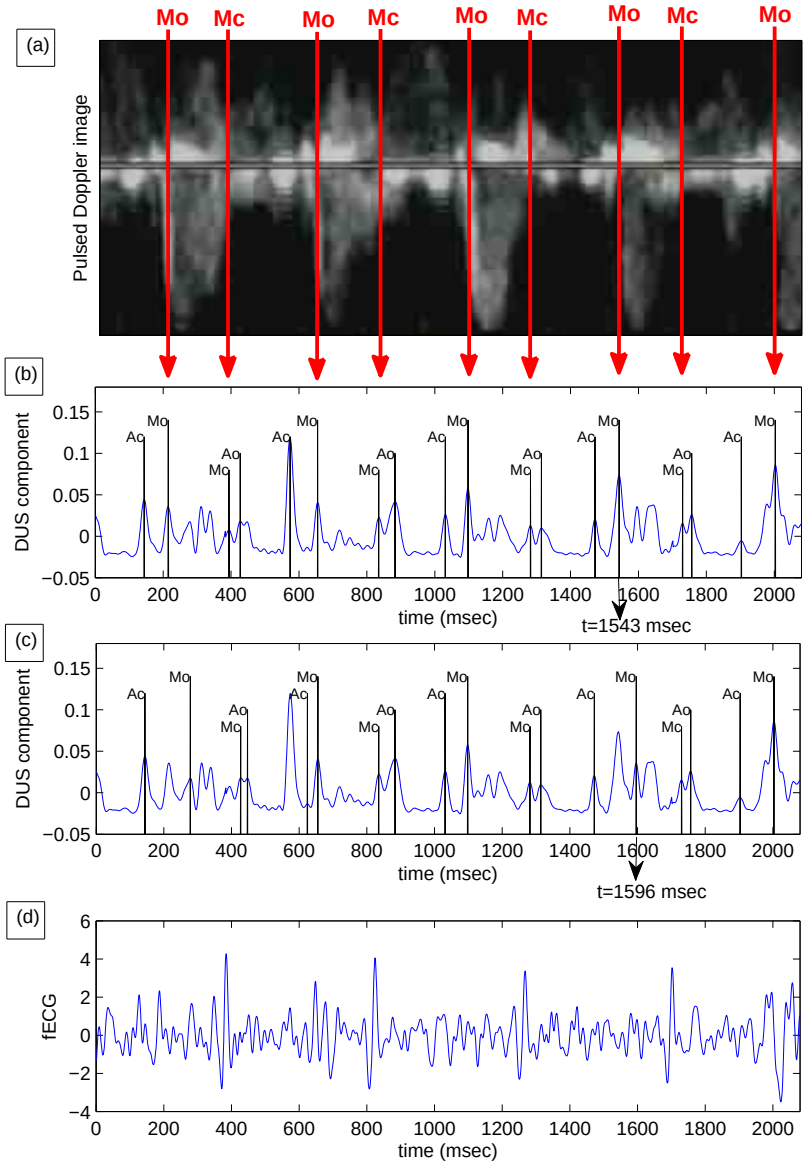

Figure 5.6: (a) Pulsed wave Doppler signal of fetal mitral valve movements annotated to show the mitral opening (Mo) and closing (Mc) for a fetus at 24 weeks of gestation, (b) The DUS component and the valve motion events identified by the proposed method (K-means and hybrid SVM-HMM), (c) The DUS component and the valve motion events identified by the hybrid SVM-HMM without clustering [123], (d) Simultaneously recorded fECG.

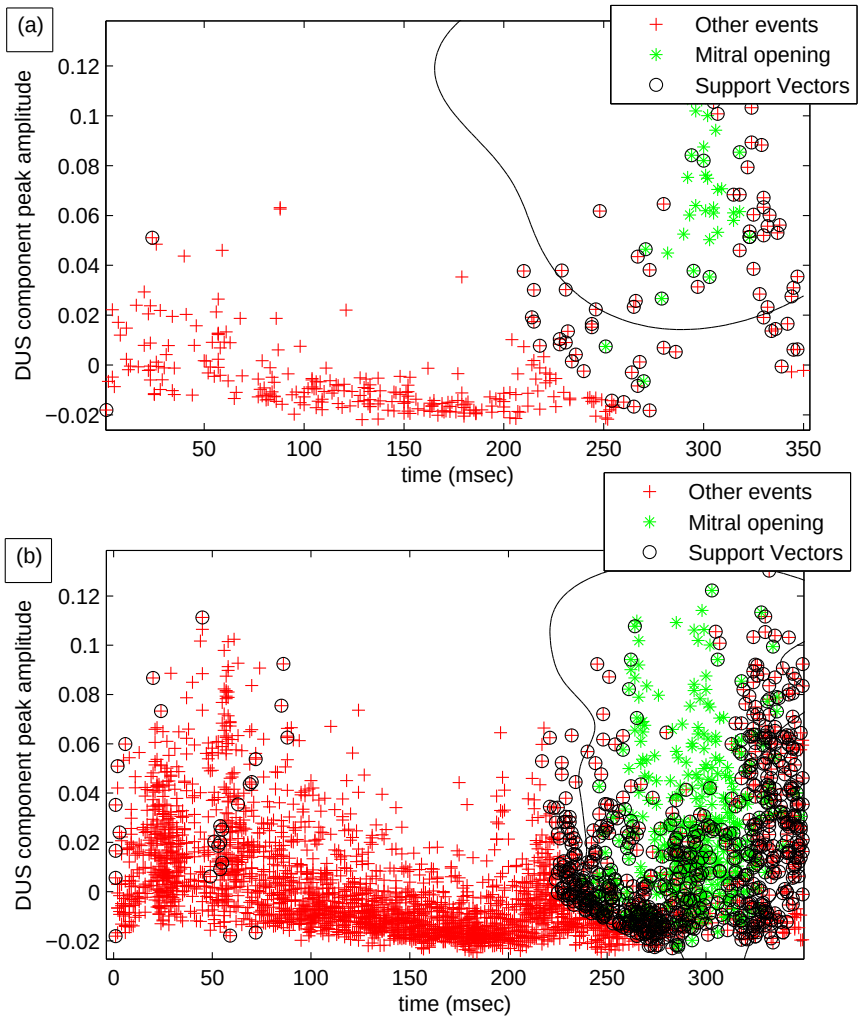

Figure 5.7: (a) The trained SVM for classification of mitral opening for the second cluster, used by the new method. (b) The trained SVM for classification of mitral opening for all training data regardless of the clusters by the previous method.

5.3.4 Cross validation results

To quantitatively compare the results of the new method with the previous method which was based on SVM-HMM without clustering [123], 10-fold cross validation was performed on the training data. Training data containing 345 segments of DUS component from 21 fetuses were partitioned into training and testing sub-sets. Partitioning was performed for each cluster to include all clusters in training and testing. The identification precision and recall of each valve timing event were calculated as follows and averaged over the 10 folds:

$$Precision_i = \frac{T_i}{T_i + \sum_j F_{ij}} \tag{5.3}$$

$$Recall_i = \frac{T_i}{T_i + \sum_j F_{ji}} \tag{5.4}$$

where i refers to one of the valve motion events (Mo, Mc, Ao or Ac), T_i is the number of true estimation of event i and F_{ij} indicates the number of times event j was mistakenly identified as event i. Table 5.2 summarizes the precision and recall of different identified events by two methods. Cross validation result shows improvement of precision and recall of identifying mitral opening by 10.8% and 9.4%, respectively and aorta closing by 10.7%. Overall, the average precision and recall were improved in the new method (precision: 83.4% and recall: 84.2%) compared to the previous approach (precision: 79.0% and recall: 79.8%)[123].

Table 5.2: Precision (%) and recall (%) of valve motion identification using the new hybrid SVM-HMM with clustering versus the previous SVM-HMM approach without clustering [123].

Parameter	Methods	Mc	Ao	Ac	Mo	Average
Precision	New	89.5	87.8	86.3	69.9	83.4
	Previous [123]	91.6	89.7	75.6	59.1	79.0
Recall	New	92.4	89.2	86.3	68.7	84.2
	Previous [123]	93.4	90.8	75.6	59.3	79.8

Table 5.3: Mean ± standard error (SE) of the intervals between R-peak of fECG and valve motion and the rate of identified events.

Intervals	Mean ± SE (msec)	Rate*
R-R	420.5 ± 34.1	100 %
R-Mc	24.2 ± 4.1	98.6 %
R-Ao	59.8 ± 5.0	99.8 %
R-Ac	220.2 ± 7.9	99.7 %
R-Mo	304.6 ± 11.0	98.8 %

* The rate is calculated from the number of identified valve motion events out of 8510 beats belonging to 61 fetuses.

5.3.5 Extended results

The proposed method was also applied on data from other fetuses not involved in training, to evaluate the identification rate and valve timing intervals. The average intervals between R-peak of the fECG and valve openings and closings for 8510 beats belonging to 61 cases and the rate of identified events are summarized in table 5.3.

5.4 Discussion

The DUS signal has a transient nature and the signal content is widely variable even on a beat-to-beat basis, depending on the orientation of the fetal heart and the DUS transducer. The DUS signal variability for inter and intra subjects was also discussed by Shakespeare et al. [174]. In this chapter, it was shown that the development and maturation of the fetal heart also take part in the variability of the patterns. Multiple factors may contribute to the observed differences of the signal patterns for the fetuses before 32 weeks and after 36 weeks, including fetal growth, physiological development and changes in the dominant positioning. It was proposed in previous studies to use STFT, Wavelet transform or EMD to extract the component linked to the valve motion, but this component does not have a single pattern for all beats and different fetuses. Figure 5.1 (c) shows an example in which the change in the pattern of DUS component is observed in successive beats. The DUS component patterns were clustered into six groups by K-means and the DUS components had peaks linked to the valve motion in a common range of timing and am-

plitude within each groups, different from other clusters. Figure 5.2 shows the centroid of each cluster and the range of valve motion events determined from the training data specific to each cluster, which demonstrates the difference in the average amplitude of peaks linked to each event across clusters. This was the point to use clustering to train the SVM-HMM for each cluster separately and decode the peaks of the DUS components based on trained SVM-HMM specific to the matched cluster.

Compared to the method in which clustering was not performed (discussed in chapter 3), this method achieved better precision and recall. Because the DUS components of the training set without clustering, had different patterns and the amplitude and timing range of the peaks representing the events were wide and disparate. When data were clustered before training, the peaks linked to each event were concentrated and more unified in a certain range of timing and amplitude, from which the valve opening and closing were better identified. For example the trained SVM for one of the clusters by the new method (figure 5.7 (a)) was compared with the SVM trained based on the whole training set regardless of their pattern (figure 5.7 (b)) according to the previous method. The first SVM could better discriminate the range of amplitudes corresponding to Mo.

As discussed in previous chapters, Systolic Time Intervals including ICT, PEP and VET, are significant indicators of myocardial function. The STIs which depend on the onset of QRS complex of fECG, Mc, Ao and Ac could be estimated with more than 98.6% identification rate and higher than 86.3% precision by this method. The pulsed wave Doppler and M-mode echocardiography may be performed to find the cardiac intervals but need skilled specialists to perform and are highly specialized compared to the Doppler Ultrasound method suggested in this study. The use of DUS signal and fECG provides a simpler way and with the automated technique proposed, beat-to-beat valve motion timings are continuously evaluated with less time and skill for operation. Furthermore, using pulsed-wave Doppler, the recording is captured in one screen size and the motion of only one valve (e.g. mitral or aorta) at a time is monitored; while DUS signal enables identification of opening and closure of mitral and aorta in each beat with a recording of DUS and fECG. In this chapter M-mode and pulsed wave doppler images were used to verify the results of automated identification. More quantitative comparisons can be

performed in future studies.

5.5 Conclusion

Opening and closing of fetal cardiac valves are reflected as peaks in the high frequency component of the DUS signal. In this study, we found six different patterns for the DUS component. The occurrence rate of five patterns for the fetuses with less than 32 weeks of age was different from the fetuses older than 36 weeks. Each pattern had different amplitude range and timing of the peaks linked to the aortic and mitral valve motion. K-means clustering was applied to the DUS components in training set and SVM-HMM was trained for each cluster separately. In this way, valve motion events were detected from each DUS component based on the trained SVM-HMM specific to its matching cluster. The identification of opening and closing of the mitral by SVM-HMM was improved using clustering compared to the method without clustering as verified by pulsed wave Doppler image. The average precision and recall of the method with clustering were 83.4% and 84.2% respectively, which were higher than the method without clustering. More than 98.6% of cardiac valve motion events were identified by the new method.

Chapter 6

Automated measurement of ICT from Doppler ultrasound signals without using fECG

Isovolumic Contraction Time (ICT) is the interval from mitral closing to aorta opening. Fetal ICT can be noninvasively measured from DUS signal by automated identification of mitral and aortic valve timings as discussed in previous chapters. Fetal ECG has a crucial role as a reference in automated methods by identifying the onset of each cardiac cycle. However simultaneous recording of abdominal ECG and DUS and separation of fECG from the noisy mixture of ECG complicate this method. In this chapter the automated identification of valves' motion without using fECG was investigated. The DUS signal was decomposed by EMD to high and low frequency components linked to valve and wall motion, respectively. The peaks of the latter were used for segmentation of the high frequency component as a substitute for fECG. Results show a significant positive linear correlation between average ICT obtained with and without using fECG.

This chapter is a slightly modified version of the published article [120]:

- *F. Marzbanrad, Y. Kimura, M. Endo, et al. Automated measurement of fetal Isovolumic Contraction Time from doppler ultrasound signal without using fetal electrocardiography, Computing in Cardiology Conference (CinC), 2014 , vol., no., pp.485-488, 2014.*

6.1 Introduction

FETAL ICT is the Mc-Ao interval which is a reliable index of fetal cardiac contractility and can sensitively detect impaired cardiac function [85,204]. A study by Koga et al., found the prolonged ICT significantly correlated with abnormalities in perinatal course and it was suggested as a prediction of adverse outcome for the fetus [85]. Automated

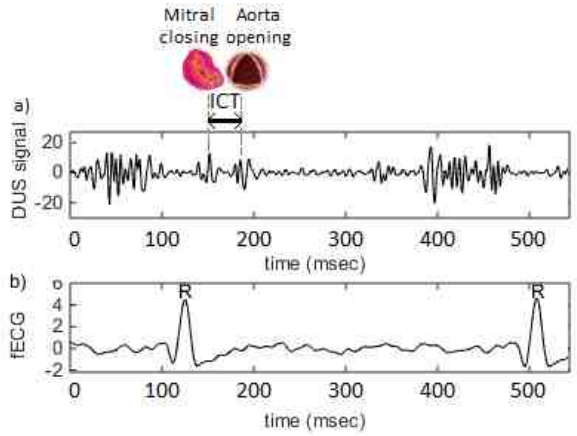

Figure 6.1: An illustrative example of mitral closing and aorta opening identification from the raw 1-D DUS signal (a), and fECG as a reference (b), to estimate ICT as Mc to Ao interval.

.

differentiation of mitral and aorta opening and closing events from the peaks of the high frequency component of DUS, was described in previous chapters. Figure 6.1 shows an illustrative example of ICT using DUS signal. Simultaneously recorded fECG has a crucial role in automated methods; by specifying the beginning of cardiac cycle for segmentation. However simultaneous recording of abdominal ECG with DUS signal and separation of fECG from a noisy mixture of maternal ECG and other interfering signals and artifacts complicate this technique.

In this chapter automated identification of valve movements from DUS signal without using fECG was investigated. To this aim the DUS signal was decomposed by EMD to IMFs. The first IMF (high frequency) was linked to the valve motion and the fourth IMF (low frequency) was related to the cardiac wall motion. The peaks of the latter were used for segmentation as a substitute for fECG R-waves. The mitral and aortic valve movements were automatically identified by hybrid SVM-HMM as described in chapter 3.

6.2 Methods

6.2.1 Data

Similar to the discussed procedure in chapter 3, DUS signal was recorded from 21 pregnant women at the gestational age of 16 to 41 weeks with normal single pregnancies at Tohoku University Hospital in Japan. The continuous DUS data were obtained with 1 minute in length and sampled at 1 kHz with 16-bit resolution. For comparison purposes, abdominal ECG signals were also recorded simultaneous with DUS. The fECG extraction process was described in previous chapters.

6.2.2 DUS signal decomposition

Similar to the chapter 3, DUS was decomposed by EMD into a set of IMFs. The first IMF i.e. the highest frequency content was used to identify the valve movements. The peaks of the absolute value of this IMF can be linked to the opening and closing of the mitral and aortic valves. The fourth IMF, i.e. the low frequency component, includes peaks associated with fetal cardiac wall motion. The atrial wall contractions (Atc) were represented by the prominent peaks of the fourth component occurring once per each cardiac cycle. They were used as a reference for segmentation of the first IMF, as explained in the next section. The envelope of the first and fourth IMFs were obtained using low-pass filter. Their peaks were then detected based on the sign of the first and second derivatives.

6.2.3 Segmentation and normalization

The sequence of Atc-to-Atc intervals was calculated from the detected Atc peaks of the fourth IMF. This sequence was processed to fix misidentified Atc peaks as follows. For each window of five consecutive Atc-Atc intervals, the middle interval which was deviated from the mean of the four other intervals by more than 10%, was replaced by that mean value. The first envelope of the first IMF was then divided into segments of Atc-Atc intervals. Then each segment was normalized by subtracting the mean and dividing by the standard deviation of the segment.

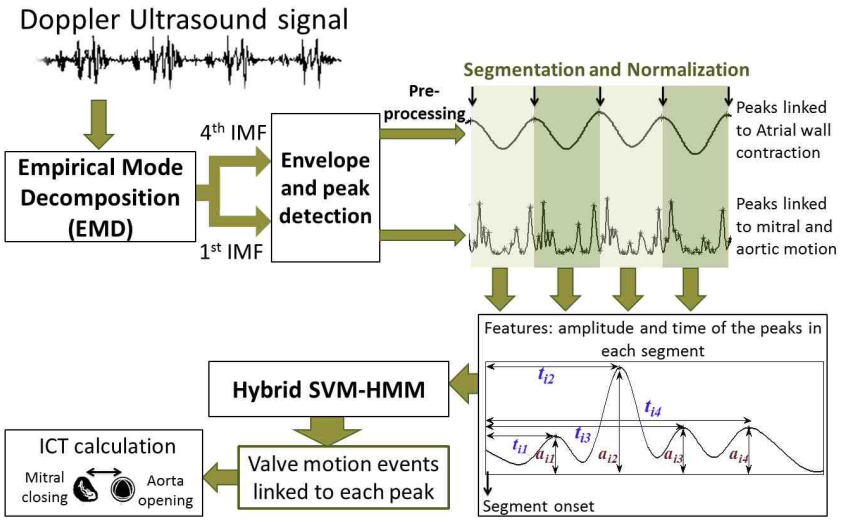

Figure 6.2: Schematic illustration of the ICT estimation process without using fECG.

6.2.4 Identification of valve movements

The hybrid SVM-HMM method was proposed for identification of valve movements as described in chapter 3. The hybrid model was trained once and then the trained model was used for identification of valve events from the new data. In this study we were particularly interested in Mc and Ao versus the other states. The observation sequence is the amplitude of the peaks of the first IMF envelope, as well as the time interval between each peak and its proceeding Atc peak (the beginning of the segment). Details of the hybrid SVM-HMM process can be found in chapter 3. After performing hybrid SVM-HMM, ICT was calculated from the interval between mitral closing and aorta opening. Then beat to beat ICT values were averaged over all cardiac cycles in one minute for each fetus. The whole process is illustrated in figure 6.2

6.2.5 Comparison

For comparison of the new method with the previous technique, fECG for all 21 fetuses were used as a reference to find ICT with the method in chapter 3. The BlandAltman method [17, 157] was used to investigate the agreement between previous and new method and to calculate the variability of the estimates. Pearson's coefficient of correla-

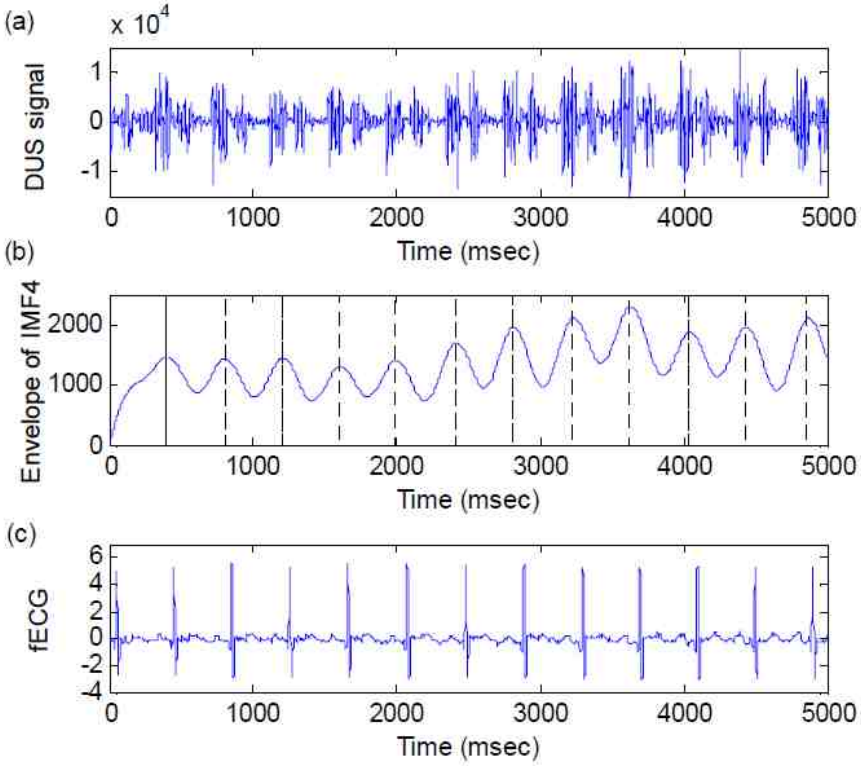

Figure 6.3: (a) 5 second recording of DUS signal. (b) Reference from the envelope of IMF 4, which is a low frequency component of the DUS signal. Dashed lines show the segmentation reference points found from peaks. (c) Simultaneous fECG.

tion was calculated to measure the association between the ICT intervals obtained using two methods.

6.3 Results

Regular wall movement peaks were detected from the fourth IMF and used as a reference for segmentation. Figure 6.3 shows an example of the segments found using peaks of the envelope of IMF4 (figure 6.3(b)), which can be compared with the reference from R-peak of fECG as in figure 6.3(c). ICT was measured for 21 fetuses using the new method (without using fECG) and previous method (using fECG) described in chapter 3. Mean and standard error of the averaged ICT over 1 minute for each fetus are summarized in table 6.1. The relationship between ICT measured with two methods was almost linear

Table 6.1: Mean and standard error (SE) of ICT averaged over all cardiac cycles (in 1 minute) for 21 fetuses using the new method (without using fECG) and previous method (using fECG).

Method	Mean (msec)	SE (msec)
New method	37.3	3.6
Previous method	36.8	2.8

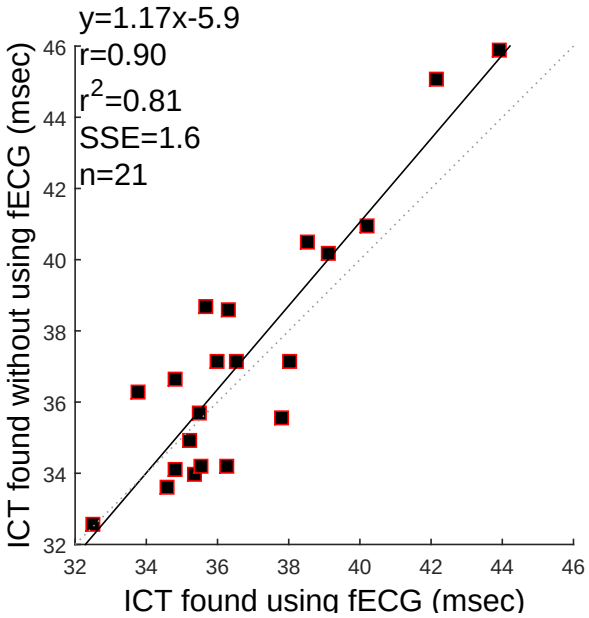

Figure 6.4: Bland-Altman analysis for comparing the average ICT from 21 fetuses measured by the new method (without using fECG) versus the previous method (using fECG). r: Pearson correlation r-value, r2 : Pearson r-value squared, SSE: sum of squared error, n: number of fetuses.

($r^2 = 0.81$) (figure 6.4). The agreement between these measurements is shown in figure 6.4 and figure 6.5, which show the average differences of changes between ICT measured by different algorithms, the variability of the estimates, limits of agreement ($\pm 1.96 * SD$), and the strength of the associations between the two measurements. The agreement between methods was high, difference was not significant and had a low variability of the estimate. The correlation coefficient $r = 0.90$ shows a strong association between methods. Although for the new method fECG was not used, the mean of absolute difference of 1.4 msec was obtained which is small compared to the large range of variability of ICT.

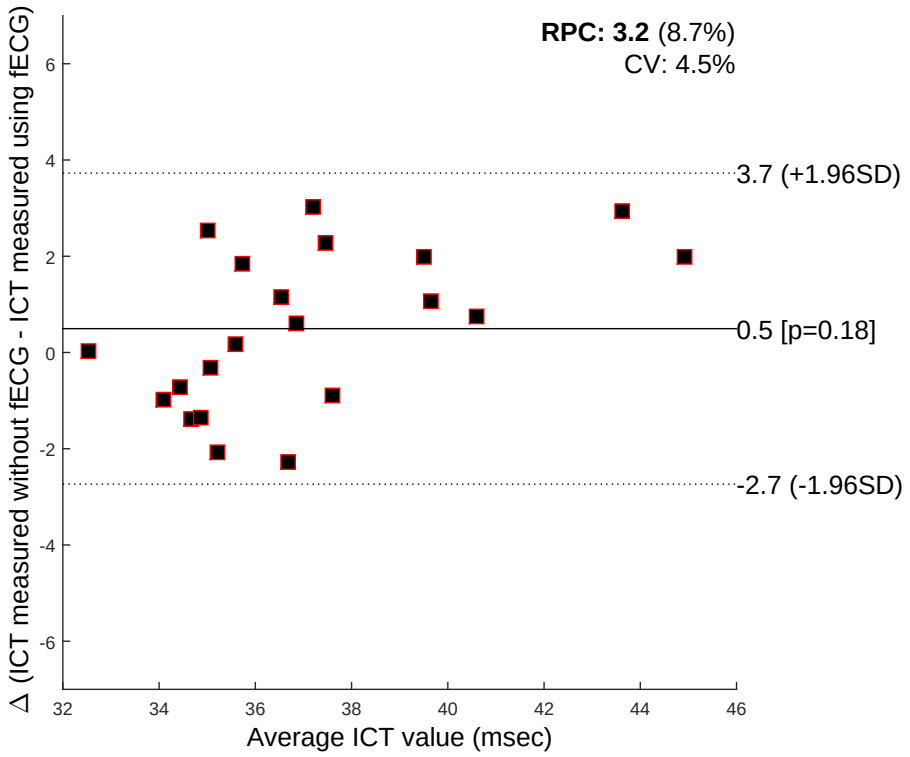

Figure 6.5: Bland-Altman plot (bias and 95% limits of agreement: 1.96SD) for the average ICT from 21 fetuses measured by the new method (without using fECG) versus the previous method (using fECG). RPC(%): reproducibility coefficient and % of mean values, CV: coefficient of variation (SD of mean values in %).

6.4 Discussion

ICT is a significant index which can be estimated from the timing of mitral closure and aorta opening. Although fECG was not involved in manual measurement of ICT proposed in previous studies [85, 204], it was required as a reference for automated methods as described in previous chapters. R-peaks of the extracted fECG from the abdominal ECG provide a stable and accurate reference for segmentation of DUS signal component into cardiac cycles. However, to this aim, abdominal ECG should be recorded simultaneous with DUS signal and fECG should be extracted from the mixtures; which require extra cost, equipment and processing. The new automated method without fECG provided ICT measurement in acceptable agreement (limit of agreement (-2.7 to 3.7 msec)) with the average ICT obtained from the previous method. However larger differences were found for beat to beat ICA measured with and without using fECG (6.1 $\pm$ 3.8 msec). Further studies are required for more accurate segmentation. A combination of DUS components (IMFs) may provide a more stable reference for segmentation. Other processing methods for correction of the false segmentation points may also improve this task.

6.5 Conclusion

Fetal ICT can be estimated noninvasively from DUS signal. Different from the previous automated methods for identifying ICT, fECG was not used as reference for the technique proposed in this chapter. Instead, the low frequency component of DUS signal was used for segmentation. Results showed that the measured average ICT with this new method was in agreement with the average ICT measured by the previous method which required fECG as reference (correlation coefficient: r = 0.9, bias = 0.5 msec, 95% limits of agreement: -2.7 to 3.7 msec).

Chapter 7

Classification of Doppler Ultrasound Signal Quality

1-D DUS is a commonly applied technique for fetal heart rate monitoring, but as discussed in the previous chapters, it can also be used to identify the fetal cardiac valve motion timings. However DUS is highly susceptible to noise and variable on a beat-to-beat basis. Therefore it is crucial to assess the signal quality to ensure its validity for a reliable estimation of the valve movement timings. An automated quality assessment can provide the operator with an online feedback on the quality of DUS during data collection. This chapter investigates automated classification of the DUS signal quality using Naive Bayes (NB) classifier.

This chapter is a slightly modified version of the article [118]:

- *F. Marzbanrad, A. Khandoker, M. Endo, et al. Classification of Doppler Ultrasound Signal Quality for the Application of Fetal Valve Motion Identification, Computing in Cardiology Conference (CinC), 2015.*

7.1 Introduction

SEVERAL automated techniques for identification of valve movements were proposed in previous chapters to overcome the shortcomings of manual methods including their time consuming process and vulnerability to inter and intra observer errors [116, 117, 123]. However the pattern and the quality of the DUS signal were found to be variable, even on a beat-to-beat basis [117]. The signal is highly contaminated by noise and its extensive variability and nonstationary characteristics complicate the valve motion identification. Therefore, an automated DUS quality assessment is required for a reliable estimation of the valve timings and also providing a real time feedback to the

operator during data collection. The importance of DUS signal quality assessment for its classic application in FHR monitoring, was investigated in previous studies [107,179]. This chapter focuses on the signal quality assessment for the extended application of DUS signal in valve motion identification.

7.2 Methods

7.2.1 Data acquisition and processing

Data acquisition and processing methods were described in previous chapters. A multichannel data acquisition system was used to collect the simultaneous DUS and ECG data. Fetal ECG was extracted using BSSR and used as a reference for segmentation of the DUS signal into cardiac cycles. To isolate the high frequency component of the DUS signal linked to the valves' movement, the DUS signal was decomposed by the multiresolution Wavelet analysis, the same as in chapter 5 [79,117]. The signal segments were then normalized by subtracting the mean and dividing by the standard deviation. Considering that the valve motion events mostly happen within 350 msec following the R-peak [79,117,123], this section of the DUS segments was used for quality assessment.

7.2.2 Signal quality annotation

Signal quality annotation was performed in two phases, using 345 DUS segments. In the first phase, five beats with the closest heart rate to the median of FHR were selected from each recording for training. Total of 285 DUS segments were presented to two medical doctors and two researchers to rate the quality independently. The scoring was based on observing the data to identify four peaks, corresponding to Mc, Ao, Ac and Mo. Five quality levels were defined as described in table 7.1 and given to the annotators as instructions on quality rating. Examples of a very good and a very bad quality signal scored by the annotators are shown in figure 7.1. The possible ranges of Mc, Ao, Ac, and Mo events were shaded with yellow, green, magenta and cyan colors respectively, as guides for the annotators.

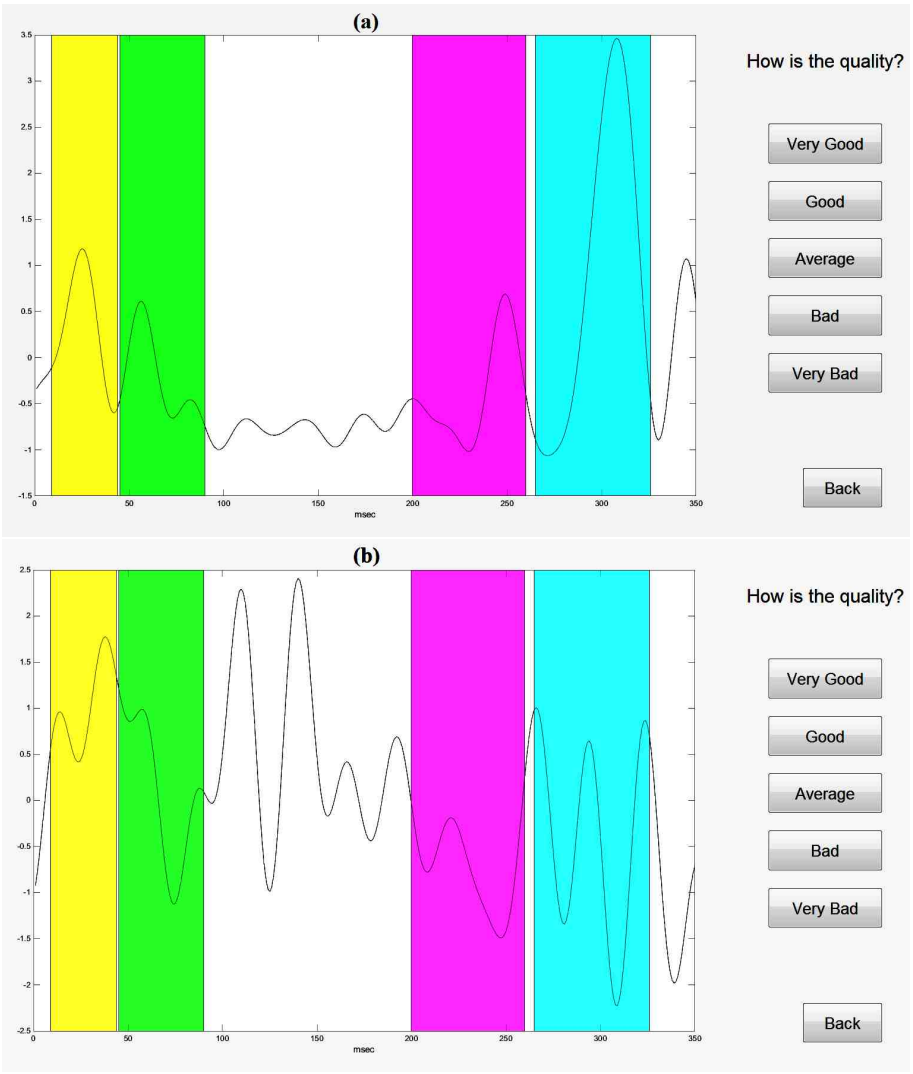

Figure 7.1: Two examples of annotated signals as very good (a) and very bad (b). The possible ranges of Mc, Ao, Ac, and Mo events were shaded with yellow, green, magenta and cyan colors respectively, as guides for the annotators.

Inter-rater agreement was tested by Fleiss kappa test [23, 52]. It calculates the degree of

Table 7.1: Description of the quality levels used for annotation

Quality Level	Quality Description
very good	Mc, Ao, Ac, Mo peaks are clearly detectable with no doubt.
good	Although the signal is slightly noisy, at least 3 events can be clearly detected.
borderline	It is difficult to detect the events, but some traces are observed, or at least two events can be detected.
bad	There is mostly noise, it is impossible to detect the events.
very bad	No trace of the events, only noise.

agreement in classification against the completely random rating. Scores of 1 to 5 were assigned to very bad to very good labels. The signals with the average score of below 2.5 and above 3.5 were labeled as unacceptable (60 signals) and acceptable (121 signals), respectively; while others were labeled as ambiguous (104 signals). In the second phase in order to balance the classes, 60 additional poor quality DUS segments as confirmed by the annotators were selected from the recordings and labeled as unacceptable.

7.2.3 Signal quality indices

Twelve features were selected mostly based on the signal properties in the valve motion ranges compared to the remaining time intervals. The plausible valve motion ranges were defined as: Mc: (9-44), Ao: (45-90), Ac: (200-260), Mo: (265-326), all in msec following the segment onset (preceding R-peak) [79, 117]. The features were as follows and all normalized:

- The ratio of the power (SQI_1), number of peaks (SQI_2), mean peak amplitude (SQI_3) and variance (SQI_4) in the valve motion range to the values in the remaining time intervals.

- kurtosis (SQI_5), skewness (SQI_6), Hjorth (SQI_7) parameters and sample entropy

(SQI_8: $m = 1, r = 0.1$, SQI_9: $m = 1, r = 0.2$, SQI_{10}: $m = 2, r = 0.1$, SQI_{11}: $m = 2, r = 0.2$) as described in previous studies [29,177].

- Minimum ratio of the 2nd to 1st singular value (SQ_{12}) from Singular Value Decomposition (SVD) of a matrix containing consecutive windows of the signal with various sizes: 10, 15, 20,...,100 [89,177].

7.2.4 Classification

An overall quality metric was obtained from the quality features $SQI_{1,2,..,12}$. A naive Bayes (NB) classifier with kernel density estimate was used for this purpose. NB classifier is a widely used supervised learning method which is fast and simple to implement [75,131]. It uses the training data to estimate the conditional distribution of the features given the classes and also distribution of the classes. Then it assumes conditional independence of the features given the classes which dramatically simplifies the estimation of the probabilities. It estimates the posterior probability through the Bayes rule and classifies a sample to the most probable class. It is important to note that in practice the features may not be independent while NB still works properly. Since some features did not have normal distribution, kernel density estimate was performed based on the training data [75].

10-fold cross validation was used to evaluate the classification performance, and the accuracy, sensitivity and specificity in train and test sets were calculated.

7.3 Results

Inter-rater agreement results of Fleiss kappa test showed a fair agreement with overall $\kappa = 0.300$, C.I. (95%) of $\kappa = [0.293 - 0.307]$, and $p < 0.0001$ confirming that the observed agreement was not accidental. Kappa values for the score 1 to 5 were: 0.224, 0.257, 0.232, 0.277, 0.507, respectively.

Sensitivity (Se), was measured as the proportion of unacceptable signals that were correctly identified as unacceptable. Specificity (Sp), was also calculated as the proportion

of acceptable signals that were correctly classified as acceptable. Finally, Accuracy (Ac) was measured as the proportion of correctly classified quality of the signals. Results are summarized in table 7.2.

Table 7.2: Average classification results (mean $\pm$ standard deviation) for the train and test data, based on 10-fold cross validation.

	Accuracy	Sensitivity	Specificity
Train	0.863$\pm$0.007	0.832$\pm$0.016	0.894$\pm$0.013
Test	0.842$\pm$0.038	0.800$\pm$0.070	0.884$\pm$0.059

7.4 Discussion and conclusion

The quality of the DUS signal is usually affected by noise and also depends on the fetus-transducer orientation. Although the DUS quality assessment has been previously investigated, it was only targeted for improving FHR monitoring [107, 179]. Results of our study show that the DUS quality can also be assessed in more detail, based on its reliability for valve motion identification.

A real time feedback on the signal quality during data collection would improve the quality of DUS signal for a more accurate estimation of fetal cardiac intervals. Results show that the NB classifier can be used for an accurate classification of the signal quality. NB also requires a short computational time, can be simply implemented and is not sensitive to irrelevant features. However further investigation of other classification techniques are required particularly to improve the sensitivity, in order to provide a reliable feedback to recollect or exclude the poor quality data for further analysis. The classification performance can also be improved by investigating better discriminative features in future studies.

A limitation of the proposed method is the dependance of features on the predefined range of the valve motions. Although the ranges were assumed wide enough to accommodate the variation of the intervals with age or heart rate, the validity of the measures should be assessed for abnormal cases in future studies.

Chapter 8
Identification of fetal heart anomalies

In this chapter the automated valve motion identification method was applied to the fetuses with heart anomalies to investigate the effect of anomalies on fetal cardiac intervals. Results show that the Pre-ejection period (PEP) and Isovolumetric Contraction Time (ICT) were affected by the anomalies. They were both shortened for three out of four anomalies and lengthened for one heart anomaly case. Results will be a background for a further study on more heart anomaly cases to develop a reliable marker for early diagnosis.

This chapter is a slightly modified version of the published article [124]:

- *F. Marzbanrad, Y. Kimura, M. Palaniswami, et al. Application of Automated Fetal Valve Motion Identification to Investigate Fetal Heart Anomalies. IEEE EMBS Healthcare Innovation Conference (HIC), 2014 IEEE , vol., no., pp.243-246, 2014.*

8.1 Introduction

EACH year, at least 8 in 1,000 infants are born with a congenital heart and cardiovascular defects, comprising about 1% of live births [1]. Even in developed countries, perinatal mortality rates of 10/1000 births was accounted [27] mostly caused by congenital malformations and perinatal hypoxia. Despite the advances in fetal surveillance for high risk pregnancies, which reduced perinatal morbidity and mortality rate in the high risk population, the majority of stillbirths and anomalies still occur in low risk pregnancies [27]. Therefore there is a need for more effective and sensitive methods of identifying fetal risks, as well as simple and less specialized methods applicable to the larger population of low risk pregnancies.

As discussed in chapter 2, fetal heart rate monitoring as NST is currently used for assessment of fetal wellbeing, which is not enough for a thorough assessment of fetal risks and

has not significantly reduced the fetal mortality rate. Noninvasive and automated techniques to estimate the cardiac intervals based on the DUS signal and fECG as a reference were discussed in previous chapters. In this chapter we applied the method described in chapter 3 to 56 normal fetuses as well as four fetuses with heart anomalies. Therefore the application of the method for these abnormal cases and the effects of anomalies on fetal cardiac indices were investigated with a focus on PEP and ICT intervals.

8.2 Methods

8.2.1 Data acquisition and processing

Similar to the previous chapters, simultaneous recordings of the abdominal ECG signals and DUS signals. It was decided to study only the normal fetuses and the fetuses with heart anomalies excluding two cases one with bradycardia and one with an abnormal FHR. Furthermore, three cases with very low quality of DUS signal were excluded, to avoid the influence of their quality on the comparison of the normal with the abnormal cases. Therefore the total number of cases considered for this study were 60 cases and included 56 normal fetuses, while fetal heart anomalies were present for four fetuses. The gestational age of the fetuses ranging from 16 to 41 weeks, was 33 ± 6 weeks for normal fetuses and 33, 36, 30 and 28 weeks for four fetuses (1 to 4) with heart anomalies. A total of 60 recordings (each of 1 min. length) were sampled at 1 kHz with 16-bit resolution. The detailed procedure for experimental setup and fECG extraction can be found in previous chapters.

8.2.2 Automated estimation of cardiac intervals

DUS signal was decomposed by EMD, then the envelope of the first component i.e. IMF 1 was taken. Then it was segmented into the cardiac cycles using R-R intervals of the fECG and normalized. The valve motions were automatically identified from the observed peaks of the IMF, using hybrid SVM-HMM trained for 21 normal fetuses as described in detail in chapter 3. The valve motion timings and Q waves of fECG were used to estimate

PEP (Q-Ao) and ICT (Mc-Ao) beat by beat for all fetuses. An average of these intervals over 1 minute was calculated for each fetus for further analysis. The statistical parameters of the ICT and PEP intervals for normal fetuses including median, first and third quartiles and 95% confidence interval (using t-test) of the means were calculated. Then the ICT and PEP of fetuses with heart anomalies were compared with normal parameters.

8.3 Results

PEP and ICT were both measured beat by beat in milliseconds and averaged over 1 minute recording for 56 normal fetuses. The statistical parameters are summarized in table 8.1. The PEP and ICT values averaged for fetuses with heart anomaly, over 1 minute as shown in table 8.2. Comparison of the results of tables 8.1 and 8.2 shows that, ICT of

Table 8.1: Median, first and third quartiles and 95% confidence interval (CI) of the mean ICT and PEP in milliseconds for 56 normal fetuses.

Parameter	ICT (msec)	PEP (msec)
Minimum	33.42	61.67
First quartile	37.38	73.44
Median	39.62	75.88
Third quartile	43.39	78.99
Maximum	47.20	89.89
95% CI	(38.87 , 40.85)	(74.34 , 77.14)

Table 8.2: ICT and PEP measured in milliseconds and averaged over all beats for four fetuses with heart anomaly.

Abnormal Fetuses	ICT (msec)	PEP (msec)
Fetus 1	42.61	85.46
Fetus 2	30.52	72.72
Fetus 3	33.27	67.49
Fetus 4	33.01	70.32

three fetuses with heart anomaly was less than the minimum ICT of 56 normal fetuses. For these fetuses, PEP was also shorter than the first quartile of the normal PEP. ICT of the abnormal fetus 1 was longer than median of ICT for normal fetuses but shorter than the third quartile. It was also larger than the upper 95% CI of the mean ICT for normal

fetuses. For this particular fetus, PEP was longer than the third quartile of the normal PEP and also larger than the upper 95% CI value. Figure 8.1 shows a joint plot of ICT and PEP for normal and abnormal fetuses. It gives a better insight for comparing normal and abnormal fetuses, considering ICT and PEP together. As demonstrated in this figure three cases with heart anomaly had both ICT and PEP shortened, while one abnormal fetus had comparatively long PEP and ICT.

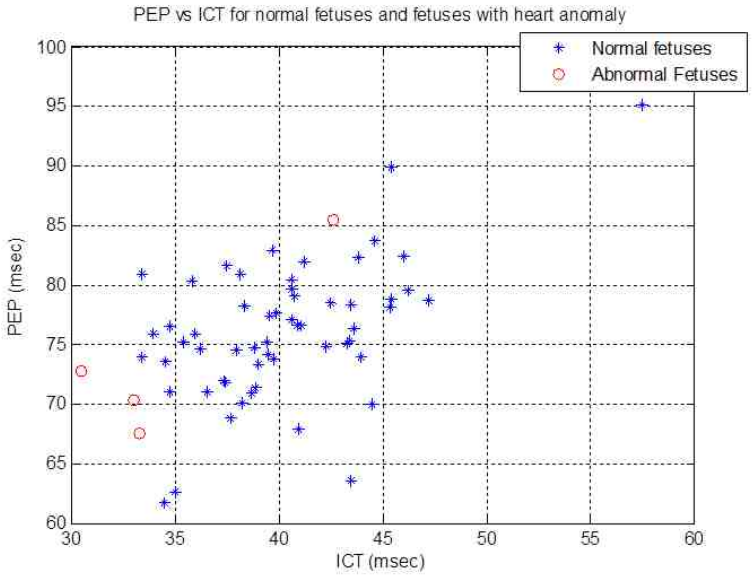

Figure 8.1: Joint plot of PEP versus ICT measured in msec and averaged over 1 minute for 56 normal fetuses and four fetuses with heart anomaly.

8.4 Discussion

A SVM-HMM model was developed based on normal fetuses for automated beat by beat identification of valve motions. In this chapter it is suggested that the developed SVM-HMM model is applicable to the fetal heart anomaly cases and can demonstrate shortened or prolonged indices. The focus of this study was on PEP and ICT. Previous studies have shown that PEP and ICT are the most useful systolic time intervals for clinical purposes [134]. PEP was found as an index of both myocardial contractility and the loading conditions of the heart, which can indicate the fetal cardiac performance [47, 127]. Shortened PEP was also found for acute hypoxemia, while prolonged PEP was

found during sustained and severe hypoxemia [144]. The current study showed prolongation and shortening of these indices deviated from the normal ranges for the fetuses with heart anomalies. Considering PEP and ICT together provided a better insight for discrimination of normal and abnormal cases.

Correlation of R-R intervals with R-peak to Aorta opening and mitral closing times were also suggested to discriminate between normal and abnormal fetuses [79]. Investigation of the changes of the electromechanical coupling indices or their combination for detecting different types of fetal heart anomalies is recommended for future studies. Further investigation based on a larger number of fetuses with different types of heart anomalies are required to develop a model and a conclusive marker for a reliable detection of heart anomalies. Based on a larger number of fetal anomaly cases, a Neural Network model or a Support Vector Machine classifier can be developed to classify normal and abnormal cases using electromechanical coupling indices. Incorporation of this classifier with the automated method of identifying valve motions provides a fully automated tool to detect abnormalities from simultaneous recording of DUS and fECG.

8.5 Conclusion

PEP and ICT were automatically estimated for 56 normal fetuses and four fetuses with heart anomalies, using hybrid SVM-HMM developed for normal fetuses. Results show that the model is able to estimate PEP and ICT for the fetuses with heart anomalies, which were both shortened for three cases and lengthened for one case. Further studies on a larger number of fetuses with heart anomalies can be performed to develop a conclusive marker for automated detection of fetal heart anomalies during pregnancy.

Part III

Fetal-Maternal Heart Rate Interactions

Introduction to Part III

THE fetus interacts with the mother during pregnancy, while their physiological relationship may evolve with gestational progression or be affected by pathologic conditions. The focus of this chapter is on the relationship between maternal and fetal heart rates and its changes with gestation. Results suggest that the assessment of the relationship throughout gestation can provide clinical markers of the fetal development.

Chapter 9

Analysis of fetal-maternal heart rate coupling

Although evidence of the short term relationship between maternal and fetal heart rates has been found in previous model-based studies, knowledge about the mechanism and patterns of the coupling during gestation is still limited. In this chapter, Transfer Entropy (TE) was used to quantify directed interactions between maternal and fetal heart rates at various time delays and gestational ages. Experimental results using maternal and fetal electrocardiograms showed significant coupling for 97% of fetuses, by statistically validating against surrogate pairs. Analysis of TE showed a decrease in transfer of information from fetus to the mother with gestational age, alongside the maturation of the fetus. On the other hand, maternal to fetal TE was significantly greater in mid and late gestation compared to early gestation. Delay in the information transfer from mother to fetus significantly decreased from mid to late gestation, implying a decrease in fetal response time. These changes occur concomitant with the maturation of the fetal sensory and autonomic nervous systems with advancing gestational age. The application of TE with delays revealed detailed information on the fetal-maternal heart rate coupling strength and latency throughout gestation, which could provide novel clinical markers of fetal development and well-being.

This chapter is a slightly modified version of the following articles [121,125]:

- *F. Marzbanrad, M. Endo, Y. Kimura, et al. Transfer Entropy Analysis of Maternal and Fetal Heart Rate Coupling, IEEE Engineering in Medicine and Biology Conference EMBC 2015.*
- *F. Marzbanrad, Y. Kimura, M. Palaniswami, et al. Quantifying the Interactions between Maternal and Fetal Heart Rates by Transfer Entropy. Plos One journal, 10.12, 2015.*

9.1 Introduction and literature review

MONITORING of FHR has been widely used for a reliable assessment of fetal wellbeing and development. In particular, acquisition of FHR through noninvasive fetal electrocardiogram (fECG), even in its current stage of development, provides an accurate estimation of FHR and its beat-to-beat variability [74,82,166]. FHR is influenced by not only the fetal conditions including behaviorial state and maturation, but also the maternal psychological and physiological conditions [71, 132]. These maternal conditions may affect FHR through the hormones transferred via the placenta or the changes in the oxygen and nutrition supply for the fetus. For example, a correlation was previously found between FHR and maternal stress and anxiety level [32, 132]. It was found to be linked to the transferred glucocorticoids and corticosteroid hormones through the placenta or released catecholamines, causing maternal vasoconstriction and limitation of the fetal oxygen and nutrient supply [32, 132]. Maternal relaxation was found to be associated with decreased FHR and increased variability [43]. In addition to the effect of maternal emotion, a significant correlation between the fetal and maternal diurnal heart rate rhythms was found with a phase lag of -2 to +2 hours, in a study by Lunshof et al. [104]. They hypothesized that the fetal suprachiasmatic nucleus, although not completely mature, is involved in transferring the maternal diurnal rhythm information to the fetal heart [104].

In addition to the relationship between maternal and fetal heart rates in large time scales discussed above, evidence of synchronization epochs between the heart rates at the beat-to-beat level was also reported [71,160,189,198]. This short time coupling was found by Van Leeuwen et al., using phase synchronization analysis, as the phase locking of the rhythmic maternal and fetal heartbeats [189]. It was further shown by a model based approach, using the additive autoregressive processes with external contributing factors [160]. Fetal-maternal heart rate synchronization was further investigated in different settings, including controlled maternal respiration and maternal aerobic exercise [190,191]. Results of those studies suggested that high maternal breathing rate may induce the synchronization as it occurred significantly more often at fast maternal breathing and less at slow respiratory rates [190]. Synchronization was found less often where mothers had exercised regularly, possibly due to an increased beat-to-beat differences, higher vagal tone

and slower breathing rates [191]. As previously suggested, the short time fetal-maternal heart rate coupling might be via mechanical or auditory stimuli associated with the maternal rhythms, perceived by the fetus [160, 188]. However, the certain determination of the underlying mechanisms requires further investigation.

A factor which might contribute to the short time coupling of the maternal and fetal heart beats is the delay between them. For example, if the acoustic stimulation is assumed to be the reason behind the coupling, it is reasonable to consider the fetal auditory processing time, causing the latency of the fetal response. The latency of FHR changes in response to the Vibroacoustic Stimulation (VAS), maternal voice or displacement was reported in previous studies [83, 84, 97]. Therefore in the current chapter, this time delay was investigated by analyzing the maternal-fetal heart rate coupling at different lags. The variation of the coupling strength and lag was further analyzed against gestational age, in order to assess the influence of fetal maturation.

Fetal behaviorial state may also affects FHR, particularly after 36 weeks of gestation, when the states can be identified by FHR analysis [151]. It may also have an influence on the maternal-fetal heart rate couplings. The behaviorial states are characterized by the simultaneous occurrence of specific FHR patterns, with or without eye and body movements and divided into: 1F (quiet sleep), 2F (active sleep), 3F (quiet awake), 4F (active awake) [138]. Although the states are commonly identified using long-term FHR monitoring and sonographic observation, they can also be classified based on the short-term FHR variability, such as RMSSD or SDNN, as reported by Lange et al. [93]. In this study we analyzed the effect of these parameters on the coupling for the fetuses in 32nd or later weeks of gestation.

Different from the previous studies on the fetal-maternal heart rate coupling, in this chapter an approach based on the information transfer is used. We applied Transfer Entropy (TE) to investigate the interactions between fetal and maternal heart rates. TE is a non-parametric measure which can determine the coupling of two variables by quantifying the information transferred between them [171]. Using TE, we found the transfer of information between two variables on both directions, i.e. from maternal to fetal heart rate and vice versa. Without assuming any underlying model, TE can capture any linear

and nonlinear link between the time series. Therefore it is more suitable than (linear) model-based measures such as Granger Causality (GC) for analyzing the physiological time series with nonlinear interactions [48]. TE has been used for investigating the coupling of physiological variables in various applications [49, 194, 200]. Improved methods and toolboxes for TE estimation have been recently proposed [98, 133].

9.2 Methods

9.2.1 Data

Different from the previous chapters, the study described in this chapter only required fECG and maternal ECG. Therefore in addition to 61 cases as described previously, the data from 4 extra cases were added which did not include synchronous DUS to be used in the previous chapters, but did have fECG and maternal ECG and therefore were only used in this chapter. Similar to previous chapters, maternal and abdominal ECG signals were recorded from 65 pregnant women in Tohoku University Hospital. The pregnancies were all healthy, single and at the gestational age between 16 to 41 weeks. The cases were further divided into three age groups: early (16-25 weeks, 25 cases), mid (26-31 weeks, 18 cases) and late (32-41 weeks, 22 cases). The recording and extraction procedure of fECG can be found in previous chapters. All signals were collected for 1 minute and sampled at 1 kHz with 16-bit resolution. Pregnant volunteers undergoing their routine prenatal tests had lain on the bed for five minutes before the one minute ECG measurement started.

9.2.2 Estimation of RR Intervals

A Pan and Tompkins-like QRS detector was used with refractory periods of 250 and 150 msec for detecting the maternal and fetal QRS, respectively; as proposed in previous studies [14, 147]. Maternal and fetal RR intervals (fRR and mRR) were then preprocessed by taking a moving window of five RR-intervals and replacing the middle sample by the average of the other four, if deviated by more than 20%. The fRRs and mRRs were resampled at 4 Hz, using cubic interpolation.

9.2.3 Transfer Entropy Analysis

The transfer entropy between two time series $X = \{x_1, x_2, ..., x_N\}$ and $Y = \{y_1, y_2, ..., y_N\}$ on X to Y direction, is calculated as:

$$TE_{X\to Y} = H(y_i|y^l_{i-t}) - H(y_i|y^l_{i-t}, x^k_{i-\tau}) \tag{9.1}$$

$$= \sum_{y_i, y^l_{i-t}, x^k_{i-\tau}} p(y_i, y^l_{i-t}, x^k_{i-\tau}) log(\frac{p(y_i|y^l_{i-t}, x^k_{i-\tau})}{p(y_i|y^l_{i-t})}) \tag{9.2}$$

where i is a given time point, τ and t are the time lags of X and Y, respectively; k and l are the lengths of the blocks containing the past values of X and Y, respectively. In this study TE was calculated for two directions: fetal to maternal ($F \to M$) and maternal to fetal ($M \to F$) heart rates. Therefore X and Y in the equations above denote fetal and maternal RR intervals after preprocessing and resampling. The conditional probabilities in (9.2) are conditioned on $x^k_{i-\tau} = \{x_{i-\tau-k+1}, x_{i-\tau-k+2}, ..., x_{i-\tau}\}$ and $y^l_{i-t} = \{y_{i-t-l+1}, y_{i-t-l+2}, ..., y_{i-t}\}$. The transfer entropy is a non-negative measure of the reduction in uncertainty of y_i given $x^k_{i-\tau}$ and y^l_{i-t}, compared to given only y^l_{i-t} [98].

As suggested in [98], due to the small sample size and computational reasons, the lag of the target and block lengths were all assumed to be one ($k = l = t = 1$). In this study 40 sample delays were considered for the source signal of TE, ranging from 250 msec to 10 sec in equal steps of 250 msec ($= T_{sampling}$). The classic approach of fixed bins was used to estimate the probabilities in (9.2), by allocating the data points to equally-spaced bins. Furthermore, RR-intervals were transformed by replacing them with their integer ranks sorted from smallest (1) to largest (N) values, to enhance the robustness of the measure against outliers and sparse regions of the distribution [98].

The same number of bins, $Q = 10$, was arbitrarily selected in each dimension, as well as $Q = 6$ and $Q = 8$ bins tested for comparison. Using fixed number of bins, the computation of TE was simplified as follows:

$$TE_{X\to Y}(\tau) \approx \sum_{a=1,b=1,c=1}^{Q} \frac{m_{a,b,c}}{P} log \frac{m_{a,b,c} m_b}{m_{b,c} m_{a,b}} \tag{9.3}$$

where a, b, and c are the index of bins along the transformed y_i, y_{i-1}, and $x_{i-\tau}$ time series, respectively, and P is the total number of triplets of transformed y_i, y_{i-1}, and $x_{i-\tau}$. The number of data points in the intersection of the one-dimensional bins are denoted by $m_{a,b,c}$, $m_{a,b}$, and $m_{b,c}$, indexed by their subscript, and m_b is the number of data points at the b^{th} bin in the transformed y_{i-1} dimension. More details on the computation of TE can be found in a previous study [98].

9.2.4 Surrogate Analysis

The significance of TE was statistically evaluated by surrogates using temporal shuffling of the time series. In our experiment, TE was computed for 100 surrogates of the source time series (fRR or mRR for $F \rightarrow M$ or $M \rightarrow F$ directions, respectively). Given the TE from the original source was greater than the 95th percentile of the surrogate TE results, it was assumed to be significant. Only significant TE values were used for further analysis, e.g. mean TE was calculated over the delays at which TE was significant.

9.2.5 Maternal Respiratory Rate Estimation

Maternal respiratory rate was estimated through single lead ECG-Derived Respiration (EDR). Kernel Principal Component Analysis (K-PCA) technique was used, which was previously shown by Widjaja et al., to outperform PCA and R-peak amplitude methods in the extraction of the EDR [201]. The procedure of the EDR extraction can be found in [201] and summarized as follows. An input matrix X was formed by assembling n (no. of R-peaks) columns, each composed of a symmetric window of length $m = 121$ around each R-peak. Then K-PCA was applied to the input matrix, using Least Squares Support Vector Machines (LSSVM) toolbox LS-SVMlab v1.8 (http://www.esat.kuleuven.be/sista/ lssvmlab/, Leuven, Belgium) [180]. Radial Basis Function (RBF) was used as a kernel with various parameter values ranging from $\sigma^2 = 0.1\sigma_0^2$ to $\sigma^2 = 100\sigma_0^2$, where $\sigma_0^2 = m.\text{mean}(\text{var}(X))$. The σ^2 value which resulted in the largest difference between the first and the sum of the remaining eigenvalues was selected. Using this value for kernel, the input data was reconstructed from the resulting first eigenvector in the feature space

via preimage_rbf function of the LS-SVMlab toolbox. EDR was estimated as a row of this reconstructed observation.

The maternal respiratory rate was estimated from the EDR signal, using an algorithm proposed by Cysarz et al., summarized as follows [35]. EDR was resampled at 10 Hz using cubic spline interpolation. Then a band-pass filter was applied in the range of $0.1-0.45$ Hz using a least-square FIR filter. The filtered signal was standardized by dividing by the 75 percentile of all detected local maxima, in order to exclude the influence of single oscillations with extreme amplitudes. The local maxima which exceeded 0.3 were further used and the average of the distances between the successive local maxima was calculated.

9.2.6 Statistical Analysis

The mean and maximum of (significant) TE as well as the lags resulting in maximum TE were all compared against different age groups by nonparametric statistical analysis. Mann Whitney Wilcoxon (MWW) test was used to compare maximum transfer entropy and corresponding delay for early, mid and late age groups. P-value of 0.05 was chosen as the level of significance. MWW test was also used for comparison of TE for different ranges of RMSSD and SDNN, each divided into two groups: high RMSSD $\geq$4 msec (6, 5 and 13 fetuses in early, mid and late gestation, respectively), low RMSSD $<$4 msec (19, 13 and 9 fetuses in early, mid and late gestation, respectively), high SDNN $\geq$12 msec (5, 8 and 15 fetuses in early, mid and late gestation, respectively), low SDNN $<$12 msec (20, 10 and 7 fetuses in early, mid and late gestation, respectively). The correlation of mean FHR, RMSSD and SDNN with TE on both directions were also tested. In each case linear partial correlation was evaluated while controlling for the gestational age. The correlation of maternal respiratory rate and mean TE was analyzed through Pearson's correlation and MWW was also used to compare TE for various breathing ranges; i.e. lower than 14 bpm (18 subjects), between 14 and 16 bpm (21 subjects) and higher than 16 bpm (26 subjects).

9.3 Results

9.3.1 Results of surrogate analysis

TE was calculated for lags up to 10 seconds and on two directions. Based on the surrogate analysis, for 63 out of 65 cases, $TE_{M\to F}$ was significant, while not being significant for one early and one late gestation cases. $TE_{F\to M}$ was also not significant for that late gestation case, as well as another case in late gestation, while being significant for the rest of the cases. The fetuses with insignificant $TE_{F\to M}$ had the highest mean FHR (160.649 bpm and 166.736 bpm) among all 65 fetuses. The mean FHR for the fetuses with insignificant $TE_{M\to F}$ was also high compared to other cases (160.649 bpm and 154.698 bpm). The cases with insignificant TE were excluded from further analysis.

9.3.2 Comparison between gestational age groups

Both mean of and maximum of significant $TE_{M\to F}$ over the lags were significantly different for three age groups according to MWW test results (table 9.1). Figure 9.1(a) shows the boxplot of the mean $TE_{M\to F}$ for different age groups. According to MWW results as shown in figure 9.1(a) and table 9.1, both mean and maximum of $TE_{M\to F}$ significantly increased from early to mid and to late gestation, however no significant change was observed from mid to late gestation. This was further investigated by analyzing fetal heart rate variability as discussed in the following section. Mean and maximum of TE on the other direction ($F \to M$) did not change significantly with gestation. However a decreasing trend was found in the mean $TE_{F\to M}$ with gestational progression, as it was negatively correlated with age ($r = -0.393, p = 0.001$ while controlling for the mean fHR).

Similar results were obtained when the number of bins was changed to $Q = 8$; an increase in $TE_{M\to F}$ was found with gestational age (KW $p = 0.025$), particularly from early to mid gestation (MWW $p = 0.037$), as well as a decreasing trend for $TE_{F\to M}$ from early to late gestation (nearly significant MWW $p = 0.056$). Similarly for $Q = 6$ bins, an increase was found in mean $TE_{M\to F}$ with gestational age (MWW $p = 0.066$, nearly signifi-

(a)

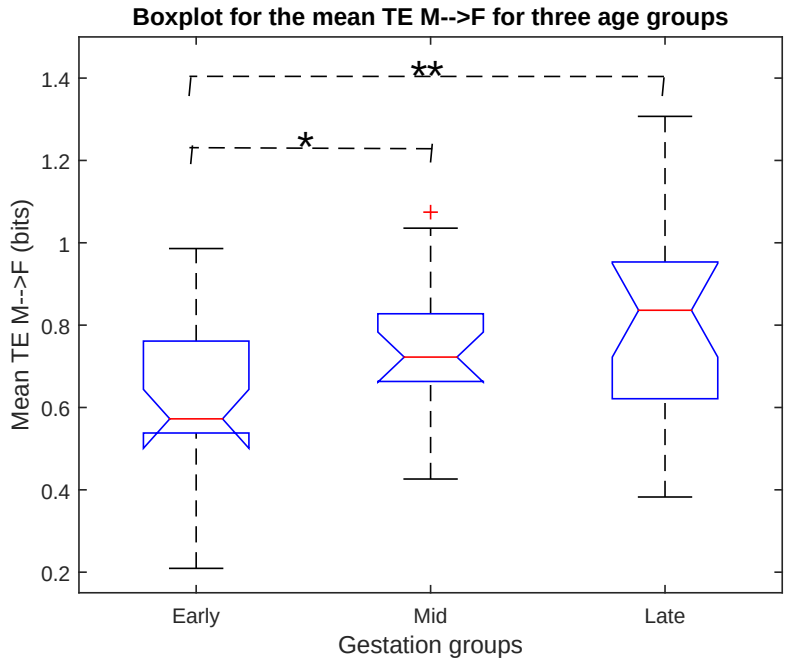

(b)

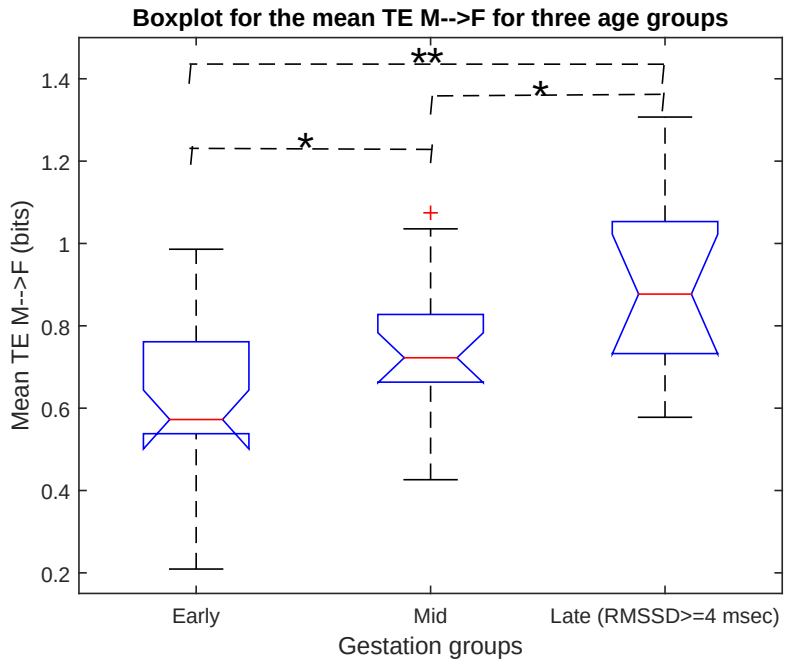

Figure 9.1: Comparison of the mean $TE_{M\to F}$ for different age groups is shown. Significant differences according to the pairwise comparison by MWW test with p-value < 0.05 and p-value < 0.01 are marked with (*) and (**), respectively. (a) Boxplot of mean $TE_{M\to F}$ for different age groups, (b)Boxplot of mean $TE_{M\to F}$ for different age groups, excluding the cases in late gestation group with RMSSD being smaller than 4 msec.

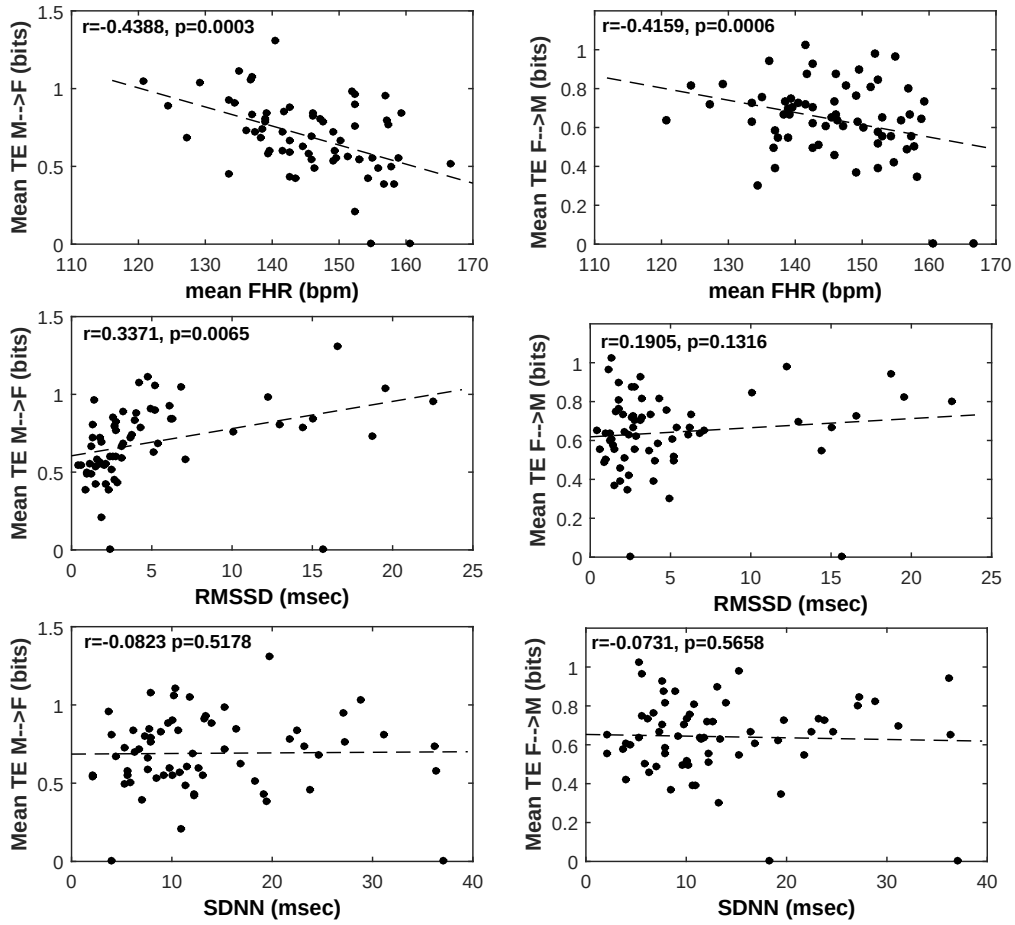

Figure 9.2: Regression plots of mean TE on both directions with mean, RMSSD and SDNN of FHR are shown. coefficient and p-values of partial correlation controlled for gestational age are also indicated. The cases shown with zero TE had insignificant TE according to the surrogate analysis.

Table 9.1: Results of MannWhitneyWilcoxon test for changes of the estimated mean, maximum and delay of TE, as well as the maternal respiratory rate with gestational age

	Early Gestation	Mid Gestation	Late Gestation
Mean $TE_{M\to F}$ (bits)	0.618±0.178 (A*,B**)	0.728±0.187 (A*)	0.808±0.227 (B**)
Max $TE_{M\to F}$ (bits)	0.698±0.196 (A*,B**)	0.816±0.201 (A*)	0.895±0.250 (B**)
Delay $TE_{M\to F}$ (sec)	4.490±2.844 (A*)	5.931±2.818 (A*,C*)	4.012±3.025 (C*)
Mean $TE_{F\to M}$ (bits)	0.673±0.170	0.687±0.160	0.626±0.156
Max $TE_{F\to M}$ (bits)	0.756±0.192	0.777±0.184	0.702±0.170
Delay $TE_{F\to M}$ (sec)	4.810±3.058	3.958±2.701	5.000±3.070
Maternal respiratory rate (bpm)	14.833±2.301 (B*)	15.218±2.074	15.904±2.587 (B*)

The mean ± Standard Error (SE) (msec) of the values for different age groups are shown. Significant differences between pairs of age groups: early vs mid, early vs late and mid vs late gestations are marked by (A), (B) and (C), respectively. The letters are also marked with (*) or (**) depending on the p-value of MWW test being < 0.05 or < 0.01, respectively.

cant for early to late gestation). Also a slight decrease in mean $TE_{F\to M}$ with age (MWW $p = 0.081$ from mid to late gestation) was observed and it was negatively correlated with age ($r = -0.244$, $p = 0.051$ while controlling for the mean FHR).

Delays which resulted in maximum TE were also analyzed for different gestation groups, as summarized in table 9.1. The lag associated with maximum $TE_{M\to F}$ significantly decreased from mid to late gestation and increased from early to mid gestation. However the latter is not as valued as the former, considering the small value of $TE_{M\to F}$ at the early gestation. No significant change in delay was found on the other direction ($F \to M$). By changing the number of bins from $Q = 10$ to $Q = 6$, similarly the delay decreased with age in both directions (e.g. MWW $p = 0.05$ for delay of $TE_{M\to F}$ for mid to late gestation, and for the delay of $TE_{F\to M}$ MWW $p = 0.02$ and $p = 0.09$ were found for early to late and mid to late gestation, respectively). For the choice of $Q = 8$, the delay was also slightly decreased with gestational age in both directions, but it was not statistically significant.

9.3.3 Effect of short-term FHR variability

The correlation of mean TE was tested with mean, RMSSD and SDNN of FHR, all controlled for the gestational age. The regression plots with all correlation coefficients are shown in figure 9.2. Mean $TE_{M\to F}$ was found only positively correlated with RMSSD ($r = 0.337, p = 0.006$) and negatively with mean FHR ($r = -0.439, p < 0.001$), while it was not significantly correlated with fetal SDNN ($r = -0.082, p = 0.518$). Considering that a significant increase in mean $TE_{M\to F}$ was found from early to mid, but not from mid to late gestation, we tested the changes in mean $TE_{M\to F}$ for the fetuses in late gestation with RMSSD $\geq$4 msec. As shown in figure 9.1(b), for the fetuses with RMSSD $\geq$4 msec, there was a further increase from mid to late gestation (MWW p=0.039), while no significant change for the fetuses with RMSSD $<$4. We also tested the relationship with the maternal heart rate variability features (mean heart rate, SDNN and RMSSD) and found no significant correlation. Finally, mean $TE_{F\to M}$ was only correlated significantly with mean FHR ($r = -0.416, p = 0.001$).

9.3.4 Effect of maternal respiration

No significant correlation was found between maternal breathing rate and mean $TE_{M\to F}$ or $TE_{F\to M}$, with or without controlling for fetal heart rate, RMSSD or age. MWW was also used to compare TE for various breathing ranges; lower than 14 bpm, between 14 and 16 bpm and higher than 16 bpm. According to MWW results, no significant difference was found between mean TE with different breathing rate ranges, over all or specific age groups and on any directions. Overall no relationship was found between the average maternal respiratory rate and $TE_{M\to F}$ or $TE_{F\to M}$.

9.4 Discussion

Assessing the responses of the fetuses to the stimuli in their environment, provides markers of their well-being and development. One of the common and easy-to-measure responses is the change in FHR. It was previously hypothesized that the fetus responds to mechanical or auditory stimuli associated with the maternal rhythms, which results in short time coupling between the fetal and maternal heart rates [160,188]. Different from previous model based approaches, we used an analysis of the coupling as a nonparametric measure which could detect any linear and nonlinear relationship of two variables, based on the transferred information. Moreover using transfer entropy enables analysis of coupling in each separate direction. The significance of the coupling was statistically validated against surrogate pairs, and evidence of significant transfer of information was found on both directions for 97% of fetuses.

The results of this study showed that the coupling from the mother to the fetus becomes stronger with advancing gestation. Particularly, the transfer entropy from the mother to the fetus significantly increases after 26 weeks of gestation compared to 16-25 weeks. This result is in agreement with the maturation process of the fetal response to the stimuli from the maternal rhythms, since both tactile and auditory systems become operational after 26 weeks of gestation [84]. It was previously reported that the maturation of human fetal response (in form of changes in FHR) to vibroacoustic stimulation starts at around 26 weeks and reaches maturity at about 32 weeks [84]. Our result is also in line with the increasing sympathetic activity with gestational progression, alongside the development of fetal autonomic nervous system and its function in regulation of FHR [148]. Development of the sympathetic control during mid gestation is also concomitant to the nonlinear heart period dynamics, which is suggested to be involved with sympathetic regulation and also possibly the sympatho-vagal interactions [154]. The nonlinearity of the FHR dynamics particularly in mid and late gestation was also our motivation for using TE. With advancing gestation particularly around mid gestation, the fetus receives more information from the mother and reacts better, while the FHR shows more complexity and nonlinear dynamics. Therefore, the transfer entropy from the mother to the fetus may provide a marker to assess the development of fetal sensory and autonomic nervous sys-

tems.

Although we found an increase in $TE_{M\to F}$ from early (16-25 weeks) to mid (26-31 weeks) gestation, no significant increase was found from mid to late (32-41) gestation. A factor which might be involved in the coupling in late gestation, is the fetal behavioral state. A higher FHR variability is generally observed in active periods after 28th week, and the states can be identified by FHR analysis after 36 weeks of gestation [151]. As previously reported by Lange et al., the fetal behavioral states can be classified based on the differences in short-term FHR variability such as RMSSD or SDNN [93]. In this study a positive correlation was found between RMSSD and $TE_{M\to F}$, and there was a further increase in $TE_{M\to F}$ from mid to late gestation for the fetuses with RMSSD $\geq$4 msec, which is associated with active state of the fetus [93]. However, a thorough assessment of the fetal behavioral state can be better performed through long-term FHR monitoring and sonographic observation, which is suggested for future studies.

The fetus also provides feedback to maternal systems throughout its own development, which can evoke a maternal physiological response. Our results showed that the transfer of information from fetal to maternal heart rate was negatively correlated with age. The decrease in $TE_{F\to M}$ with gestational progression is possibly because the fetus requires less from the mother when most organs are developed towards delivery. The mature fetuses have also more stable and developed ANS in the late gestation. TE on both directions was negatively correlated with mean FHR and the cases with insignificant TE had higher FHR compared to other fetuses. Although it is not possible to comment on the causal link between FHR and TE, but this negative correlation implies that at high FHR it may be difficult for the fetus to maintain the link with the maternal heart rate.

In this study the coupling between maternal and fetal heart rate was observed at various delays. These lags may reflect the fetal (e.g. auditory or tactile) processing time before responding to the stimuli from mother. Similarly, a latency was previously found for FHR changes in response to the VAS, maternal voice or displacement [83, 84, 97]. The lags for the short-term relationship between maternal and fetal heart rates were also considered in a model-based analysis by Riedl et al. [160]. They found a short-term synchronization through which, the maternal beats described the FHR fluctuations as a predecessor with

a lag of 4 to 5 fetal beats. Considering that the fetuses in their study were at 34 to 40 weeks of gestation, their finding is consistent with our results for the late gestation group. We further included the delays up to 10 sec (around 20-28 fetal beats) in our analysis to allow for detection of longer delays particularly for the fetuses in earlier gestation.

In addition, the changes of the lag corresponding to the maximum TE was analyzed for different gestational ages. The lag for $TE_{M\to F}$ was significantly shorter in the late gestation. This is an evidence of faster fetal sensory processing time and shorter latency of fetal response to the stimuli from maternal rhythms, according to the maturation of sensory systems and ANS. Previous studies observed similar results for the late gestation stage, such as decreased latency of fetal response to maternal voice [83].

Previous studies tested the relationship between fetal and maternal heart rates in controlled maternal respiration setting and suggested that the relationship may be induced by high maternal respiratory rates [190]. They found that the synchronization occurred significantly more often at fast maternal breathing and less at slow respiratory rates [188, 190]. In this study we tested TE for average maternal respiratory rate, derived from maternal ECG. No significant relationship was found between maternal respiratory rate and $TE_{M\to F}$ or $TE_{M\to F}$. Our analysis was only based on the average respiratory rate for each mother. An accurate breath-by-breath measurement of maternal respiration is suggested for future studies, to be considered as a confounding variable in TE analysis. Therefore, it would be possible to evaluate the causal effect between maternal-fetal heart rates, conditioned on the maternal respiration.

In this study transfer entropy was evaluated based on one-minute recordings, which is the standard fetal ECG measurement protocol to minimize the inconvenience for the participating mothers. For future studies, it is recommended to use longer recordings to investigate the effect of sample size and study the temporal changes in information transfer for each fetus. Furthermore, application of other methods for measuring the coupling, for example to improve the quantification of coupling for small sample sizes [153], is recommended for future investigations. Longer recordings also provide the analysis of nonstationarity in FHR, as a factor with possible influence on TE analysis. Nonstationarity of FHR becomes more pronounced in the late gestation due to the fetal movement.

An accurate evaluation of the nonstationarity in the FHR requires longer recordings, e.g. to measure the inconsistency of baselines using acceleretion/deceleration patterns [73]. Analysis of the nonstationarity and its influence on TE measures are left for the future studies.

9.5 Conclusion

Using transfer entropy as a nonparametric measure, significant couplings were found between maternal and fetal heart rates on both directions for 63 of 65 fetuses. Maternal to fetal TE increased from early to mid gestation, along maturation of fetal ANS and sensory (e.g. auditory and tactile) systems. It was further increased from mid to late gestation, except for the fetuses with low RMSSD ($<$ 4msec) of heart rate, possibly due to their quiet sleep state. The fetal to maternal TE was negatively correlated with gestational age, showing a decrease in the feedback from fetus to the mother towards delivery. Furthermore, the delay at which maximum information transferred from mother to the fetus was shorter in the late gestation, implying the short fetal processing time and latency in responding to the stimuli from the mother. Results suggest that the assessment of the coupling strength and latency throughout gestation can provide clinical markers of healthy versus pathological fetal development.

Chapter 10
Contributions and further work

10.1 Summary of contributions

10.1.1 Contributions to the identification of fetal cardiac valve motion events

Although detection of valve motion events from 1-D DUS signal was performed in previous studies, all were based on manual recognition of events which is time consuming and subject to visual, inter- and intra-observer errors. The first automated method for identification of the valve motion events from 1-D DUS was developed in this thesis. Furthermore, decomposition of DUS signal to the component related to valve motion was improved using EMD which is a data-driven algorithm suitable for decomposing nonlinear and nonstationary time series. The main basis for the proposed automated valve motion identification method was HMM. This method provided beat by beat estimation of valve timings, which was published and presented in 35th Annual International Conference of the IEEE Engineering in Medicine and Biology Society (EMBC) in July 2013.
This method was then further improved by incorporating extra features of the DUS component for detecting the valve movements, through MD-HMM and Hybrid SVM-HMM. These methods were published in the proceeding of IEEE EMBC and IEEE Journal of Biomedical and Health Informatics, respectively, in 2014.
It was further shown that different patterns of the DUS components were observed which were variable on a beat to beat basis and throughout gestation. By clustering the DUS components and performing hybrid SVM-HMM for each cluster separately, more accurate detection of valve movements was achieved as described in chapter 5. This model-

based technique was the basis for the second journal paper published in IEEE Journal of Biomedical and Health Informatics, in 2014.

Simultaneous recording of fECG with Doppler has a crucial role in automated methods for segmentation. However simultaneous recording of abdominal ECG with DUS signal and extraction of fECG complicate this technique. Therefore it was proposed to use wall motion related component of DUS signal for segmentation, instead of fECG. Results showed that the measured average ICT with this new method was in agreement with the average ICT measured by the previous method which required fECG as reference. This work was described in chapter 6 and presented in Computing in Cardiology Conference in 2014.

Overall, the model-based method proposed in chapter 5 provided the highest precision and recall and is recommended for accurate estimation of valve timings in clinical practice. However in the case of computational limitations, the MD-HMM-based method proposed in chapter 4 is recommended. Finally, if simultaneous fECG is not available, the valve timings can be identified using the DUS signal only, as proposed in chapter 6.

Considering the high susceptibility of the DUS signal to noise and interferences, it is crucial to assess the signal quality to ensure its validity for a reliable estimation of the valve movement timings. Another contribution of this thesis was to automatically assess the quality of the DUS signal. Automated quality classifier was developed in this study and presented in Computing in Cardiology Conference in 2015.

The changes of the estimated valve timing intervals with gestational age were also investigated, which can provide clinical markers to assess healthy versus pathological development of fetuses. The intervals were also found to be different for the fetuses with heart anomalies compared to the normal cases, therefore can be used for detection of those anomalies. The comparison of valve intervals for different gestational ages and healthy versus heart anomaly fetuses were the bases for two conference papers presented and published in the proceeding of Computing in Cardiology, in 2013 and IEEE EMBS Healthcare Innovation Conference (HIC), in 2014.

10.1.2 Contributions to the identification of the coupling between maternal and fetal heart rates

Different from the previous studies on the coupling between maternal and fetal heart rates, in this thesis a model-free and nonparametric method based on transfer entropy was used which provided details on the linear or nonlinear relationships. The coupling was also quantified separately in fetal to maternal and maternal to fetal directions. Furthermore delay of the information transfer was considered and analysed for various gestational ages. Results of this work suggested that the assessment of the coupling strength and latency throughout gestation can provide clinical markers of healthy versus pathological fetal development. This study was the basis for a paper presented in IEEE Engineering in Medicine and Biology Society Conference (EMBC) in 2015 and a journal paper submitted to PlosOne, in 2015.

10.2 Future research

10.2.1 Future studies in the identification of fetal cardiac valve motion events

- Valve motion events were identified based on the timing and amplitude of the peaks of the DUS component. Additional features, such as width and power spectral density of the peaks can be used to improve the identification of valve events.

- This research provided an automated method for estimation of fetal cardiac valve intervals, which were also tested for four heart anomaly cases. Further investigation based on a larger number of fetuses with certain types of heart anomalies are required to develop a classifier for automated detection of abnormalities. Incorporation of this classifier with the automated method of detecting valve movements provides a fully automated tool to detect abnormalities from simultaneous recording of DUS and fECG.

- Finally, quantitative comparison of the intervals estimated from 1-D DUS with M-Mode and pulsed wave Doppler images is recommended for future studies.

10.2.2 Future studies in the investigation of the relationship between maternal and fetal heart rates

- The relationship between fetal and maternal heart rates was investigated based one minute recordings. It was suggested that fetal behavioral state may affect this relationship. Longer recordings together with fetal behavioral state reliably detected by sonography is recommended for future studies.

- Although no relationship was found between average maternal breathing rate and the maternal-fetal coupling, an accurate breath-by-breath measurement of maternal respiration is suggested for future studies, to be considered as a confounding variable in TE analysis.

- Finally, testing the coupling for pathological fetal and maternal conditions requires further investigation.

Bibliography

[1] "Annual report of the victor chang cardiac research institute," 1999. [Online]. Available: http://www.victorchang.edu.au/pdfs/1999Report.pdf

[2] S. Abe, *Support vector machines for pattern classification*. Springer, 2010.

[3] A. Z. Abuhamad and R. Chaoui, *A practical guide to fetal echocardiography: normal and abnormal hearts*. Lippincott Williams & Wilkins, 2010.

[4] Z. Alfirevic and J. Neilson, "Doppler ultrasound for fetal assessment in high risk pregnancies (review)," 2009.

[5] L. D. Allan, A. C. Cook, and I. C. Huggon, *Fetal echocardiography: a practical guide*. Cambridge University Press, 2009.

[6] I. Amer-Wåhlin, C. Hellsten, H. Norén, H. Hagberg, A. Herbst, I. Kjellmer, H. Lilja, C. Lindoff, M. Månsson, L. Mårtensson *et al.*, "Cardiotocography only versus cardiotocography plus st analysis of fetal electrocardiogram for intrapartum fetal monitoring: a swedish randomised controlled trial," *The Lancet*, vol. 358, no. 9281, pp. 534–538, 2001.

[7] American Heart Association, "Congenital heart defects in children fact sheet," 2008. [Online]. Available: http://www.americanheart.org/children

[8] F. Andreotti, M. Riedl, T. Himmelsbach, D. Wedekind, N. Wessel, H. Stepan, C. Schmieder, A. Jank, H. Malberg, and S. Zaunseder, "Robust fetal ecg extraction and detection from abdominal leads," *Physiological measurement*, vol. 35, no. 8, p. 1551, 2014.

[9] Australian Bureau of Statistics, "Perinatal death," 2014. [Online]. Available: http://www.abs.gov.au/ausstats/abs@.nsf/Previousproducts/CC97737B485147C0CA257B2E000D7826?opendocument

[10] E. Bacharakis, A. Nandi, and V. Zarzoso, "Foetal ecg extraction using blind source separation methods," *Signal Processing Division. University of Srathclyde*, 1996.

[11] L. E. Baum, T. Petrie, G. Soules, and N. Weiss, "A maximization technique occurring in the statistical analysis of probabilistic functions of markov chains," *The annals of mathematical statistics*, vol. 41, no. 1, pp. 164–171, 1970.

[12] J. Behar, J. Oster, and G. D. Clifford, "Combining and benchmarking methods of foetal ecg extraction without maternal or scalp electrode data," *Physiological Measurement*, vol. 35, no. 8, p. 1569, 2014. [Online]. Available: http://stacks.iop.org/0967-3334/35/i=8/a=1569

[13] J. Behar, F. Andreotti, S. Zaunseder, Q. Li, J. Oster, and G. D. Clifford, "An ecg simulator for generating maternal-foetal activity mixtures on abdominal ecg recordings," *Physiological measurement*, vol. 35, no. 8, p. 1537, 2014.

[14] J. Behar, J. Oster, and G. D. Clifford, "Non-invasive fecg extraction from a set of abdominal sensors," in *Computing in Cardiology Conference (CinC), 2013*. IEEE, 2013, pp. 297–300.

[15] M. Bennasar, J. Martinez, O. Gomez, J. Bartrons, A. Olivella, B. Puerto, and E. Gratacós, "Accuracy of four-dimensional spatiotemporal image correlation echocardiography in the prenatal diagnosis of congenital heart defects," *Ultrasound in Obstetrics & Gynecology*, vol. 36, no. 4, pp. 458–464, 2010.

[16] A. T. Bianco, S. W. Smilen, Y. Davis, S. Lopez, R. Lapinski, and C. J. Lockwood, "Pregnancy outcome and weight gain recommendations for the morbidly obese woman." *Obstetrics & Gynecology*, vol. 91, no. 1, pp. 97–102, 1998.

[17] J. M. Bland and D. Altman, "Statistical methods for assessing agreement between two methods of clinical measurement," *The lancet*, vol. 327, no. 8476, pp. 307–310, 1986.

[18] P. Blunsom, "Hidden markov models," *Lecture notes, August*, 2004.

[19] P. Bobby *et al.*, "Multiple assessment techniques evaluate antepartum fetal risks." *Pediatric annals*, vol. 32, no. 9, p. 609, 2003.

[20] H. Boudoulas, "Systolic time intervals," *Eur Heart J*, vol. 11, no. Suppl I, pp. 93–104, 1990.

[21] A. Bouzid and N. Ellouze, "Empirical mode decomposition of voiced speech signal," in *Control, Communications and Signal Processing, 2004. First International Symposium on*. IEEE, 2004, pp. 603–606.

[22] D. Callaerts, "Signal separation methods based on singular value decomposition and their application to the real-time extraction of the fetal electrocardiogram from cutaneous recordings," *status: published*, 1989.

[23] G. Cardillo, "Fleiss's kappa: compute the Fleiss's kappa for multiple raters." 2007.

[24] L. Caserta, Z. Ruggeri, L. D'Emidio, C. Coco, P. Cignini, A. Girgenti, L. Mangiafico, and C. Giorlandino, "Two-dimensional fetal echocardiography: where we are," *Journal of prenatal medicine*, vol. 2, no. 3, p. 31, 2008.

[25] S. Cerutti, G. Baselli, S. Civardi, E. Ferrazzi, A. M. Marconi, M. Pagani, and G. Pardi, "Variability analysis of fetal heart rate signals as obtained from abdominal electrocardiographic recordings," *Journal of Perinatal Medicine-Official Journal of the WAPM*, vol. 14, no. 6, pp. 445–452, 1986.

[26] S. Cerutti, A. L. Goldberger, and Y. Yamamoto, "Recent advances in heart rate variability signal processing and interpretation," *Biomedical Engineering, IEEE Transactions on*, vol. 53, no. 1, pp. 1–3, 2006.

[27] CESDI, "Confidential enquiry into stillbirths and deaths in infancy," 2001. [Online]. Available: www.cesdi.org.au

[28] R. Chaoui, J. Hoffmann, and K. Heling, "Three-dimensional (3d) and 4d color doppler fetal echocardiography using spatio-temporal image correlation (stic)," *Ultrasound in obstetrics & gynecology*, vol. 23, no. 6, pp. 535–545, 2004.

[29] G. D. Clifford, J. Behar, Q. Li, and I. Rezek, "Signal quality indices and data fusion for determining clinical acceptability of electrocardiograms," *Physiological Measurement*, vol. 33, no. 9, p. 1419, 2012.

[30] G. D. Clifford, I. Silva, J. Behar, and G. B. Moody, "Non-invasive fetal ecg analysis," *Physiological measurement*, vol. 35, no. 8, p. 1521, 2014.

[31] N. Colley, N. Abraham, P. Fayers, D. Talbert, W. Davies, and D. Southall, "The fetal phonogram: a measure of fetal activity," *The Lancet*, vol. 327, no. 8487, pp. 931–935, 1986.

[32] R. L. Copper, R. L. Goldenberg, A. Das, N. Elder, M. Swain, G. Norman, R. Ramsey, P. Cotroneo, B. A. Collins, F. Johnson *et al.*, "The preterm prediction study: Maternal stress is associated with spontaneous preterm birth at less than thirty-five weeks' gestation," *American journal of obstetrics and gynecology*, vol. 175, no. 5, pp. 1286–1292, 1996.

[33] R. Creasy and R. Resnik, "Chapter 34: Intrauterine growth restriction," *Maternal-fetal medicine: principles and practice (6th ed.), Saunders, Philadelphia*, pp. 635–650, 2008.

[34] C. S. Croom, B. B. Banias, E. Ramos-Santos, L. D. Devoe, A. Bezhadian, and A. Hiett, "Do semiquantitative amniotic fluid indexes reflect actual volume?" *American journal of obstetrics and gynecology*, vol. 167, no. 4 Pt 1, p. 995, 1992.

[35] D. Cysarz, R. Zerm, H. Bettermann, M. Frühwirth, M. Moser, and M. Kröz, "Comparison of respiratory rates derived from heart rate variability, ecg amplitude, and nasal/oral airflow," *Annals of biomedical engineering*, vol. 36, no. 12, pp. 2085–2094, 2008.

[36] A. Damen and J. Van Der Kam, "The use of the singular value decomposition in electrocardiography," *Medical and Biological Engineering and Computing*, vol. 20, no. 4, pp. 473–482, 1982.

[37] G. Davies, "Antenatal fetal assessment," *SOGC Clinical Practice Guideline*, 2000.

[38] A. K. Dayal, F. A. Manning, D. J. Berck, G. M. Mussalli, C. Avila, C. R. Harman, and S. Menticoglou, "Fetal death after normal biophysical profile score: An eighteen-year experience," *American journal of obstetrics and gynecology*, vol. 181, no. 5, pp. 1231–1236, 1999.

[39] L. De Lathauwer, B. De Moor, and J. Vandewalle, "Fetal electrocardiogram extraction by blind source subspace separation," *Biomedical Engineering, IEEE Transactions on*, vol. 47, no. 5, pp. 567–572, 2000.

[40] L. D. Devoe, "Antenatal fetal assessment: Contraction stress test, nonstress test, vibroacoustic stimulation, amniotic fluid volume, biophysical profile, and modified biophysical profile- an overview," in *Seminars in perinatology*, vol. 32, no. 4. Elsevier, 2008, pp. 247–252.

[41] G. DeVore, J. Horenstein, B. Siassi, and L. Platt, "Fetal echocardiography. vii. doppler color flow mapping: a new technique for the diagnosis of congenital heart disease." *American journal of obstetrics and gynecology*, vol. 156, no. 5, p. 1054, 1987.

[42] G. R. DeVore, "Fetal echo: Standard," 2015. [Online]. Available: http://www.fetal.com/FetalEcho/04%20Standard.html

[43] J. A. DiPietro, K. A. Costigan, P. Nelson, E. D. Gurewitsch, and M. L. Laudenslager, "Fetal responses to induced maternal relaxation during pregnancy," *Biological psychology*, vol. 77, no. 1, pp. 11–19, 2008.

[44] M. L. Druzin, A. Fox, E. Kogut, C. Carlson *et al.*, "The relationship of the nonstress test to gestational age," *Am J Obstet Gynecol*, vol. 153, no. 4, pp. 386–9, 1985.

[45] J. Echeverria, J. Crowe, M. Woolfson, and B. Hayes-Gill, "Application of empirical mode decomposition to heart rate variability analysis," *Medical and Biological Engineering and Computing*, vol. 39, no. 4, pp. 471–479, 2001.

[46] R. D. Eden, F. H. Boehm, and M. Haire, *Assessment and Care of the Fetus: Physiological, Clinical, and Medicolegal Principles*. Appleton & Lange, 1990.

[47] J. L. H. Evers, "Cardiac pre-ejection period during prenatal life," *Gynecologic and obstetric investigation*, vol. 11, no. 4, pp. 193–213, 1980.

[48] L. Faes, D. Marinazzo, F. Jurysta, and G. Nollo, "Linear and non-linear brain–heart and brain–brain interactions during sleep," *Physiological measurement*, vol. 36, no. 4, p. 683, 2015.

[49] L. Faes, D. Marinazzo, A. Montalto, and G. Nollo, "Lag-specific transfer entropy as a tool to assess cardiovascular and cardiorespiratory information transfer," 2014.

[50] N. Feinstein, K. L. Torgersen, and J. Atterbury, *Fetal Heart Monitoring: Principles and Practices*. Kendall Hunt, 1993.

[51] C. Ferencz, J. D. Rubin, R. J. Mccarter, J. I. Brenner, C. A. Neill, L. W. Perry, S. I. Hepner, and J. W. Downing, "Congenital heart disease: Prevalence at livebirth the baltimore-washington infant study," *American Journal of Epidemiology*, vol. 121, no. 1, pp. 31–36, 1985.

[52] J. L. Fleiss, "Measuring nominal scale agreement among many raters." *Psychological Bulletin*, vol. 76, no. 5, p. 378, 1971.

[53] R. Freeman, G. Anderson, and W. Dorchester, "A prospective multi-institutional study of antepartum fetal heart rate monitoring. ii. contraction stress test versus nonstress test for primary surveillance." *American journal of obstetrics and gynecology*, vol. 143, no. 7, pp. 778–781, 1982.

[54] A. Ganapathiraju, J. Hamaker, and J. Picone, "Hybrid svm/hmm architectures for speech recognition." in *INTERSPEECH*. Citeseer, 2000, pp. 504–507.

[55] A. L. Goldberger, L. A. N. Amaral, L. Glass, J. M. Hausdorff, P. C. Ivanov, R. G. Mark, J. E. Mietus, G. B. Moody, C.-K. Peng, and H. E. Stanley, "Physiobank, physiotoolkit, and physionet: Components of a new research resource for complex physiologic signals," *Circulation*, vol. 101, no. 23, pp. e215–e220, 2000. [Online]. Available: http://circ.ahajournals.org/content/101/23/e215.abstract

[56] A. Grant, L. Valentin, D. Elbourne, and S. Alexander, "Routine formal fetal movement counting and risk of antepartum late death in normally formed singletons," *The Lancet*, vol. 334, no. 8659, pp. 345–349, 1989.

[57] K. R. Greene and K. G. Rosen, "Long-term st waveform changes in the ovine fetal electrocardiogram: the relationship to spontaneous labour and intrauterine death." *Clinical Physics And Physiological Measurement: An Official Journal Of The Hospital Physicists' Association, Deutsche Gesellschaft Fr Medizinische Physik And The European Federation Of Organisations For Medical Physics*, vol. 10 Suppl B, pp. 33 – 40, 1989. [Online]. Available: https://ezp.lib.unimelb.edu.au/login?url=https://search.ebscohost.com/login.aspx?direct=true&db=cmedm&AN=2630159&scope=site

[58] A. Gretton, K. Fukumizu, C. H. Teo, L. Song, B. Schölkopf, and A. J. Smola, "A kernel statistical test of independence." in *NIPS*, vol. 20, 2007, pp. 585–592.

[59] M. Gurban and J.-P. Thiran, "Audio-visual speech recognition with a hybrid svm-hmm system," in *13th European Signal Processing Conference*, 2005.

[60] M. Haghpanahi and D. A. Borkholder, "Fetal ecg extraction from abdominal recordings using array signal processing," in *Computing in Cardiology Conference (CinC), 2013*. IEEE, 2013, pp. 173–176.

[61] A. B. Hameed and M. S. Sklansky, "Pregnancy: maternal and fetal heart disease," *Current problems in cardiology*, vol. 32, no. 8, pp. 419–494, 2007.

[62] B. Hannaford and P. Lee, "Multi-dimensional hidden markov model of telemanipulation tasks with varying outcomes," in *Systems, Man and Cybernetics, 1990. Conference Proceedings., IEEE International Conference on*. IEEE, 1990, pp. 127–133.

[63] B. Hayes-Gill, S. Hassan, F. G. Mirza, S. Ommani, J. Himsworth, M. Solomon, R. Brown, B. S. Schifrin, and W. R. Cohen, "Accuracy and reliability of uterine contraction identification using abdominal surface electrodes." *Clinical Medicine Insights: Women's Health*, no. 5, 2012.

[64] S. Haykin, *Neural networks: a comprehensive foundation*. Prentice Hall PTR, 1994.

[65] E. Hon, "The instrumentation of fetal heart rate and fetal electrocardiography. i. a fetal heart monitor." *Connecticut medicine*, vol. 24, p. 289, 1960.

[66] E. Hon and O. Hess, "The clinical value of fetal electrocardiography," *Am J Obstet Gynecol*, vol. 79, pp. 1012–1023, 1960.

[67] E. Hon and S. Lee, "Averaging techniques in fetal electrocardiography," *Medical electronics and biological engineering*, vol. 2, no. 1, pp. 71–76, 1964.

[68] N. E. Huang, Z. Shen, S. R. Long, M. C. Wu, H. H. Shih, Q. Zheng, N.-C. Yen, C. C. Tung, and H. H. Liu, "The empirical mode decomposition and the hilbert spectrum for nonlinear and non-stationary time series analysis," *Proceedings of the Royal Society of London. Series A: Mathematical, Physical and Engineering Sciences*, vol. 454, no. 1971, pp. 903–995, 1998.

[69] J. Huddleston, G. Sutliff, F. Carney, and C. Flowers, "Oxytocin challenge test for antepartum fetal assessment. report of a clinical experience." *American journal of obstetrics and gynecology*, vol. 135, no. 5, p. 609, 1979.

[70] C. Ionescu, "The benefits of 3d-4d fetal echocardiography," *Maedica*, vol. 5, no. 1, p. 45, 2010.

[71] P. C. Ivanov, Q. D. Ma, and R. P. Bartsch, "Maternal–fetal heartbeat phase synchronization," *Proceedings of the National Academy of Sciences*, vol. 106, no. 33, pp. 13 641–13 642, 2009.

[72] M. G. Jafari and J. A. Chambers, "Fetal electrocardiogram extraction by sequential source separation in the wavelet domain," *Biomedical Engineering, IEEE Transactions on*, vol. 52, no. 3, pp. 390–400, 2005.

[73] J. Jezewski, K. Horoba, A. Gasek, J. Wrobel, A. Matonia, and T. Kupka, "Analysis of nonstationarities in fetal heart rate signal: inconsistency measures of baselines using acceleration/deceleration patterns," in *Signal Processing and Its Applications, 2003. Proceedings. Seventh International Symposium on*, vol. 2. IEEE, 2003, pp. 9–12.

[74] J. Jezewski, A. Matonia, T. Kupka, D. Roj, and R. Czabanski, "Determination of fetal heart rate from abdominal signals: evaluation of beat-to-beat accuracy in relation to the direct fetal electrocardiogram," *Biomedizinische Technik/Biomedical Engineering*, vol. 57, no. 5, pp. 383–394, 2012.

[75] G. H. John and P. Langley, "Estimating continuous distributions in bayesian classifiers," in *Proceedings of the Eleventh Conference on Uncertainty in Artificial Intelligence*. Morgan Kaufmann Publishers Inc., 1995, pp. 338–345.

[76] P. Kanjilal, S. Palit, and G. Saha, "Fetal ecg extraction from single-channel maternal ecg using singular value decomposition," *Biomedical Engineering, IEEE Transactions on*, vol. 44, no. 1, pp. 51–59, Jan 1997.

[77] V. Karsdorp, J. Van Vugt, H. Van Geijn, P. Kostense, D. Arduim, N. Montenegro, and T. Todros, "Clinical significance of absent or reversed end diastolic velocity waveforms in umbilical artery," *The Lancet*, vol. 344, no. 8938, pp. 1664–1668, 1994.

[78] A. Khamene and S. Negahdaripour, "A new method for the extraction of fetal ecg from the composite abdominal signal," *Biomedical Engineering, IEEE Transactions on*, vol. 47, no. 4, pp. 507–516, 2000.

[79] A. H. Khandoker, Y. Kimura, T. Ito, N. Sato, K. Okamura, and M. Palaniswami, "Antepartum non-invasive evaluation of opening and closing timings of the cardiac valves in fetal cardiac cycle," *Medical & biological engineering & computing*, vol. 47, no. 10, pp. 1075–1082, 2009.

[80] A. H. Khandoker, Y. Kimura, M. Palaniswami, and S. Marusic, "Identifying fetal heart anomalies using fetal ecg and doppler cardiogram signals," in *Computing in Cardiology, 2010*. IEEE, 2010, pp. 891–894.

[81] Y. Kimura, K. Okamura, T. Watanabe, J. Murotsuki, T. Suzuki, M. Yano, and A. Yajima, "Power spectral analysis for autonomic influences in heart rate and blood pressure variability in fetal lambs," *American Journal of Physiology-Heart and Circulatory Physiology*, vol. 271, no. 4, pp. H1333–H1339, 1996.

[82] Y. Kimura, N. Sato, J. Sugawara, C. Velayo, T. Hoshiai, S. Nagase, T. Ito, Y. Onuma, A. Katsumata, K. Okamura *et al.*, "Recent advances in fetal electrocardiography," *Open Medical Devices Journal*, vol. 4, pp. 7–12, 2012.

[83] B. S. Kisilevsky and S. M. Hains, "Onset and maturation of fetal heart rate response to the mother's voice over late gestation," *Developmental science*, vol. 14, no. 2, pp. 214–223, 2011.

[84] B. S. Kisilevsky, D. W. Muir, and J. A. Low, "Maturation of human fetal responses to vibroacoustic stimulation," *Child development*, vol. 63, no. 6, pp. 1497–1508, 1992.

[85] T. Koga, N. Athayde, B. Trudinger, and H. Nakano, "A new and simple doppler method for measurement of fetal cardiac isovolumetric contraction time," *Ultrasound in obstetrics & gynecology*, vol. 18, no. 3, pp. 264–267, 2001.

[86] T. Koga, N. Athayde, and B. Trudinger, "The fetal cardiac isovolumetric contraction time in normal pregnancy and in pregnancy with placental vascular disease: the first clinical report using a new ultrasound technique," *British Journal of Obstetrics and Gynaecology*, vol. 108, no. 2, pp. 179–185, 2001.

[87] F. Kovács, C. Horváth, Á. T. Balogh, and G. Hosszú, "Fetal phonocardiography-past and future possibilities," *Computer methods and programs in biomedicine*, vol. 104, no. 1, pp. 19–25, 2011.

[88] B. Krupa, M. M. Ali, and E. Zahedi, "The application of empirical mode decomposition for the enhancement of cardiotocograph signals," *Physiological measurement*, vol. 30, no. 8, p. 729, 2009.

[89] D. Kumar, P. Carvalho, M. Antunes, R. Paiva, and J. Henriques, "Noise detection during heart sound recording using periodicity signatures," *Physiological Measurement*, vol. 32, no. 5, p. 599, 2011.

[90] T. Kupka, J. Jezewski, A. Matonia, K. Horoba, and J. Wrobel, "Timing events in doppler ultrasound signal of fetal heart activity," in *Engineering in Medicine and Biology Society, 2004. IEMBS'04. 26th Annual International Conference of the IEEE*, vol. 1. IEEE, 2004, pp. 337–340.

[91] D. C. Lagrew Jr, "The contraction stress test," *Clinical Obstetrics and Gynecology*, vol. 38, no. 1, pp. 11–25, 1995.

[92] K.-C. Lai and J. J. Shynk, "A successive cancellation algorithm for fetal heart-rate estimation using an intrauterine ecg signal," *Biomedical Engineering, IEEE Transactions on*, vol. 49, no. 9, pp. 943–954, 2002.

[93] S. Lange, P. Van Leeuwen, U. Schneider, B. Frank, D. Hoyer, D. Geue, and D. Grönemeyer, "Heart rate features in fetal behavioural states," *Early human development*, vol. 85, no. 2, pp. 131–135, 2009.

[94] S. D. LARKS and L. D. LONGO, "Electrocardiographic studies of the fetal heart during delivery." *Obstetrics & Gynecology*, vol. 19, no. 6, pp. 740–747, 1962.

[95] S. Larks and G. Larks, "Components of the fetal electrocardiogram and intrauterine electrical axis: Quantitative data," *Neonatology*, vol. 10, no. 3-4, pp. 140–152, 1966.

[96] J. P. Lavin Jr, M. Miodovnik, and T. P. Barden, "Relationship of nonstress test reactivity and gestational age," *Obstetrics & Gynecology*, vol. 63, no. 3, pp. 338–344, 1984.

[97] J.-P. Lecanuet and A.-Y. Jacquet, "Fetal responsiveness to maternal passive swinging in low heart rate variability state: effects of stimulation direction and duration," *Developmental psychobiology*, vol. 40, no. 1, pp. 57–67, 2002.

[98] J. Lee, S. Nemati, I. Silva, B. A. Edwards, J. P. Butler, and A. Malhotra, "Transfer entropy estimation and directional coupling change detection in biomedical time series," *Biomedical engineering online*, vol. 11, no. 1, pp. 1–17, 2012.

[99] M. J. Lewis, "Review of electromagnetic source investigations of the fetal heart," *Medical engineering & physics*, vol. 25, no. 10, pp. 801–810, 2003.

[100] R. P. Lewis, S. Rittogers, W. Froester, and H. Boudoulas, "A critical review of the systolic time intervals." *Circulation*, vol. 56, no. 2, pp. 146–158, 1977.

[101] C. Li, C. Zheng, and C. Tai, "Detection of ecg characteristic points using wavelet transforms," *Biomedical Engineering, IEEE Transactions on*, vol. 42, no. 1, pp. 21–28, 1995.

[102] J. A. Lipponen and M. P. Tarvainen, "Principal component model for maternal ecg extraction in fetal qrs detection," *Physiological Measurement*, vol. 35, no. 8, p. 1637, 2014. [Online]. Available: http://stacks.iop.org/0967-3334/35/i=8/a=1637

[103] R. Liston, D. Sawchuck, and D. Young, "Fetal health surveillance: antepartum and intrapartum consensus guideline." *Journal of obstetrics and gynaecology Canada: JOGC= Journal d'obstétrique et gynécologie du Canada: JOGC*, vol. 29, no. 9 Suppl 4, pp. S3–56, 2007.

[104] S. Lunshof, K. Boer, H. Wolf, G. van Hoffen, N. Bayram, and M. Mirmiran, "Fetal and maternal diurnal rhythms during the third trimester of normal pregnancy: Outcomes of computerized analysis of continuous twenty four hour fetal heart rate recordings," *American journal of obstetrics and gynecology*, vol. 178, no. 2, pp. 247–254, 1998.

[105] J. MacQueen *et al.*, "Some methods for classification and analysis of multivariate observations," in *Proceedings of the fifth Berkeley symposium on mathematical statistics and probability*, vol. 1. California, USA, 1967, pp. 281–297.

[106] E. F. Magann, S. P. Chauhan, J. A. Bofill, and J. N. Martin, "Comparability of the amniotic fluid index and single deepest pocket measurements in clinical practice,"

Australian and New Zealand journal of obstetrics and gynaecology, vol. 43, no. 1, pp. 75–77, 2003.

[107] G. Magenes, M. Signorini, and R. Sassi, "Automatic diagnosis of fetal heart rate: comparison of different methodological approaches," in *Engineering in Medicine and Biology Society, 2001. Proceedings of the 23rd annual international conference of the IEEE*, vol. 2. IEEE, 2001, pp. 1604–1607.

[108] K. Mäkikallio, P. Jouppila, and J. Räsänen, "Human fetal cardiac function during the first trimester of pregnancy," *Heart*, vol. 91, no. 3, pp. 334–338, 2005.

[109] P. Malcus, "Antenatal fetal surveillance," *Current Opinion in Obstetrics and Gynecology*, vol. 16, no. 2, pp. 123–128, 2004.

[110] F. A. Manning, "Fetal biophysical profile," *Obstetrics and gynecology clinics of North America*, vol. 26, no. 4, pp. 557–577, 1999.

[111] F. Manning, C. Harman, I. Morrison, S. Menticoglou, I. Lange, and J. Johnson, "Fetal assessment based on fetal biophysical profile scoring: Iv. an analysis of perinatal morbidity and mortality," *American journal of obstetrics and gynecology*, vol. 162, no. 3, pp. 703–709, 1990.

[112] F. Manning, I. Morrison, C. Harman, and S. Menticoglou, "The abnormal fetal biophysical profile score: V. predictive accuracy according to score composition," *American journal of obstetrics and gynecology*, vol. 162, no. 4, pp. 918–927, 1990.

[113] F. Manning, I. Morrison, I. Lange, C. Harman, and P. Chamberlain, "Fetal biophysical profile scoring: selective use of the nonstress test," *Hypertension*, vol. 4711, p. 173, 1987.

[114] F. A. Manning, "Dynamic ultrasound-based fetal assessment: the fetal biophysical profile score," *Clinical Obstetrics and Gynecology*, vol. 38, no. 1, pp. 26–44, 1995.

[115] S. M. Martens, C. Rabotti, M. Mischi, and R. J. Sluijter, "A robust fetal ecg detection method for abdominal recordings," *Physiological measurement*, vol. 28, no. 4, p. 373, 2007.

[116] F. Marzbanrad, A. Khandoker, M. Endo, Y. Kimura, and M. Palaniswami, "A multi-dimensional hidden markov model approach to automated identification of fetal cardiac valve motion," in *Engineering in Medicine and Biology Society (EMBC), 2014 36th Annual International Conference of the IEEE*, Aug 2014, pp. 1885–1888.

[117] F. Marzbanrad, Y. Kimura, M. Endo, S. Oshio, K. Funamoto, N. Sato, M. Palaniswami, and A. Khandoker, "Model based estimation of aortic and mitral valves opening and closing timings in developing human fetuses," *Biomedical and Health Informatics, IEEE Journal of*, vol. PP, 2014.

[118] F. Marzbanrad, Y. Kimura, M. Endo, M. Palaniswami, and A. H. Khandoker, "Classification of doppler ultrasound signal quality for the application of fetal valve motion identification," in *2015 Computing in Cardiology Conference (CinC)*, Sept 2015, pp. 365–368.

[119] F. Marzbanrad, A. H. Khandoker, K. Funamoto, R. Sugibayashi, M. Endo, C. Velayo, Y. Kimura, and M. Palaniswami, "Automated identification of fetal cardiac valve timings," in *Engineering in Medicine and Biology Society (EMBC), 2013 35th Annual International Conference of the IEEE*. IEEE, 2013, pp. 3893–3896.

[120] F. Marzbanrad, Y. Kimura, M. Endo, M. Palaniswami, and A. H. Khandoker, "Automated measurement of fetal isovolumic contraction time from doppler ultrasound signals without using fetal electrocardiography," in *Computing in Cardiology Conference (CinC), 2014*. IEEE, 2014, pp. 485–488.

[121] ——, "Transfer entropy analysis of maternal and fetal heart rate coupling," in *Engineering in Medicine and Biology Society (EMBC), 2015 37th Annual International Conference of the IEEE*. IEEE, 2015, pp. 7865–7868.

[122] F. Marzbanrad, Y. Kimura, K. Funamoto, R. Sugibayashi, M. Endo, T. Ito, M. Palaniswami, and A. Khandoker, "Development of fetal cardiac intervals throughout 16 to 41 weeks of gestation," in *Computing in Cardiology Conference (CinC), 2013*. IEEE, 2013, pp. 1155–1158.

[123] F. Marzbanrad, Y. Kimura, K. Funamoto, R. Sugibayashi, M. Endo, T. Ito, M. Palaniswami, and A. H. Khandoker, "Automated estimation of fetal cardiac timing events from doppler ultrasound signal using hybrid models," *Biomedical and Health Informatics, IEEE Journal of*, vol. 18, no. 4, pp. 1169–1177, 2014.

[124] F. Marzbanrad, Y. Kimura, M. Palaniswami, and A. H. Khandoker, "Application of automated fetal valve motion identification to investigate fetal heart anomalies," in *Healthcare Innovation Conference (HIC), 2014 IEEE*. IEEE, 2014, pp. 243–246.

[125] ——, "Quantifying the interactions between maternal and fetal heart rates by transfer entropy," *PloS one*, vol. 10, no. 12, p. e0145672, 2015.

[126] A. Matonia, J. Jezewski, T. Kupka, K. Horoba, J. Wrobel, and A. Gacek, "The influence of coincidence of fetal and maternal qrs complexes on fetal heart rate reliability," *Medical and Biological Engineering and Computing*, vol. 44, no. 5, pp. 393–403, 2006. [Online]. Available: http://dx.doi.org/10.1007/s11517-006-0054-0

[127] N. A. Mensah-Brown, R. T. Wakai, B. Cheulkar, S. Srinivasan, and J. F. Strasburger, "Assessment of left ventricular pre-ejection period in the fetus using simultaneous magnetocardiography and echocardiography," *Fetal diagnosis and therapy*, vol. 28, no. 3, pp. 167–174, 2010.

[128] E. Merz, *Ultrasound in Obstetrics and Gynecology.* Georg Thieme Verlag, 2004.

[129] B. Mijovic, M. De Vos, I. Gligorijevic, J. Taelman, and S. Van Huffel, "Source separation from single-channel recordings by combining empirical-mode decomposition and independent component analysis," *Biomedical Engineering, IEEE Transactions on*, vol. 57, no. 9, pp. 2188–2196, 2010.

[130] D. A. Miller, Y. A. Rabello, and R. H. Paul, "The modified biophysical profile: antepartum testing in the 1990s," *American journal of obstetrics and gynecology*, vol. 174, no. 3, pp. 812–817, 1996.

[131] T. M. Mitchell, *Machine learning. 1997*, 1997, vol. 45.

[132] C. Monk, W. P. Fifer, M. M. Myers, R. P. Sloan, L. Trien, and A. Hurtado, "Maternal stress responses and anxiety during pregnancy: effects on fetal heart rate," *Developmental Psychobiology*, vol. 36, no. 1, pp. 67–77, 2000.

[133] A. Montalto, L. Faes, and D. Marinazzo, "Mute: a matlab toolbox to compare established and novel estimators of the multivariate transfer entropy," *PloS one*, vol. 9, no. 10, p. e109462, 2014.

[134] Y. Murata and J. Chester B Martin, "Systolic time intervals of the fetal cardiac cycle," *Obstetrics & Gynecology*, vol. 44, no. 2, pp. 224–232, 1974.

[135] Y. Murata, C. B. Martin, T. Ikenoue, and P. Lu, "Antepartum evaluation of the preejection period of the fetal cardiac cycle," *Am J Obstet Gynecol*, vol. 132, pp. 278–284, 1978.

[136] M. P. Nageotte, C. V. Towers, T. Asrat, and R. K. Freeman, "Perinatal outcome with the modified biophysical profile," *American journal of obstetrics and gynecology*, vol. 170, no. 6, pp. 1672–1676, 1994.

[137] K. Nicolaides, C. Bilardo, P. Soothill, and S. Campbell, "Absence of end diastolic frequencies in umbilical artery: a sign of fetal hypoxia and acidosis." *BMJ: British Medical Journal*, vol. 297, no. 6655, p. 1026, 1988.

[138] J. Nijhuis, H. F. Prechtl, C. J. Martin, and R. Bots, "Are there behavioural states in the human fetus?" *Early human development*, vol. 6, no. 2, pp. 177–195, 1982.

[139] H. Norén, S. Blad, A. Carlsson, A. Flisberg, A. Gustavsson, H. Lilja, M. Wennergren, and H. Hagberg, "Stan in clinical practicethe outcome of 2 years of regular use in the city of gothenburg," *American journal of obstetrics and gynecology*, vol. 195, no. 1, pp. 7–15, 2006.

[140] H. Norn, I. Amer-Whlin, H. Hagberg, A. Herbst, I. Kjellmer, K. Marl *et al.*, "Fetal electrocardiogram in labor and neonatal outcome: data from the swedish randomized controlled trial on intrapartum fetal monitoring. fetal electrocardiography in labor and neonatal outcome: data from the swedish randomized controlled trial on

intrapartum fetal monitoring," *American Journal of Obstetrics and Gynecology*, vol. 188, pp. 183–192, 2003.

[141] J. C. Nunes, Y. Bouaoune, E. Delechelle, O. Niang, and P. Bunel, "Image analysis by bidimensional empirical mode decomposition," *Image and vision computing*, vol. 21, no. 12, pp. 1019–1026, 2003.

[142] G. Ogge, P. Gaglioti, S. Maccanti, F. Faggiano, and T. Todros, "Prenatal screening for congenital heart disease with four-chamber and outflow-tract views: a multicenter study," *Ultrasound in obstetrics & gynecology*, vol. 28, no. 6, pp. 779–784, 2006.

[143] OpenStaxCollege, "Anatomy and physiology II," 2015. [Online]. Available: http://www.ubooks.pub/Books/ON/B0/E28R8369/P4C2S3U27.html

[144] L. Organ, A. Bernstein, and P. Hawrylyshyn, "The pre-ejection period as an antepartum indicator of fetal well-being." *American journal of obstetrics and gynecology*, vol. 137, no. 7, p. 810, 1980.

[145] M. Ounsted, V. Moar, and W. A. Scott, "Perinatal morbidity and mortality in small-for-dates babies: the relative importance of some maternal factors," *Early human development*, vol. 5, no. 4, pp. 367–375, 1981.

[146] N. Outram, E. Ifeachor, P. Van Eetvelt, and S. Curnow, "Techniques for optimal enhancement and feature extraction of fetal electrocardiogram," *IEE Proceedings-Science, Measurement and Technology*, vol. 142, no. 6, pp. 482–489, 1995.

[147] J. Pan and W. J. Tompkins, "A real-time qrs detection algorithm," *Biomedical Engineering, IEEE Transactions on*, no. 3, pp. 230–236, 1985.

[148] J. G. Papp, "Autonomic responses and neurohumoral control in the human early antenatal heart," *Basic research in cardiology*, vol. 83, no. 1, pp. 2–9, 1988.

[149] M. Peters, J. Crowe, J. F. Piri, H. Quartero, B. Hayes-Gill, D. James, J. Stinstra, and S. Shakespeare, "Monitoring the fetal heart non-invasively: a review of methods." *Journal Of Perinatal Medicine*, vol. 29, no. 5, pp. 408 – 416, 2001.

[Online]. Available: https://ezp.lib.unimelb.edu.au/login?url=https://search.ebscohost.com/login.aspx?direct=true&db=cmedm&AN=11723842&scope=site

[150] M. Peters, J. Stinstra, S. Van Den Broek, J. Huirne, H. Quartero, H. Ter Brake, and H. Rogalla, "On the fetal magnetocardiogram," *Bioelectrochemistry and bioenergetics*, vol. 47, no. 2, pp. 273–281, 1998.

[151] M. Pillai and D. James, "The development of fetal heart rate patterns during normal pregnancy." *Obstetrics & Gynecology*, vol. 76, no. 5, pp. 812–816, 1990.

[152] J. Platt *et al.*, "Probabilistic outputs for support vector machines and comparisons to regularized likelihood methods," *Advances in large margin classifiers*, vol. 10, no. 3, pp. 61–74, 1999.

[153] A. Porta, G. Baselli, D. Liberati, N. Montano, C. Cogliati, T. Gnecchi-Ruscone, A. Malliani, and S. Cerutti, "Measuring regularity by means of a corrected conditional entropy in sympathetic outflow," *Biological cybernetics*, vol. 78, no. 1, pp. 71–78, 1998.

[154] A. Porta, V. Bari, A. Marchi, B. De Maria, D. Cysarz, P. Van Leeuwen, A. C. Takahashi, A. M. Catai, and T. Gnecchi-Ruscone, "Complexity analyses show two distinct types of nonlinear dynamics in short heart period variability recordings," *Frontiers in physiology*, vol. 6, 2015.

[155] L. Rabiner, "A tutorial on hidden markov models and selected applications in speech recognition," *Proceedings of the IEEE*, vol. 77, no. 2, pp. 257–286, 1989.

[156] G. Ramanathan and S. Arulkumaran, "Antenatal fetal surveillance," *Obstetrics and Gynecology for Postgraduates*, vol. 1.

[157] K. Ran, "Bland-altman and correlation plot code," Mathworks, 2014. [Online]. Available: http://www.mathworks.com/matlabcentral/fileexchange/45049-bland-altman-and-correlation-plot

[158] M. Ray, R. Freeman, S. Pine, and R. Hesselgesser, "Clinical experience with the oxytocin challenge test," *Am J Obstet Gynecol*, vol. 114, no. 1, pp. 1–9, 1972.

[159] M. Richter, T. Schreiber, and D. T. Kaplan, "Fetal ecg extraction with nonlinear state-space projections," *Biomedical Engineering, IEEE Transactions on*, vol. 45, no. 1, pp. 133–137, 1998.

[160] M. Riedl, P. Van Leeuwen, A. Suhrbier, H. Malberg, D. Grönemeyer, J. Kurths, and N. Wessel, "Testing foetal–maternal heart rate synchronization via model-based analyses," *Philosophical Transactions of the Royal Society A: Mathematical, Physical and Engineering Sciences*, vol. 367, no. 1892, pp. 1407–1421, 2009.

[161] R. Rodrigues, "Fetal ecg detection in abdominal recordings: a method for qrs location," in *Computing in Cardiology Conference (CinC), 2013*. IEEE, 2013, pp. 325–328.

[162] D. Rouvre, D. Kouamé, F. Tranquart, and L. Pourcelot, "Empirical mode decomposition (emd) for multi-gate, multi-transducer ultrasound doppler fetal heart monitoring," in *Signal Processing and Information Technology, 2005. Proceedings of the Fifth IEEE International Symposium on*. IEEE, 2005, pp. 208–212.

[163] S. E. Rutherford, J. P. PHELAN, C. V. SMITH, and N. JACOBS, "The four-quadrant assessment of amniotic fluid volume: an adjunct to antepartum fetal heart rate testing," *Obstetrics & Gynecology*, vol. 70, no. 3, pp. 353–356, 1987.

[164] R. Sameni, C. Jutten, and M. Shamsollahi, "Multichannel electrocardiogram decomposition using periodic component analysis," *Biomedical Engineering, IEEE Transactions on*, vol. 55, no. 8, pp. 1935–1940, Aug 2008.

[165] R. Sameni, "Extraction of fetal cardiac signals from an array of maternal abdominal recordings," Ph.D. dissertation, Sharif University of Technology, Tehran, Iran, 2008.

[166] R. Sameni and G. D. Clifford, "A review of fetal ecg signal processing; issues and promising directions," *The open pacing, electrophysiology & therapy journal*, vol. 3, p. 4, 2010.

[167] R. Sameni, M. B. Shamsollahi, C. Jutten, and G. D. Clifford, "A nonlinear bayesian filtering framework for ecg denoising," *Biomedical Engineering, IEEE Transactions on*, vol. 54, no. 12, pp. 2172–2185, 2007.

[168] M. B. Sampson, "Antepartum measurement of the preejection period in high-risk pregnancy," *Obstetrics & Gynecology*, vol. 56, no. 3, pp. 289–290, 1980.

[169] M. Sato, Y. Kimura, S. Chida, T. Ito, N. Katayama, K. Okamura, and M. Nakao, "A novel extraction method of fetal electrocardiogram from the composite abdominal signal," *Biomedical Engineering, IEEE Transactions on*, vol. 54, no. 1, pp. 49–58, 2007.

[170] Save the Children, "Ending newborn deaths," 2014. [Online]. Available: http://www.savethechildren.org/atf/cf/%7B9def2ebe-10ae-432c-9bd0-df91d2eba74a%7D/ENDING-NEWBORN-DEATHS.PDF

[171] T. Schreiber, "Measuring information transfer," *Physical review letters*, vol. 85, no. 2, p. 461, 2000.

[172] T. Schreiber and D. T. Kaplan, "Signal separation by nonlinear projections: The fetal electrocardiogram," *Physical Review E*, vol. 53, no. 5, p. R4326, 1996.

[173] P. J. Schwartz, M. Periti, and A. Malliani, "The long qt syndrome," *American heart journal*, vol. 89, no. 3, pp. 378–390, 1975.

[174] S. Shakespeare, J. Crowe, B. Hayes-Gill, K. Bhogal, and D. James, "The information content of doppler ultrasound signals from the fetal heart," *Medical and Biological Engineering and Computing*, vol. 39, no. 6, pp. 619–626, 2001.

[175] M. Shao, K. E. Barner, and M. H. Goodman, "An interference cancellation algorithm for noninvasive extraction of transabdominal fetal electroencephalogram (tafeeg)," *Biomedical Engineering, IEEE Transactions on*, vol. 51, no. 3, pp. 471–483, 2004.

[176] D. Sim, R. Beattie, and J. Dornan, "Evaluation of biophysical fetal assessment in high-risk pregnancy to assess ultrasound parameters suitable for screening in the low-risk population," *Ultrasound in Obstetrics & Gynecology*, vol. 3, no. 1, pp. 11–17, 1993.

[177] D. Springer, T. Brennan, L. Zuhlke, H. Abdelrahman, N. Ntusi, G. D. Clifford, B. Mayosi, and L. Tarassenko, "Signal quality classification of mobile phone-

recorded phonocardiogram signals," in *Acoustics, Speech and Signal Processing (ICASSP), 2014 IEEE International Conference on*. IEEE, 2014, pp. 1335–1339.

[178] P. Steer and P. Danielian, "Fetal distress in labour," *High Risk Pregnancy Management Options.*, 1999.

[179] L. Stroux and G. D. Clifford, "The importance of biomedical signal quality classification for successful mhealth implementation," in *2014 Tech4Dev International Conference UNESCO Chair in Technologies for Development: What is Essential?*, June 2014.

[180] J. A. Suykens, T. Van Gestel, J. De Brabanter, B. De Moor, J. Vandewalle, J. Suykens, and T. Van Gestel, *Least squares support vector machines*. World Scientific, 2002, vol. 4.

[181] C. M. Sweeney-Reed and S. J. Nasuto, "A novel approach to the detection of synchronisation in eeg based on empirical mode decomposition," *Journal of Computational Neuroscience*, vol. 23, no. 1, pp. 79–111, 2007.

[182] E. M. Symonds, D. Sahota, and A. Chang, *Fetal electrocardiography*. OECD Publishing, 2001.

[183] E. Symonds, D. Sahota, and A. Chang, *Fetal Electrocardiology*. London: Imperial College Press, 2001.

[184] K. Tan and A. Sabapathy, "Fetal manipulation for facilitating tests of fetal wellbeing," *Cochrane Database Syst Rev*, vol. 4, 2001.

[185] S. Theodoridis, A. Pikrakis, K. Koutroumbas, and D. Cavouras, *Introduction to Pattern Recognition: A Matlab Approach: A Matlab Approach*. Academic Press, 2010.

[186] I. Timor-Tritsch, L. Dierker, I. Zador, R. Hertz, and M. Rosen, "Fetal movements associated with fetal heart rate accelerations and decelerations." *American journal of obstetrics and gynecology*, vol. 131, no. 3, p. 276, 1978.

[187] M. Ungureanu, J. W. Bergmans, S. G. Oei, and R. Strungaru, "Fetal ecg extraction during labor using an adaptive maternal beat subtraction technique," *Biomedizinische Technik*, vol. 52, no. 1, pp. 56–60, 2007.

[188] P. Van Leeuwen, D. Geue, M. Thiel, D. Cysarz, S. Lange, M. Romano, N. Wessel, J. Kurths, and D. Grönemeyer, "Influence of paced maternal breathing on fetal–maternal heart rate coordination," *Proceedings of the National Academy of Sciences*, vol. 106, no. 33, pp. 13 661–13 666, 2009.

[189] P. Van Leeuwen, D. Geue, S. Lange, D. Cysarz, H. Bettermann, and D. H. Grönemeyer, "Is there evidence of fetal-maternal heart rate synchronization?" *BMC physiology*, vol. 3, no. 1, p. 2, 2003.

[190] P. Van Leeuwen, D. Geue, M. Thiel, S. Lange, D. Cysarz, M. C. Romano, J. Kurths, and D. H. Grönemeyer, "Fetal maternal heart rate entrainment under controlled maternal breathing," in *17th International Conference on Biomagnetism Advances in Biomagnetism–Biomag2010*. Springer, 2010, pp. 262–265.

[191] P. Van Leeuwen, K. M. Gustafson, D. Cysarz, D. Geue, L. E. May, and D. Grönemeyer, "Aerobic exercise during pregnancy and presence of fetal-maternal heart rate synchronization," *PloS one*, vol. 9, no. 8, p. e106036, 2014.

[192] P. Van Leeuwen, S. Lange, A. Klein, D. Geue, and D. H. Grönemeyer, "Dependency of magnetocardiographically determined fetal cardiac time intervals on gestational age, gender and postnatal biometrics in healthy pregnancies," *BMC pregnancy and childbirth*, vol. 4, no. 1, p. 6, 2004.

[193] V. Vapnik, *The nature of statistical learning theory*. springer, 2000.

[194] R. Vicente, M. Wibral, M. Lindner, and G. Pipa, "Transfer entropy-a model-free measure of effective connectivity for the neurosciences," *Journal of computational neuroscience*, vol. 30, no. 1, pp. 45–67, 2011.

[195] V. Vigneron, A. Paraschiv-Ionescu, A. Azancot, O. Sibony, and C. Jutten, "Fetal electrocardiogram extraction based on non-stationary ica and wavelet denoising,"

in *Signal Processing and Its Applications, 2003. Proceedings. Seventh International Symposium on*, vol. 2. IEEE, 2003, pp. 69–72.

[196] A. M. Vintzileos, W. A. Campbell, C. J. Ingardia, and D. J. Nochimson, "The fetal biophysical profile and its predictive value," *Obstetrics & Gynecology*, vol. 62, no. 3, pp. 271–278, 1983.

[197] R. Von Kries, R. Kimmerle, J. Schmidt, A. Hachmeister, O. Böhm, and H. Wolf, "Pregnancy outcomes in mothers with pregestational diabetes: a population-based study in north rhine (germany) from 1988 to 1993," *European journal of pediatrics*, vol. 156, no. 12, pp. 963–967, 1997.

[198] Q. Wang, A. H. Khandoker, F. Marzbanrad, K. Funamoto, R. Sugibayashi, M. Endo, Y. Kimura, and M. Palaniswami, "Investigating the beat by beat phase synchronization between maternal and fetal heart rates," in *Engineering in Medicine and Biology Society (EMBC), 2013 35th Annual International Conference of the IEEE*. IEEE, 2013, pp. 3821–3824.

[199] A. M. Weissler, W. S. Harris, and C. D. Schoenfeld, "Systolic time intervals in heart failure in man," *Circulation*, vol. 37, no. 2, pp. 149–159, 1968.

[200] M. Wibral, B. Rahm, M. Rieder, M. Lindner, R. Vicente, and J. Kaiser, "Transfer entropy in magnetoencephalographic data: Quantifying information flow in cortical and cerebellar networks," *Progress in biophysics and molecular biology*, vol. 105, no. 1, pp. 80–97, 2011.

[201] D. Widjaja, C. Varon, A. C. Dorado, J. A. Suykens, and S. Van Huffel, "Application of kernel principal component analysis for single-lead-ecg-derived respiration," *Biomedical Engineering, IEEE Transactions on*, vol. 59, no. 4, pp. 1169–1176, 2012.

[202] B. Widrow, J. R. Glover Jr, J. M. McCool, J. Kaunitz, C. S. Williams, R. H. Hearn, J. R. Zeidler, E. Dong Jr, and R. C. Goodlin, "Adaptive noise cancelling: Principles and applications," *Proceedings of the IEEE*, vol. 63, no. 12, pp. 1692–1716, 1975.

[203] L. Yang, Y. Xu, and C. S. Chen, "Hidden markov model approach to skill learning and its application to telerobotics," *Robotics and Automation, IEEE Transactions on*, vol. 10, no. 5, pp. 621–631, 1994.

[204] Y. Yumoto, S. Satoh, Y. Fujita, T. Koga, N. Kinukawa, and H. Nakano, "Noninvasive measurement of isovolumetric contraction time during hypoxemia and acidemia: Fetal lamb validation as an index of cardiac contractility," *Early human development*, vol. 81, no. 7, pp. 635–642, 2005.

[205] I. E. Zador, R. N. Wolfson, S. K. Pillay, I. E. Timor-Tritsch, and R. H. Hertz, "Fetal cardiac time intervals and their potential clinical applications," *Clinical Obstetrics and Gynecology*, vol. 22, no. 3, pp. 651–663, 1979.

[206] V. Zarzoso, J. Millet-Roig, and A. Nandi, "Fetal ecg extraction from maternal skin electrodes using blind source separation and adaptive noise cancellation techniques," in *Computers in Cardiology 2000*. IEEE, 2000, pp. 431–434.

[207] V. Zarzoso and A. Nandi, "Noninvasive fetal electrocardiogram extraction: blind separation versus adaptive noise cancellation," *Biomedical Engineering, IEEE Transactions on*, vol. 48, no. 1, pp. 12–18, Jan 2001.

[208] V. Zarzoso, A. Nandi, and E. Bacharakis, "Maternal and foetal ecg separation using blind source separation methods," *Mathematical Medicine and Biology*, vol. 14, no. 3, pp. 207–225, 1997.

Author/s:
Marzbanrad, Faezeh

Title:
Modeling fetal cardiac valve intervals and fetal-maternal interactions

Date:
2015

Persistent Link:
http://hdl.handle.net/11343/91726

File Description:
Modeling fetal cardiac valve intervals and fetal-maternal interactions